SUMMARY OF UNCERTAINTY AND SENSITIVITY ANALYSIS RESULTS FOR THE EPA-MANDATED PERFORMANCE ASSESSMENT VERIFICATION TEST

WPO # 46912

August 22, 1997

August 22, 1997

TABLE OF CONTENTS

TABLE OF CONTENTS (continued)

1.0 INTRODUCTION

Two prior reports (WPO #46674 and WPO #46702) describe the results obtained from the U.S. Environmental Protection Agency (EPA)-Mandated Performance Assessment Verification Test (PAVT) of the U.S. Department of Energy's Performance Assessment Analyses supporting the Waste Isolation Pilot Plant (WIPP) Compliance Certification Application (CCA). This report presents a summary of the uncertainty and sensitivity analysis results obtained from the PAVT calculations.

This report is divided into the following sections: Introduction and Summary of Uncertainty and Sensitivity Results (Section 1); Salado Flow (Section 2); Direct Release to the Accessible Environment: Cuttings, Cavings, and Spallings (Section 3); Direct Release to the Accessible Environment: Direct Brine Release (Section 4); Release from the Culebra to the Accessible Environment (Section 5); and Total Normalized Releases to the Accessible Environment (Section 6). Descriptions of variables used in the sensitivity analysis are provided in Appendix A. Codes used to perform the uncertainty and sensitivity analysis are listed in Appendix B.

1.1 Summary of Uncertainty and Sensitivity Results

As described in previous reports (WPO #46674 and WPO #46702), the PAVT mean CCDF for total normalized releases to the accessible environment is shifted to the right of the CCA mean CCDF by a factor of 2 or 3 for all probabilities of exceedance. The shifting of the mean CCDF to the right is primarily due to an increase in cuttings and cavings releases and, to a lesser extent, an increase in spallings releases. Direct brine releases are slightly more important in the PAVT than in the CCA, but have only a minor effect on the mean CCDF for total normalized releases. Releases to the Culebra from the repository in the PAVT and CCA are similar. Subsurface releases due to Culebra groundwater transport are not significant in the PAVT and nonexistent in the CCA. Salado interbed releases are not significant and Dewey Lake releases are nonexistent in both the PAVT and CCA.

In general, the uncertainty and sensitivity analysis of the PAVT calculations yields results similar to those obtained from the preliminary CCA uncertainty and sensitivity analysis (WPO # 42912). However, as a result of several parameter changes in the PAVT (WPO # 46674), differences in both the order of importance of key variables and the appearance of new important variables occurs. Similarities and differences in important variables contributing to the uncertainty in releases for both the PAVT and CCA are summarized below.

1.1.1 Releases Due to Cuttings and Cavings

The important variable contributing to uncertainty in cuttings and cavings releases in both the PAVT and CCA is the waste shear strength W*TAUFAIL*. In the PAVT, the range of uncertain *WTAUFAIL* values is increased and the distribution of W*TAUFAIL* values is changed from a uniform to loguniform distribution. The impact of the higher maximum W*TAUFAIL* value results

in an increased number of small releases, while the impact of converting the distribution to loguniform results in an increased number of large releases.

1.1.2 Releases Due to Spallings

In the PAVT, the most important variable contributing to uncertainty in spallings releases is borehole permeability *BHPRM*, with expected releases tending to increase with decreasing values of *BHPRM* due to the important influence of this variable on repository pressure. The second most important variable is *VOLSPALL*, the spallings volume released if repository pressure is above 8 MPa. The next most important variable is *WMICDFLG*, which controls the amount of gas generated by microbial degradation of cellulose. Spallings releases tend to increase with increasing values of *WMICDFLG* due to the important influence of this variable on repository pressure. In the CCA, uncertainty in spallings release is dominated by *WMICDFLG*.

1.1.3 Releases Due to Direct Brine Release

In the PAVT, the dominant variables contributing to uncertainty in direct brine releases are permeability *DRZPRM* of the disturbed rock zone (DRZ) surrounding the repository and initial pressure of the Castile brine reservoir *BPINTPRS*. These variables tend to cause increases in brine saturation and repository pressure, which lead to increases in direct brine releases. In the CCA, the dominant variables are residual brine saturation *WRBRNSAT* and halite porosity *HALPOR*. Increasing values of *WRBRNSAT* tend to decrease the size of releases by decreasing the amount of mobile brine available for direct release. Increasing values of *HALPOR* have the opposite effect by increasing the amount of brine in the repository.

1.1.4 Releases From the Culebra

Releases from the Culebra are determined by first calculating releases to the Culebra; these release rates are then used in conjunction with Culebra transport results to estimate releases to the accessible environment. Because of the small number of nonzero releases from the Culebra to the accessible environment, a meaningful sensitivity analysis for total releases from the Culebra could not be performed. However, sensitivity analyses for releases to the Culebra and for transport in the Culebra were performed and are summarized herein.

In the PAVT, the only radionuclide released from the Culebra is U-234. The most important variable contributing to uncertainty in releases to the Culebra is borehole permeability *BHPRM*. Increasing values of *BHPRM* tend to cause increased releases to the Culebra (1) by reducing resistance to brine flow from the Castile brine reservoir to the repository and also from the repository to the Culebra, and (2) by facilitating the filling of the repository due to brine flow down an intruding borehole. In the CCA, *BHPRM* and brine reservoir compressibility *BPCOMP* are nearly equally important contributors to uncertainty in releases to the Culebra.

In the PAVT, the dominant variables contributing to uncertainty in Culebra transport are the

pointer variable for oxidation state *WOXYSTAT* and the matrix distribution coefficient *CMKDU6*, with the size of release tending to increase as *WOXYSTAT* increases and decrease as *CMKDU6* increases. The positive effect for *WOXYSTAT* results from its role in determining which set of distribution coefficients are used in the transport calculations. In particular, smaller distribution coefficients (*CMKDU6*) for U-234 are associated with *WOXYSTAT* = 1 (i.e., oxidation state of +VI), hence the positive effect for *OXYSTAT*. The negative effect for *CMKDU6* results because increasing *CMKDU6* increases adsorption of U-234 in the matrix and thus reduces transport. In the CCA meaningful regression analysis of transport of U-234 across the land withdrawal boundary could not be completed because of the fact that only one Latin Hypercube Sample (LHS) element produced releases.

1.1.5 Total Normalized Releases to the Accessible Environment

In the PAVT, the two dominant variables with respect to uncertainty in the expected total release are *WTAUFAIL* and *BHPRM*, with the size of the expected release tending to decrease as these variables increase. The negative effect for *WTAUFAIL* results from its influence on the size of the cuttings release, as *WTAUFAIL* increases cuttings releases decrease. The negative effect for *BHPRM* results from its influence on repository pressure, as *BHPRM* decreases repository pressures increase. The primary determinant of the uncertainty in releases due to spallings is the pressure condition in repository, with no spallings releases taking place at pressures less than 8 MPa. In addition, minor positive effects are contributed by *VOLSPALL*, *WMICDFLG*, *DRZPRM*, *HALPOR*, and *PBRINE* due to their influence on the size of spallings and direct brine releases.

In the CCA, the two dominant variables with respect to uncertainty in the expected total release are *WMICDFLG* and *WTAUFAIL*, with the size of the expected release tending to increase as *WMICDFLG* increases and tending to decrease as *WTAUFAIL* increases. The positive effect for *WMICDFLG* results from its influence on the size of spallings release, as *WMICDFLG* increases spallings releases increase in size. The negative effect for *WTAUFAIL* results from its influence on the size of cuttings releases. In addition, minor effects are contributed by corrosion rate for steel under inundated conditions *WGRCOR* (positive), waste particle diameter *WPRTDIAM* (negative), *HALPOR* (positive), and *BHPRM* (negative), primarily because of their effects on spallings release.

2.0 SALADO FLOW

In this section, PAVT uncertainty and sensitivity analysis results are presented for Salado flow. The presentation of results closely follows the presentation given in Sections 2 and 3 of the preliminary CCA sensitivity and analysis report (WPO #42912). At the end of each subsection, figure numbers in the CCA report that correspond to figures presented in this PAVT report are listed. Note that CCA figures typically included more than one plot, therefore there are fewer CCA figures listed.

2.1 Fluid Flow in the Vicinity of the Repository: Undisturbed Conditions

2.1.1 Undisturbed Conditions: Brine Inflow

The anhydrite marker beds provide the only significant pathway by which brine can flow from the Salado Formation to the repository from areas beyond the DRZ (Figure 2.1.1.1). However, as in the CCA, the dominant source of brine into the repository is drainage from the DRZ, which primarily takes place over the first 50 to 100 years of the calculation (Figure 2.1.1.2). Total brine inflow to the repository is greater than the total flow from the marker beds because of drainage from the DRZ. An examination Figures 2.1.1.1 and 2.1.1.2 shows that considerable uncertainty exists both with respect to the volume of brine inflow from the marker beds and the volume of brine flow into the repository.

Three important variables contributing to uncertainty in brine inflow from the marker beds are *ANHPRM*, *DRZPRM*, and *WMICDFLG* (Figure 2.1.1.3). The negative effect indicated for *WMICDFLG* results because increasing *WMICDFLG* increases gas generation and thus pressure in the repository, which in turn decreases flow out of the marker beds and into the DRZ. The positive effects indicated for *DRZPRM* and *ANHPRM* result from decreased resistance to brine flow in the DRZ and marker beds.

The dominant variables for cumulative brine flow into the repository are *HALPOR* and *DRZPRM* (Figure 2.1.1.4). The positive effect for *HALPOR* results because increasing *HALPOR* increases the volume of brine in the DRZ that is available to drain into the repository. The positive effect indicated for *DRZPRM* results from decreased resistance to brine flow in the DRZ.

The important variables contributing to brine inflow under undisturbed conditions, described above, are similar to the CCA. The only difference is that *DRZPRM*, sampled for the PAVT but constant in the CCA, is an important PAVT variable. *HALPRM*, is less important in the PAVT due to the increased importance of *DRZPRM*. For brine inflow to the repository, *SALPRES* and *WMICDFLG* were also less important due to the increased importance of *DRZPRM*.

[Corresponding Figures From CCA: 2.1.1, 2.1.3]

2.1.2 Undisturbed Conditions: Gas Generation

Gas generation results from the corrosion of steel and the microbial degradation of cellulose (Figures 2.1.2.1 and 2.1.2.2). The discretized character of cumulative gas generation for microbial degradation derives from the variable *WMICDFLG*, which takes on three values. One value, which has a probability of 0.25, specifies the inclusion of rubber and plastics in the inventory of cellulose available for microbial degradation and results in the upper group of curves in Fig. 2.1.2.2; one value, which also has a probability of 0.25, specifies the exclusion of rubber and plastics from the inventory of cellulose available for microbial degradation and results in the middle group of curves in Fig. 2.1.2.2; and one value, which has a probability of 0.5, specifies that no microbial degradation of cellulose will take place and results in the lower group of curves in Fig. 2.1.2.2.

Total gas generation is obtained by combining gas generation due to corrosion and gas generation due to microbial degradation (Fig. 2.1.2.3), with the larger contribution coming from corrosion (Fig. 2.1.2.1). However, microbial degradation still makes a substantial contribution to the total uncertainty in gas generation.

As in the CCA, gas generation due to microbial degradation is dominated by *WMICDFLG*. For gas generation due to corrosion, the dominant variables are *WGRCOR*, *HALPOR*, and *DRZPRM* with a smaller effect indicated for *WASTWICK* (Fig. 2.1.2.4). The variables *WGRCOR* and *WASTWICK* are important at early times because increasing each of these variables increases the rate at which gas is generated. However, over the longer term, the amount of gas generated by corrosion depends on the amount of steel undergoing corrosion, which in turn depends on the volume of brine available for the corrosion process. Brine is consumed in the corrosion process, with the result that the amount of gas generated by corrosion can be limited by the amount of brine present in the repository. The positive effect indicated for *HALPOR* and *DRZPRM* results because *HALPOR* and *DRZPRM* are dominant variables with respect to the amount of brine entering the repository (Fig. 2.1.1.4).

For total gas generation due to corrosion of steel and microbial degradation of cellulose, the dominant variables are *WMICDFLG*, *HALPOR*, and *DRZPRM* with *WMICDFLG* controlling the uncertainty in the amount of gas generated by microbial degradation and *HALPOR* and *DRZPRM* controlling the uncertainty in the amount of gas generated by corrosion (Fig. 2.1.2.5). Smaller positive effects are indicated for *WGRCOR* and *WASTWICK*, which affect the rate at which corrosion takes place, with these effects becoming less important with increasing time.

The BRAGFLO computational grid used in both the PAVT and the CCA is based on dividing the repository into a single lower, or downdip, waste panel (identified as Waste Panel in BRAGFLO output) and nine upper waste panels (identified as Rest of Repository in BRAGFLO output), with the panel closures placed between these two groups of panels. For disturbed conditions, BRAGFLO calculations are performed with the assumption that the associated drilling intrusion takes place into the single lower panel. Further, spallings and direct brine release calculations

distinguish between drilling intrusions into upper and lower waste panels. The rationale for this selection was based on the belief that intrusions into a downdip panel might be somewhat worse from a release perspective than intrusions into an updip panel due to brine flow down the 1° dip on which the repository is constructed. Given the role that distinctions between intrusions into upper and lower waste panels will play in the release calculations, it is useful to examine the differences in conditions in these two sets of panels.

On a fractional basis, less steel is consumed in the upper waste panels (Fig. 2.1.2.6) than in the lower waste panel (Fig. 2.1.2.7). This pattern occurs because the lower waste panel receives more brine inflow relative to its volume than the upper waste panels. As indicated by the many level curves for fraction of steel in the upper waste panels, the corrosion of steel ceases for many sample elements due to brine depletion. In contrast, this behavior is less pronounced for the lower waste panel, which receives more brine inflow from the marker beds relative to its volume than do the upper waste panels. Also, the lower waste panel receives brine that initially enters the upper waste panels and then flows down dip into the lower waste panel.

The dominant variables with respect to gas production in the upper and lower waste panels are *WGRCOR*, *WASTWICK*, *HALPOR*, and *DRZPRM* (Figs. 2.1.2.8 and 2.1.2.9). These variables have negative effects on the amount of steel remaining in both the upper and lower waste panels. Increasing *WGRCOR* and *WASTWICK* increases the gas generation rate, which decreases the fraction of steel remaining. Increasing *HALPOR* and *DRZPRM* increases brine inflow, which increases gas generation and decreases the fraction of steel remaining.

These PAVT sensitivity results are similar to the CCA. The only difference is the addition of *DRZPRM* as an important PAVT variable influencing gas generation due to its effect on brine inflow to the repository.

[Corresponding Figures From CCA: 2.2.1, 2.2.4, 2.2.5, 2.2.9]

2.1.3 Undisturbed Conditions: Pressure

Pressure in the repository under undisturbed conditions influences the extent to which contaminated brine migrates from the repository into the marker beds and also the size of the spallings and direct brine releases associated with initial drilling intrusions into the repository. Thus, repository pressure is one of the most important results obtained from modeling brine and gas flow in the vicinity of the repository.

The pressure in the repository tends to initially increase rapidly and then to either approach an asymptote or show a decreased rate of increase (Fig. 2.1.3.1). The results in Fig. 2.1.3.1 are for the lower waste panel; however, due to limited resistance to gas flow in the DRZ and panel closures, pressure is almost the same throughout the repository, operations area and experimental area. As in the CCA, the PAVT was performed with three replicated LHSs of size 100, with the results for repository pressure being quite stable across replicates. (WPO #46702). Thus, the

distribution of this important variable that results from subjective uncertainty is being estimated quite well within the analysis.

The dominant contributor to the uncertainty in pressure is *WMICDFLG* (Fig. 2.1.3.2), with pressure tending to increase as *WMICDFLG* increases. As previously discussed, *WMICDFLG* controls the amount of gas generated by microbial degradation of cellulose. At early times *WGRCOR* and *WASTWICK* are also important with respect to pressure, with pressure tending to increase as each of these variables increases. Increases in *WGRCOR* and *WASTWICK* tend to increase gas pressure at early times by increasing the rate at which steel is consumed by corrosion. However, neither variable affects the total amount of corrosion that will take place, with the result that their influence on pressure tends to decrease with time. In contrast, *HALPOR* and *DRZPRM* have little effect on pressure at early times, but they increase steadily in importance with time. This effect results because corrosion occurs only under inundated conditions. Given that corrosion consumes brine, increased brine in the repository results in more corrosion and hence in higher pressures. As discussed in Section 2.1.1, *HALPOR* and *DRZPRM* strongly influence the volume of brine that enters the repository and hence of the amount of gas produced by corrosion. The variables *HALPOR* and *DRZPRM* have little or no effect on pressure at earlier times because of the availability of brine from other sources; however, at later times it is the brine inflow associated with *HALPOR* and *DRZPRM* that allows corrosion to continue. Note that *DRZPRM* initially has a negative effect during a short period where brine available from other sources is being consumed and lower DRZ permeabilities tend to cause pressures to be higher.

As in the CCA, there is a strong correlation between total gas generation and repository pressure. This is demonstrated by the similarity between the partial regression correlation coefficients (PRCCs) for gas generation (Fig. 2.1.2.5) and repository pressure (Fig. 2.1.3.2).

[Corresponding Figure From CCA: 2.3.1]

2.1.4 Undisturbed Conditions: Brine Saturation

Unlike pressure, there is considerable variation between the brine saturation conditions in the upper waste panels (at the up-dip northern end of the repository) (Fig. 2.1.4.1) and lower waste panel (at the down-dip southern end of the repository) (Fig. 2.1.4.2). At both ends of the repository, brine saturation increases rapidly in the first 50 to 1000 years due to brine flow from the DRZ and reduction in pore volume due to compaction of the waste. After this period of rapid increase, brine saturation tends to decrease as brine is consumed more rapidly by corrosion than it is replaced by inflow. Due to the computational grid in use, the lower waste panel receives more brine inflow from the marker beds relative to its size than the upper waste panels. The lower panel is also at the downdip end of the repository, with the result that it can also receive brine flowing down from the upper panels. As a result, the lower panel receives more brine on a unit volume basis than the upper panels and thus tends to have a higher brine saturation.

As examination of Figs. 2.1.4.1 and 2.1.4.2 shows, brine saturation is dropping to zero for some

sample elements, with this tending to occur less often for the lower waste panel than for the upper waste panels. Further, brine saturation is more likely to remain at zero for the upper waste panels than the lower waste panel. When brine saturation goes to zero in a given computational cell, corrosion stops but will resume if brine saturation subsequently increases.

The dominant variables with respect to the uncertainty in brine saturation in the lower waste panel are *DRZPRM, HALPOR, WGRCOR, WMICDFLG,* and *WASTWICK* (Fig. 2.1.4.3). The positive effect for *DRZPRM and HALPOR* results because increasing *DRZPRM* and *HALPOR* increases the flow of brine into the lower waste panel from the DRZ in the first 50 to 100 years of the calculation and thus contributes to the rapid rise in brine saturation during this early time period (Fig. 2.1.4.2). Some of this rapid initial increase in brine saturation is also due to the compaction of the repository at early times. The negative effect for *WMICDFLG* results because increasing *WMICDFLG* increases pressure in the repository, which in turn increases pore volume and decreases brine inflow from the marker beds. Both of the preceding effects will tend to reduce brine saturation. The negative effects for *WGRCOR* and *WASTWICK* result from increasing the rate at which brine is consumed by corrosion, which in turn tends to reduce brine saturation by both removing brine and increasing pore volume due to increased pressure.

Similar effects are also indicated for *DRZPRM, HALPOR, WGRCOR,* and *WASTWICK* in the analysis for brine saturation in the upper waste panels (Fig. 2.1.4.4). However, the patterns of importance for *DRZPRM* and *HALPOR* are changed, with *HALPOR* showing greater importance over the entire 10000 year period than for the lower waste panel and *DRZPRM* showing a significant effect at only early times. These changes occur because brine inflow from the marker beds (which is sensitive to *DRZPRM* but not to *HALPOR*) is less important in determining saturation in the upper waste panels than in the lower waste panel.

These PAVT sensitivity results are similar to the CCA. Again, the difference is the addition of *DRZPRM* as an important PAVT variable influencing brine saturation in the repository due to its effect on brine inflow to the repository. The additional importance of *DRZPRM* reduced the importance of *ANHPRM* for brine saturation in the lower panel and *WMICDFLG* for brine saturation in the upper panels.

[Corresponding Figure From CCA: 2.4.1]

2.1.5 Undisturbed Conditions: Brine Outflow

The anhydrite marker beds provide a possible pathway by which brine can flow away from the repository. As in the CCA, brine flow volumes out of DRZ to the markers beds tend to be smaller than brine flow in from the marker beds and brine flow volumes across the land withdrawal boundary (LWB) are zero or very small for most sample elements. Brine that flows across the LWB is uncontaminated brine that originated in the marker beds and never had contact with the waste in the repository.

2.2. Fluid Flow in Vicinity of Repository: Disturbed Conditions

2.2.1 Disturbed Conditions: Brine Inflow for E1 and E2 Intrusions

For undisturbed conditions, the two main pathways by which brine enters the repository are flow from the Salado Formation through the anhydrite marker beds and drainage from the DRZ. For E2 intrusions (i.e., drilling intrusions that pass through the repository but do not penetrate pressurized brine in the Castile Formation), an additional pathway is provided by brine flow down the intruding borehole from overlying formations. For E1 intrusions (i.e., drilling intrusions that pass through the repository and penetrate pressurized brine in the Castile Formation), additional pathways are provided by brine flow down the intruding borehole from overlying formations and by brine flow up the borehole from a pressurized brine reservoir in the Castile Formation.

For brine inflow from the marker beds, undisturbed (Fig. 2.1.1.1), E2 (Fig. 2.2.1.1), and E1 (Fig. 2.2.1.2) conditions all produce similar results. However, the inflows for E1 and E2 intrusions tend to be somewhat larger than the inflows for undisturbed conditions. This difference results because E1 and E2 intrusions result in lower repository pressures, which in turn result in reduced resistance to brine flow toward the repository and hence greater brine flow out of the marker beds. The dominant variables affecting brine flow from the marker beds are *ANHPRM*, *DRZPRM*, and *WMICDFLG* (Figs. 2.2.1.3 and 2.2.1.4). The positive effects for *ANHPRM* and *DRZPRM* result from reducing resistance to flow in the anhydrite and DRZ, respectively. The negative effect for *WMICDFLG* results from increasing pressure in the repository before the drilling intrusion at 1000 years and thus increasing resistance to flow out of the marker beds. A positive effect is also indicated for *BHPRM* after the E2 intrusion, with this effect resulting from reduced pressure in the repository and hence reduced resistance to flow out of the marker beds.

Unlike brine flow from the marker beds, there is often considerable difference in cumulative brine flow into the repository for undisturbed (Fig. 2.1.1.2), E2 (Fig. 2.2.1.5), and E1 (Fig. 2.2.1.6) conditions. Prior to 1000 years, the sensitivity analysis results for cumulative brine flow into the repository for undisturbed, E2 and E1 conditions are the same (Figs. 2.1.1.4, 2.2.1.7, and 2.2.1.8, respectively), with *DRZPRM* being a slightly more dominant variable than *HALPOR*. Under E2 conditions (Fig. 2.2.1.7), *HALPOR* becomes the more dominant variable after 1000 years and *BHPRM* increases in importance to such an extent that it exceeds *DRZPRM* in importance by 10,000 years. Under E1 conditions (Fig. 2.2.1.8), *DRZPRM* remains the dominant variable after 1000 years but *HALPOR* is quickly exceeded by *BHPRM* in importance. The reduction in importance of *HALPOR* is because flow up the borehole from the brine reservoir, rather than flow from the marker beds, dominates brine flow into the repository. The importance of *BHPRM* increases over time due to its role in controlling brine flow in the borehole. This flow takes place both down the borehole from overlying formations and, for the E1 intrusion, up the borehole from the brine reservoir. For flow down the borehole into the repository under both E2 and E1 intrusions (Figs. 2.2.1.9 and 2.2.1.10), *BHPRM* is the dominant variable (Figs. 2.2.1.11 and 2.2.1.12), with this effect resulting because increasing *BHPRM* reduces resistance to flow in the borehole.

The variable *WMICDFLG* shows a negative effect on total brine inflow to the repository after 1200 years for the E1 intrusion (Fig. 2.2.1.8) that is not present for the E2 intrusion. This behavior results because large flows of brine can take place from the brine reservoir to the repository for an E1 intrusion from 1000 to 1200 years, during which period an open borehole is assumed to connect the brine reservoir and the repository (Fig. 2.2.1.13). However, this flow will not take place when the repository pressure is too high. Thus, the negative effect for *WMICDFLG* again results from its dominant role in determining the uncertainty in repository pressure. This effect results in the negative PRCC for *WMICDFLG* for cumulative brine flow from the brine reservoir (Fig. 2.2.1.14) and thus in the negative PRCC for cumulative brine flow into the repository (Fig. 2.2.1.12). In addition to the negative effect of *WMICDFLG*, the variables *BHPRM*, *BPINTPRS*, and *DRZPRM* have positive effects on cumulative brine flow from the brine reservoir to the repository. Specifically, increasing *BPINTPRS* increases the amount of brine that leaves the brine reservoir because of an increased driving force for flow between the brine reservoir and repository and increasing *BHPRM* both reduces the pressure in the repository and reduces resistance to flow between the brine reservoir and the repository. Increasing *DRZPRM* increases the amount of brine that can flow from the brine reservoir into the DRZ thereby increasing the amount of brine that can flow out the brine reservoir.

The important variables contributing to brine inflow under disturbed conditions, described above, are similar to the CCA. One difference is that *DRZPRM*, sampled for the PAVT but constant in the CCA, is an important PAVT variable. *HALPRM*, *ANHPRM*, and *SALPRES* are less important in the PAVT due to the increased importance of *DRZPRM*. Another difference is that for brine flow up the borehole from the brine reservoir, *BPINTPRS* replaced *BPCOMP* as an important variable. This difference was caused by the increase in sampled brine reservoir volume.

[Corresponding Figures From CCA: 3.1.1, 3.1.5, 3.1.6, 3.1.7]

2.2.2 Disturbed Conditions: Gas Generation for E1 and E2 Intrusions

As most of the cellulose is consumed by microbial action by 1000 years for undisturbed conditions (WPO #46674), there is not a significant difference between gas generation due to microbial degradation under disturbed and undisturbed conditions. However, disturbed conditions result in greater gas generation from corrosion (Figs. 2.2.2.1 and 2.2.2.2) due to the increased amount of brine entering the repository.

Gas generation due to corrosion for E2 and E1 intrusions is dominated by *WGRCOR*, *HALPOR*, *DRZPRM*, *WASTWICK*, and *BHPRM*, with gas generation tending to increase as each of these variables increases (Figs. 2.2.2.3 and 2.2.2.4). The positive effect for *WGRCOR* results from increasing the rate at which steel is consumed by corrosion, and the positive effects for *HALPOR*, *DRZPRM*, *WASTWICK*, and *BHPRM* result from increasing the amount of brine available for the corrosion process. The negative effect indicated for *WMICDFLG* (Fig.2.2.2.4) results because increasing *WMICDFLG* increases microbial gas generation and thus pressure in the repository, which in turn decreases flow into the repository and corrosion. *HALPOR* and *DRZPRM*, which

control brine inflow to the repository, gradually exceed *WGRCOR* in importance because at later times gas generation due to corrosion is limited by the availability of brine. Note that for the E2 intrusion (Fig. 2.2.2.3), *HALPOR* gradually becomes the dominant variable because brine inflow from the marker beds is the main source of brine. Similar results were obtained in the PRCC analysis for gas generation under undisturbed conditions except that *BHPRM* was not a relevant variable (Fig. 2.1.2.4).

Due to the effects of corrosion, total gas generation for E2 (Fig. 2.2.2.5) and E1 (Fig. 2.2.2.6) intrusions is also elevated relative to that observed for undisturbed conditions (Fig. 2.1.2.3). Now, *WMICDFLG* appears as an important variable (Figs. 2.2.2.7 and 2.2.2.8) in addition to *WGRCOR*, *WASTWICK*, and *HALPOR*, which were also identified when only gas generation due to corrosion was considered (Figs. 2.2.2.3 and 2.2.2.4). *WMICDFLG* controls the amount of gas generated by the microbial degradation of cellulose.

The effects of the drilling intrusion are more apparent when gas generation in the intruded lower panel is compared with gas generation in the rest of the repository (upper panels). Specifically, the intruded panel often has its entire steel inventory consumed by corrosion (Figs. 2.2.2.9 and 2.2.10 for E2 and E1, respectively), which does not occur for the remainder of the repository in intrusion scenarios (Figs. 2.2.2.11 and 2.2.2.12 for E2 and E1, respectively).

The same variables that are identified as affecting the amount of gas generated by corrosion (*WGRCOR*, *HALPOR*, *DRZPRM*, *WASTWICK*, and *BHPRM* in Figs. 2.2.2.3 and 2.2.2.4) are also identified as affecting the amount of steel remaining in the upper and lower waste panels (Figs. 2.2.2.13 through 2.2.2.16). Because the fraction of steel remaining rather than the fraction of steel consumed by corrosion appears in Figs. 2.2.2.13 through 2.2.2.16, the signs on the PRCCs in these figures are reversed from the signs in Figs. 2.2.2.3 and 2.2.2.4.

These PAVT sensitivity results are similar to the CCA. The only difference is the addition of *DRZPRM* as an important PAVT variable influencing gas generation due to its effect on brine inflow to the repository.

[Corresponding Figures From CCA: 3.2.1, 3.2.5, 3.2.7, 3.2.8]

2.2.3 Disturbed Conditions: Pressure for E1 and E2 Intrusions

Pressure in the repository under undisturbed conditions tends to increase monotonically towards an asymptote for each sample element (Fig. 2.1.3.1), with the value of this asymptote determined primarily by the amount of gas generated by corrosion and microbial degradation. A very different pattern is exhibited under disturbed conditions, with pressure tending to decrease rapidly after a drilling intrusion (Figs. 2.2.3.1 and 2.2.3.2). The results in Figs. 2.2.3.1 and 2.2.3.2 are for pressure in the lower waste panel; the pressure histories for the upper waste panels are very similar.

The PRCCs in Figs. 2.2.3.3 (E2) and 2.2.3.4 (E1) prior to 1000 years are the same as those in Fig. 2.1.3.2 for undisturbed conditions. At 1000 years, pressure in the repository is dominated by *WMICDFLG* and other variables (i.e., *WGRCOR*, *WASTWICK*, and *WGRMICI*) that influence gas generation under undisturbed conditions. Immediately after 1200 years, *BHPRM* shows a negative effect on pressure because gas flow up the borehole increases with increasing values for *BHPRM* (Figs. 2.2.3.3 and 2.2.3.4). For an E1 intrusion, *BPINTPRS* has a positive effect on repository pressure after intrusion whereas at later times the effects of *WMICDFLG*, *WGRCOR*, and *WASTWICK* are negative. However, the PRCCs in Figs. 2.2.3.3 and 2.2.3.4 do not identify any dominant variables after 1200 years.

The poor performance of the sensitivity measures after 1200 years is due to patterns that cannot be identified by the regression-based procedures in use. In particular, repository pressure is dominated by *BHPRM* after 1200 years. Pressure tends to decrease as *BHPRM* increases until a value of approximately 1×10^{-13} m^2 to 3×10^{-13} m^2 (Figs. 2.2.3.5 and 2.2.3.6) is reached; at this point, pressure jumps to approximately 6×10^6 Pa, which is hydrostatic pressure at repository depth. The patterns in Figs. 2.2.3.5 and 2.2.3.6 result from an interplay of gas and brine flow in the borehole. At low permeabilities, little gas can flow out the borehole and so pressures remain high. As *BHPRM* increases, more gas can flow out the borehole and so pressure decreases. In particular, pressure stays relatively low (i.e., ~ 1.5 to 4.0×10^6 Pa) at intermediate values for *BHPRM* because a continuous brine column is not established between the repository and overlying formations. As *BHPRM* increases, more brine flows down the borehole and the repository fills with brine at higher values of *BHPRM*. When this occurs, a continuous brine column is established between the repository and overlying formation, with the result that repository pressure then jumps to hydrostatic.

These PAVT sensitivity results are similar to the CCA. The primary difference is that *BPINTPRS* had increased importance for E1 intrusions as a result of the increase in sampled brine reservoir volume and the change in the borehole permeability distribution (WPO #46674).

[Corresponding Figures From CCA: 3.3.1, 3.3.5]

2.2.4 Disturbed Conditions: Brine Saturation for E1 and E2 Intrusions

The occurrence of a drilling intrusion can have a significant effect on the brine saturation in both the upper and lower waste panels (Figs. 2.2.4.1 and 2.2.4.2 for E2, Figs. 2.2.4.3 and 2.2.4.4 for E1). In particular, the tendency is to increase the saturation due to (1) increased flow from the marker beds, (2) flow down the borehole from overlying formations, and (3) flow up from the brine reservoir in the event of an E1 intrusion. Although saturation tends to increase throughout the repository, the effect is particularly pronounced in the intruded panel (Figs. 2.2.4.2 and 2.2.4.4), which is the lower waste panel in the calculations reported in this section. As indicated by the horizontal brine saturation curves in Figs. 2.2.4.2 and 2.2.4.4, the intruded panel often becomes fully brine saturated subject to the limitations imposed by the residual gas saturation (*WRGSSAT*). Due to the brine flow from the brine reservoir, the intruded panel is more likely to

become fully brine saturated for an E1 intrusion than for an E2 intrusion.

As indicated by the PRCCs in Fig. 2.2.4.5, the uncertainty in the brine saturation in the unintruded (i.e., upper) waste panels after an E2 intrusion is determined by *HALPOR*, *DRZPRM*, *BHPRM*, *WGRCOR* and *WASTWICK*, with brine saturation tending to increase as *HALPOR*, *DRZPRM* and *BHPRM* increase and tending to decrease as *WGRCOR* and *WASTWICK* increase. The positive effects for *HALPOR*, *DRZPRM* and *BHPRM* result because increasing each of these variables allows more brine to enter the waste panels. The negative effects for *WGRCOR* and *WASTWICK* result because increasing each of these variables increases the rate at which brine is consumed by corrosion, which in turn has two effects on saturation. First, the direct loss of brine reduces saturation. Second, the generation of gas by corrosion increases repository pressure, which in turn tends to increase repository porosity due to pore space expansion and thus reduce brine saturation. Together, these two effects result in a reduced amount of brine occupying an increased pore volume.

For brine saturation in the intruded (i.e., lower) waste panel after an E2 intrusion, the PRCCs in Fig. 2.2.4.6 indicate positive effects for *HALPOR*, *DRZPRM*, and *BHPRM*, and negative effects for *WGRCOR* and *WASTWICK*. These results are similar to the sensitivities for the upper waste panels.

Brine saturation in both the upper and lower waste panels for an E1 intrusion (Figs. 2.2.4.3 and 2.2.4.4) are similar to brine saturation in the E2 intrusion (Figs. 2.2.4.1 and 2.2.4.2). Overall, the brine saturations tend to be somewhat higher for the E1 intrusion due to the additional brine inflow from the brine reservoir. The uncertainty in the brine saturation in the unintruded (i.e., upper) waste panels after an E1 intrusion (Fig. 2.2.4.7) is determined by *HALPOR*, *DRZPRM*, *WGRCOR*, *WASTWICK*, and *WMICDFLG*, with saturation tending to increase as *HALPOR*, and *DRZPRM* increase and tending to decrease as *WGRCOR*, *WASTWICK*, and *WMICDFLG* increase. As in the E2 intrusion, the positive effects for *HALPOR*, and *DRZPRM* result because increasing each of these variables allows more brine to enter the waste panels. The negative effects for *WGRCOR* and *WASTWICK* result because increasing each of these variables increases the rate at which brine is consumed by corrosion, which in turn has two effects on saturation as described above. The negative effect indicated for *WMICDFLG* results because increasing *WMICDFLG* increases microbial gas generation and thus pressure in the repository, which in turn decreases brine flow into the repository.

For brine saturation in the intruded (i.e., lower) waste panel after an E1 intrusion, the PRCCs in Fig. 2.2.4.8 indicate effects (positive) only for *BHPRM* and *DRZPRM*.

These PAVT sensitivity results are similar to the CCA. Again, the difference is the addition of *DRZPRM* as an important PAVT variable influencing brine saturation in the repository due to its effect on brine inflow to the repository.

[Corresponding Figures From CCA: 3.4.1, 3.4.2]

2.2.5 Disturbed Conditions: Brine and Gas Flow in Borehole for E1 and E2 Intrusions

The characteristics of brine and gas flow in the intruding borehole for disturbed conditions is described in detail in the CCA report (WPO#42912) and will not be repeated here. Discussion of relevant differences in borehole flow between the CCA and PAVT are noted in Section 2.2.1.

2.2.6 Disturbed Conditions: Brine and Gas Flow into Marker Beds for E1 and E2 Intrusions

As in the CCA, very little gas and brine flow takes place into the marker beds subsequent to a drilling intrusion due to the reduced pressures in the repository.

2.2.7 Disturbed Conditions: Behavior of Brine Reservoir for E1 Intrusions

Brine flow from a region of pressurized brine (i.e., a brine reservoir) is an important potential source of brine to the repository for E1 intrusions. The pressure behavior of the brine reservoir is dynamic subsequent to a drilling intrusion (Fig. 2.2.7.1). For 200 years after the intrusion, an open borehole (i.e., permeability of 10^{-9} m^2) is assumed to exist between the brine reservoir and the repository and an impermeable seal is assumed to exist at the Rustler/Salado interface. This results in rapid changes of pressure in both the brine reservoir (Fig. 2.2.7.1) and the repository (Fig. 2.2.3.2). During this period, the pressure in the repository typically increases (Fig. 2.2.3.2) and the pressure in the brine reservoir decreases (Figs. 2.2.7.1). These changes in pressure tend to be accompanied by a surge of brine up the borehole from the brine reservoir to the repository (Fig. 2.2.1.13). In the CCA, these surges resulted in a corresponding decrease in the volume of brine contained in the brine reservoir. However, in the PAVT the brine reservoir is very large and the decrease in brine volume is small compared to the volume of the brine reservoir (Fig. 2.2.7.2). Typically, most of the brine flow out of the brine reservoir takes place during these initial surges (Figs. 2.2.1.13, 2.2.7.1).

After 200 years, the seal at the Rustler/Salado interface is assumed to fail and the entire borehole is assigned a permeability of *BHPRM*. At this point, gas can escape from the repository to overlying formations, which causes a rapid drop in repository pressure in some elements (Fig. 2.2.3.2). From this point on, there is no longer an open borehole between the repository and the brine reservoir. Rather, this portion of the borehole is assumed to have a permeability of *BHPRM* for the next 1000 years. This change in permeability produces a complex pattern of pressure behavior in the brine reservoir, with pressure continuing to decrease in sample elements that have continued brine flow out of the brine reservoir and pressure remaining constant in sample elements that experience no additional brine outflow from the brine reservoir after intrusion.

After 1000 years (i.e., 1200 years after the drilling intrusion), the permeability in the borehole between the repository and the brine reservoir is reduced from *BHPRM* to *BHPRM*/10, which tends to reduce brine flow from the brine reservoir to the repository. This effect can be seen in

the decreased slope of some of the brine flow curves at 2200 years (Fig. 2.2.1.13).

Before the intrusion at 1000 years, brine pressure is completely dominated by *BPINTPRS*, which has a PRCC of 1 (Fig. 2.2.7.3). Immediately after the intrusion, a positive effect is indicated for *WMICDFLG*, but *BPINTPRS* is still the dominant variable. *WMICDFLG* tends to increase repository pressure at 1000 years and thus reduce brine flow from, and pressure change in, the brine reservoir.

These PAVT sensitivity results are similar to the CCA. The only difference is that *BPINTPRS* had increased importance because of the increase in sampled brine reservoir volume.

[Corresponding Figure From CCA: 3.7.1]

3.0 DIRECT RELEASE TO THE ACCESSIBLE ENVIRONMENT: CUTTINGS, CAVINGS, AND SPALLINGS

In this section, PAVT uncertainty and sensitivity analysis results are presented for cuttings, cavings, and spallings. The presentation of results follows the presentation given in Section 4 of the preliminary CCA sensitivity and analysis report (WPO #42912). At the end of each subsection, figure and table numbers in the CCA report that correspond to figures and tables presented in this PAVT report are listed.

3.1 Cuttings and Cavings: Uncertainty and Sensitivity Analysis

Drilling intrusions through the waste panels can penetrate CH- or RH-TRU waste. Specifically, the probabilities that a single intrusion through a waste panel will encounter CH- or RH-TRU waste are 0.880 and 0.120, respectively. As the penetration of CH-TRU waste is more likely than the penetration of RH-TRU waste and the average concentrations of CH-TRU waste are similar to those for RH-TRU waste, the cuttings and cavings release (hereafter referred to simply as the cuttings release) is dominated by CH-TRU waste.

As in the CCA, the volume of material removed by a drilling intrusion through RH-TRU waste is fixed at 0.039 m^3 (i.e., drill bit diameter fixed at 0.3115 m, intersection area of 0.076 m^2, effective height of RH-TRU waste assumed to be 0.509 m). Uncertainty in inputs used in the PAVT is due to the volume of material removed by cuttings and cavings due to a drilling intrusion through CH-TRU waste ranging from approximately 0.3 m^2 to 4 m^3 (Fig. 3.1.1). In the CCA, the cuttings volume from CH-TRU ranged from 0.4 m^2 to 3 m^3. The uncertainty in the volume of CH-TRU waste removed as cuttings is determined by the variable *WTAUFAIL* (Fig. 3.1.2). In the PAVT, *WTAUFAIL* was represented by a loguniform distribution ranging from 0.05 to 77 Pa, whereas in the CCA *WTAUFAIL* was represented by a uniform distribution ranging from 0.05 to 10 Pa (WPO #46674). The slight scatter in Fig. 3.1.2 is due to an uncertain *DOMEGA*. In the PAVT, this variable was represented by a cumulative distribution ranging from 4.2 to 23.0 with a mean value of 7.77 rad/s. In the CCA, this variable had a constant value of 7.8 rad/s. The CH-TRU waste volumes in Fig. 3.1.1 and the fixed RH-TRU waste volume noted above are the original (i.e., uncompacted) volumes of the removed waste. The use of uncompacted volumes simplifies the calculation of the radionuclide concentrations used in the determination of cuttings releases and permits a combining of removal volumes for intrusions at different times.

For each LHS element, 10,000 futures are randomly selected and the corresponding cuttings releases calculated. Resultant CCDFs for cuttings releases to the accessible environment are then constructed. The same 10,000 futures are used for all CCDF constructions for a given LHS element, which ultimately permits the combining of all release modes (i.e., cuttings, spallings, direct brine release, groundwater transport) into a single CCDF (see Section 6). As for cuttings volumes, the uncertainty in cuttings CCDFs is dominated by the sampled variable *WTAUFAIL*.

[Corresponding Figures From CCA: 4.1.2, 4.1.3]

3.2 Spallings: Uncertainty and Sensitivity Analysis

Drilling intrusions can also produce spallings releases, which are releases of solid material due to rapid gas movement toward a borehole at the time of intrusion. The spallings model predicts a released volume of solid material which, for comparability with cuttings results, is reported as volume of original, uncompacted material emplaced in the repository. For a given drilling intrusion, this volume is multiplied by the average concentration of waste in the waste panels at the time of intrusion to produce a spallings normalized release in EPA units. The primary determinant of the uncertainty in the spallings release is the pressure condition in the repository, with no spallings releases taking place at pressures less than 8 MPa. Given that the pressure is above 8 MPa, the uncertainty in the spallings release is determined by *VOLSPALL*.

A sensitivity analysis can be performed on the mean spallings releases associated with each spallings CCDF (Table 3.2.1). The stepwise regression analysis procedures are described in WPO#42912. The regressions for volume and normalized release are almost identical. The most important variable is *BHPRM*, which has a negative effect. Increasing *BHPRM* tends to reduce the pressure in the repository below the 8 MPa threshold required for a spallings release. Therefore, expected spallings releases tend to increase with decreasing values of *BHPRM*. The high importance of *BHPRM* is consistent with its high importance to repository pressure under disturbed conditions (Section 2.2.3). The second most important variable is *VOLSPALL*, the spallings volume released if the repository pressure is above 8 MPa. The next most important variable is *WMICDFLG*, with expected releases tending to increase with increasing values of *WMICDFLG* due to the important influence of this variable on the pressure in the repository. Positive effects are also indicated for *DRZPRM, HALPOR,* and *PBRINE*. Increasing *DRZPRM* and *HALPOR* increases brine inflow to the repository which tends to increase gas generation and pressure in the repository. Increasing *PBRINE* increases the probability of an intrusion borehole encountering a pressurized brine reservoir, which also tends to increase repository pressure.

These PAVT sensitivity results for spallings releases differ somewhat from the CCA. The most sensitive PAVT parameters are *BHPRM* and *VOLSPALL*. The increased importance in *BHPRM* results from its increased importance in controlling repository pressure. The importance of *VOLSPALL* results from the new PAVT approach for calculating spallings releases. The importance of *WMICDFLG* is lower in the PAVT than in the CCA due to the increased importance of *BHPRM* and *VOLSPALL*. Other parameters with increased importance in the PAVT are *DRZPRM,* and *PBRINE*.

Table 3.2.1. Stepwise Regression Analysis with Rank-Transformed Data for Expected Volume and Expected Normalized Release Associated with Individual CCDFs for Spallings

	Expected Volume			Expected Normalized Release		
Step [a]	Variable [b]	SRRC [c]	R^2 [d]	Variable	SRRC	R^2
1	BHPRM	-0.64	0.42	BHPRM	-0.60	0.38
2	VOLSPALL	0.41	0.58	VOLSPALL	0.42	0.54
3	WMICDFLG	0.33	0.68	WMICDFLG	0.37	0.68
4	DRZPRM	0.16	0.71	DRZPRM	0.17	0.71
5	PBRINE	0.13	0.73	HALPOR	0.14	0.73
6	HALPOR	0.13	0.74	PBRINE	0.13	0.74

[a] Steps in stepwise regression analysis.
[b] Variables listed in order of selection of regression analysis.
[c] Standardized regression coefficients in final regression model with *ANHCOMP* and *HALCOMP* excluded from entry into regression model.
[d] Cumulative R^2 value with entry of each variable into regression model.

[Corresponding Table From CCA: 4.4.3]

4.0 DIRECT RELEASE TO THE ACCESSIBLE ENVIRONMENT: DIRECT BRINE RELEASE

In this section, PAVT uncertainty and sensitivity analysis results are presented for direct brine release (DBR). The presentation of results follows the presentation given in Section 5 of the preliminary CCA sensitivity and analysis report (WPO #42912). At the end of each subsection, table numbers in the CCA report that correspond to tables presented in this PAVT report are listed.

4.1 Direct Brine Release: Uncertainty and Sensitivity Analysis

Drilling intrusions through CH-TRU waste can produce direct brine releases, which are releases of brine and hence dissolved radionuclides, due to rapid fluid movement toward a borehole at the time of intrusion. Due to the low permeability of the region surrounding each RH-TRU waste canister, intrusions into RH-TRU waste are assumed not to produce direct brine releases.

The direct brine release model predicts a volume release of brine (m^3). For a given drilling intrusion, the volume of released brine is multiplied by the concentration (EPA units/m^3) of dissolved radionuclides in CH-TRU waste at the time of the intrusion to produce the direct brine release in EPA units. Prior to an E1 intrusion, solubilities associated with brines derived from the Salado Formation are used; after an E1 intrusion, solubilities associated with brines derived from the Castile Formation are used. The primary determinants of the uncertainty in direct brine releases are the pressure and brine saturation conditions in the repository, with no releases taking place for low saturations (less than about 0.25) and low pressures (less than about 8 MPa).

As was done for spallings releases, a sensitivity analysis can be performed on the mean direct brine releases associated with each DBR CCDF (Table 4.1.1). The regressions for volume and normalized release are almost identical. The dominant variables are *DRZPRM* and *BPINTPRS*, with the size of release tending to increase as these variables increase. The positive effect for *DRZPRM* results from increasing the volume of brine and, hence, pressure in the repository, while the positive effect for *BPINTPRS* results from increasing both the brine volume and the pressure in the repository. Smaller positive effects are also indicated for *PBRINE* and *HALPOR*. The negative effect indicated for *WMICDFLG* results because increasing *WMICDFLG* increases microbial gas generation and thus pressure in the repository, which in turn decreases brine flow into the repository. Note that the final regression models have R^2 values of only 0.50 and 0.49. Thus, these models are not very effective in accounting for the uncertainty in the analysis outcomes. This lack of resolution is due to the large number of sample elements that have no direct brine release.

These PAVT sensitivity results for direct brine release differ somewhat from the CCA. The most important PAVT parameters are *DRZPRM* and *BPINTPRS*. In the CCA, the most important parameters were *WRBRNSAT* and *HALPOR*. Other parameters with increased importance in the PAVT are *WMICDFLG*, *BHPRM*, and *PBRINE*.

Table 4.1.1. Stepwise Regression Analysis with Rank-Transformed Data for Expected Volume and Expected Normalized Release Associated with Individual CCDFs for Direct Brine Release

	Expected Volume			Expected Normalized Release		
Step[a]	Variable[b]	SRRC[c]	R^2[d]	Variable	SRRC	R^2
1	DRZPRM	0.47	0.23	DRZPRM	0.50	0.26
2	BPINTPRS	0.32	0.33	BPINTPRS	0.30	0.35
3	WMICDFLG	-0.22	0.37	PBRINE	0.20	0.39
4	BHPRM	-0.20	0.42	WBRNSAT	-0.16	0.42
5	PBRINE	0.18	0.45	WMICDFLG	-0.16	0.44
6	WBRNSAT	-0.18	0.48	HALPOR	0.14	0.47
7	HALPOR	0.15	0.50	BHPRM	-0.15	0.49

a Steps in stepwise regression analysis.

b Variables listed in order of selection of regression analysis.

c Standardized regression coefficients in final regression model with *ANHCOMP* and *HALCOMP* excluded from entry into regression model.

d Cumulative R^2 value with entry of each variable into regression model.

[Corresponding Table From CCA: 5.5.3]

5.0 RELEASE FROM THE CULEBRA TO THE ACCESSIBLE ENVIRONMENT

In this section, PAVT uncertainty and sensitivity analysis results are presented for release to the Culebra. The presentation of results is similar to the presentation given in Section 6 of the preliminary CCA sensitivity and analysis report (WPO #42912). At the end of each subsection, figure and table numbers in the CCA report that correspond to figures and tables presented in this PAVT report are listed. Note that CCA figures include multiple plots.

5.1 Release to the Culebra: Uncertainty and Sensitivity Analysis

Radionuclide releases to the Culebra did not occur under undisturbed conditions. Thus, it is only for disturbed conditions (i.e., subsequent to a drilling intrusion) that the potential for a radionuclide release to the Culebra exists.

Radionuclide release from the repository to the Culebra depends on both the amount of brine flow and the amount of radionuclide that can be transported in this flow. Radionuclides are assumed to exist in five states that can be transported from the repository by flowing groundwater: dissolved, humic colloids, microbial colloids, mineral fragment colloids, and actinide intrinsic colloids. Radionuclide releases to the Culebra only occur for sample elements for which BRAGFLO predicts nonzero brine flows from the repository to the Culebra. For most sample elements, brine flow from the repository is zero or very small (WPO #46674 and WPO #46702) and so little or no radionuclide transport takes place (Figs. 5.1.1 through 5.1.6). For E1 (Figs. 5.1.1 and 5.1.2) and E2E1 (Figs. 5.1.5 and 5.1.6) intrusions, most of the release takes place over a relatively short period of time and then continues at a reduced rate or stops entirely. This behavior results from (1) an initial 200 year period during which an open borehole exists between the repository and the brine reservoir, (2) a subsequent 1000 year period in which the borehole over its entire length has permeability *BHPRM*, and (3) a reduction of the permeability below the repository to *BHPRM*/10 after 1200 years.

Results are presented in Figs. 5.1.1 through 5.1.6 for only two of the intrusion times used in the NUTS and PANEL calculations. A summary of the cumulative releases over 10000 years for all intrusion times is given in Figs. 5.1.7 (E1), 5.1.8 (E2), and 5.1.9 (E2E1). As should be the case, the size of the release decreases with increasing intrusion time due to increased time for radioactive decay and decreased time for transport from the repository to the Culebra. However, at all times, most sample elements result in no significant releases to the Culebra.

The total normalized releases in Figs. 5.1.1 through 5.1.9 are based on Am-241, Pu-238, Pu-239, U-234 and Th-230. At early times (i.e., 100 and 350 years), the release tends to be dominated by Am-241, with an additional contribution from Pu-238 at very early times. With increasing time, Am-241 is lost due to decay and the release is dominated by Pu-239 due to its long half life and large inventory.

Due to the large number of zero releases, a stepwise regression analysis is not a very revealing

sensitivity analysis procedure for E1 and E2 intrusions. However, the greater number of nonzero releases associated with E2E1 intrusions makes stepwise regression analysis a possibility for this intrusion mode (Table 5.1.1). In constructing the regression models in Table 5.1.1, the candidate independent variables included the original sampled variables and also the solubilities for individual elements. As a reminder, elemental solubilities change as a function of brine type (i.e., Salado or Castile) and several sampled variables (WPO #46674). By including the actual solubilities used in the PANEL calculations for E2E1 intrusions rather than only the sampled variables, the effects of the actual solubility used in the calculation will be shown. In interpreting the analysis results, two properties of the analysis should be kept in mind. First, calculations for E2E1 intrusions use the solubilities for Castile brine. Second, solubilities are only realized if there is a sufficient quantity of the element in the waste panel; otherwise, the amount of material that can go into solution is limited by the amount present. Such inventory limits occur for both Am-241 and Pu-238.

The regressions in Table 5.1.1 for the individual radionuclides and also for the total release in EPA units are very similar. The releases are dominated by *BHPRM*, with the size of the release tending to increase as this variable increases. This positive effect results because increasing *BHPRM* tends to increase the rate at which the intruded waste panel fills with brine due to flow up the borehole from the brine reservoir and flow down the borehole from overlying formations. Also, increasing *BHPRM* tends to increase flow from the waste panel to the Culebra. Other important variables having positive effects are *BPINTPRS*, *WOXYSTAT*, and the factor used to scale the total solubility for the radionuclide under consideration (i.e., *WSOLAM3C*, *WSOLPU4C* or *WSOLU6C*). Increasing *BPINTPRS* tends to increase the rate at which the intruded waste panel fills with brine due to flow up the borehole from the brine reservoir. *WOXYSTAT* is the oxidation-state parameter that is sampled uniformly from 0 to 1. If *WOXYSTAT* is greater than 0.5, higher oxidation-state solubilities are used and releases to the Culebra are increased. The effects of *WOXYSTAT* and the total solubility scale factors are much less than that of *BHPRM*, which is due in part to the significant number of observations that have no brine flow and hence no radionuclide release to the Culebra.

In addition, negative effects are indicated for *DRZPRM*, *WGRCOR* , and *WMICDFLG*. Increasing *WGRCOR* and *WMICDFLG* decreases the rate at which the waste panel fills with brine. For *WGRCOR*, this effect results from an increased loss of brine due to corrosion; it is also possible that the resultant increased gas flow up the borehole may retard the filling of the waste panel due to brine flow down the borehole. For *WMICDFLG*, the negative effect results primarily from reduced brine flow during the initial 200 year period that an open borehole is assumed to exist between the brine reservoir and the waste panel. For *DRZPRM*, negative effects result from an increased flow of brine from the repository and into the surrounding DRZ as opposed to going up the borehole to the Culebra.

These PAVT sensitivity results are similar to the CCA. The main difference is that *BPINTPRS* has increased importance and *BPCOMP* has decreased importance because of the increase in the sampled brine reservoir volume.

Table 5.1.1. Stepwise Regression Analysis with Rank-Transformed Data for Cumulative Radionuclide Releases over 10000 years from the Repository to the Culebra Dolomite for an E2E1 Intrusion, with an E1 Intrusion Occurring at 1000 years.

	Am-241			Pu-238		
Step[a]	Variable[b]	SRRC[c]	R^{2}[d]	Variable	SRRC	R^2
1	BHPRM	0.91	0.84	BHPRM	0.90	0.82
2	BPINTPRS	0.12	0.86	WOXYSTAT	0.13	0.85
3	WSOLAM3C	0.11	0.87	BPINTPRS	0.10	0.86
4	DRZPRM	-0.09	0.88	WSOLPU4C	0.09	0.86
5	WMICDFLG	-0.08	0.88	DRZPRM	-0.08	0.87
6	WGRCOR	-0.07	0.89	HALPRM	-0.06	0.87

	Pu-239			U-234		
Step	Variable	SRRC	R^2	Variable	SRRC	R^2
1	BHPRM	0.89	0.83	BHPRM	0.87	0.79
2	WOXYSTAT	0.12	0.84	WOXYSTAT	0.19	0.83
3	BPINTPRS	0.12	0.85	BPINTPRS	0.13	0.85
4	WSOLPU4C	0.08	0.86	WMICDFLG	-0.09	0.85
5	WMICDFLG	-0.08	0.87	WGRCOR	-0.08	0.86
6	WGRCOR	-0.07	0.87	DRZPRM	-0.07	0.87
7	DRZPRM	-0.07	0.88	WSOLU6C	0.07	0.87

	Th-230			Total		
Step	Variable	SRRC	R^2	Variable	SRRC	R^2
1	BHPRM	0.91	0.84	BHPRM	0.91	0.84
2	BPINTPRS	0.13	0.86	BPINTPRS	0.12	0.86
3	DRZPERM	-0.09	0.86	WSOLAM3C	0.10	0.87
4	WMICDFLG	-0.08	0.87	DRZPRM	-0.09	0.88
5	WGRCOR	-0.07	0.88	WMICDFLG	-0.08	0.88
6	HALPRM	-0.06	0.88	WGRCOR	-0.07	0.89

[a] Steps in stepwise regression analysis.

[b] Variables listed in order of selection of regression analysis.

[c] Standardized regression coefficients in final regression model with *ANHCOMP* and *HALCOMP* excluded from entry into regression model.

[d] Cumulative R^2 value with entry of each variable into regression model.

[Corresponding Figures From CCA: 6.1.2, 6.1.3]
[Corresponding Table From CCA: 6.1.2]

5.2 Release to the Culebra: CCDFs

For each LHS element, a CCDF for groundwater releases to the accessible environment due to transport through the Culebra is constructed using a three-step process: (1) time-dependent release rates to the Culebra are calculated for each isotope and each randomly sampled future; (2) these release rates are then used in conjunction with SECOTP2D Culebra transport results to estimate a normalized release to the accessible environment for each randomly sampled future; (3) these estimated normalized releases are used to construct a CCDF for normalized release from the Culebra to the accessible environment. This process, which uses 10,000 randomly-sampled futures for each LHS element, results in 100 CCDFs for each of the three PAVT replicates.

While WIPP compliance with respect to the EPA limits specified in 40 CFR 191.13(a) is based on CCDFs of normalized releases to the accessible environment (Section 6), it is helpful as an interim performance measure to also examine CCDFs for normalized releases to the Culebra. The difference between releases to the Culebra (from the repository) and releases from the Culebra (to the accessible environment at the LWB) represents the attenuation of radionuclides due to transport through the Culebra.

Overall CCDF mean and quantile values are shown in Fig. 5.2.1 for all three PAVT replicates pooled together. Individual CCDFs for each of the three replicates are shown in Figs 5.2.2 through 5.2.4. As a reminder, a release up the borehole to the Culebra is not a release to the accessible environment. If the EPA limit boundary line specified in 40 CFR 191.13(a) was shown in these figures, the reader would observe that most sample elements produce releases into the Culebra that would require no attenuation to be in compliance. With eight exceptions, all the replicate R1 CCDFs (Fig. 5.2.2) would fall beneath the EPA limit boundary line for release to the accessible environment. A similar pattern is also shown by the other two replicates, with eight CCDFs requiring attenuation for replicate R2 (Fig. 5.2.3) and seven CCDFs requiring attenuation for replicate R3 (Fig 5.2.4).

As shown by the distributions in Figs. 5.2.5 through 5.2.8, Am-241 and Pu-239 are the dominant contributors to the CCDFs for release to the Culebra, with the largest releases coming from Pu-239. Lesser contributions are made by Th-230 and U-234, with the contribution from Th-230 tending to be larger than that from U-234.

A sensitivity analysis can be performed on the expected release to the Culebra for the CCDFs for individual isotopes and also for the CCDFs for total release (Table 5.2.1). The dominant variable is *BHPRM* , with this variable consistently selected first (with SRRCs of about 0.9) in the regression analyses in Table 5.2.1. The positive effect for *BHPRM* results from facilitating the filling of the repository due to brine flow down an intruding borehole and reducing resistance to both flow into the repository from a brine reservoir and flow from the repository to the Culebra. *WMICDFLG* is the second most important variable for total release and the release of each individual radionuclide except U-234. The negative effect results because increasing *WMICDFLG* tends to decrease the amount of brine in the repository by preventing brine flow from the brine

reservoir to the repository during the 200 year period subsequent to an E1 intrusion that an open borehole exists between the repository and the brine reservoir. In the case of U-234, *WOXYSTAT* is the second important variable, with release size tending to increase as *WOXYSTAT*, and therefore U-234 solubility, increases. *BPINTPRS* and *PBRINE* are consistently the third and fourth most important variables. Increasing *BPINTPRS* tends to increase the amount of brine entering the repository. The positive effect for *PBRINE* results from a higher probability of futures containing an E1 intrusion. In addition, small negative effects are indicated for *WGRCOR* and *DRZPRM*. Increasing *WGRCOR* tends to decrease the amount of brine in the repository by increasing the amount of brine that is consumed by corrosion. Increasing *DRZPRM* tends to increase the amount of brine that enters the repository and hence repository pressure. Higher repository pressure tends to decrease the amount of brine flowing upward from the brine reservoir and to the Culebra.

These CCDF sensitivity results are very similar to the sensitivity results for normalized releases to the Culebra (Section 5.1) and are also similar to the CCA sensitivity results. The main difference from the CCA is that *BPINTPRS* has increased importance (larger SRRC) and *BPCOMP* has decreased importance.

Table 5.2.1. Stepwise Regression Analysis with Rank-Transformed Data for Expected Normalized Release Associated with Individual CCDFs for Release to Culebra Dolomite

	Am-241			Pu-239		
Step[a]	Variable[b]	SRRC[c]	R^2[d]	Variable	SRRC	R^2
1	BHPRM	0.91	0.84	BHPRM	0.90	0.83
2	WMICDFLG	-0.14	0.86	WMICDFLG	-0.14	0.85
3	BPINTPRS	-0.13	0.87	BPINTPRS	0.12	0.86
4	PBRINE	0.11	0.88	PBRINE	0.11	0.87
5	WGRCOR	-0.09	0.89	DRZPRM	-0.09	0.88
6	DRZPRM	-0.09	0.90	WGRCOR	-0.09	0.89

	U-234			Th-230		
Step	Variable	SRRC	R^2	Variable	SRRC	R^2
1	BHPRM	0.88	0.80	BHPRM	0.92	0.85
2	WOXYSTAT	0.17	0.82	WMICDFLG	-0.13	0.86
3	WMICDFLG	-0.14	0.84	BPINTPRS	0.12	0.88
4	BPINTPRS	0.13	0.86	PBRINE	0.10	0.89
5	PBRINE	0.10	0.87	DRZPRM	-0.09	0.90
6	WGRCOR	-0.10	0.88	WGRCOR	-0.09	0.90

	Total		
Step	Variable	SRRC	R^2
1	BHPRM	0.91	0.84
2	WMICDFLG	-0.13	0.86
3	BPINTPRS	-0.12	0.87
4	PBRINE	0.11	0.88
5	DRZPRM	-0.09	0.89
6	WGRCOR	-0.09	0.90

[a] Steps in stepwise regression analysis.
[b] Variables listed in order of selection of regression analysis.
[c] Standardized regression coefficients in final regression model with *ANHCOMP* and *HALCOMP* excluded from entry into regression model.
[d] Cumulative R^2 value with entry of each variable into regression model.

[Corresponding Figures From CCA: 6.2.3, 6.2.4]
[Corresponding Table From CCA: 6.2.2]

5.3 Transport in the Culebra: Uncertainty and Sensitivity Analysis

As described in Section 7 of WPO #42912, the computational strategy used in the Culebra transport analysis takes advantage of the linearity of the system of partial differential equations that underlies the Culebra transport code SECOTP2D. That is, transport calculations were performed for unit kg releases to the Culebra. These calculations identify conditional releases from the Culebra. Using linearity of the system, the conditional releases were then used to construct transport results for time-dependent releases into the Culebra associated with randomly selected futures using NUTS and PANEL calculated radionuclide sources.

Because of the computational strategy described above, a total of only 600 SECOTP2D calculations were actually performed (i.e., 100 for partially mined conditions and 100 for fully mined conditions for each of three replicates). In each calculation, a 1 kg release of each radionuclide (i.e., Am-241, Pu-239, U-234, Th-230) was assumed to take place between 0 and 50 years and then the transport of this release over 10,000 years was calculated. Of the 600 transport calculations, there were only 40 realizations under partially mined conditions and 43 realizations under fully mined conditions that produced conditional releases across the land withdrawal boundary greater than 1.0×10^{-5} kg, with substantial releases only occurring for U-234. As noted in WPO #46674 insignificant amounts of Th-230 were also released.

A regression analysis was performed on the conditional releases of U-234 and the results are presented in Table 5.3.1. The regressions for partially and fully mined conditions are very similar. The dominant variables are *WOXYSTAT* and *CMKDU6*, with the size of release tending to increase as *WOXYSTAT* increases and decrease as *CMKDU6* increases. The positive effect for *WOXYSTAT* results from its role in determining which set of distribution coefficients are used in the transport calculations. In particular, smaller distribution coefficients (*CMKDU6*) for U-234 were associated with *WOXYSTAT* = 1 (i.e., oxidation state of +VI), hence the positive effect for *OXYSTAT* in Table 5.3.1. The negative effect for *CMKDU6* results because increasing *CMKDU6* increases adsorption of U-234 in the matrix and thus reduces transport. In the partially mined case, the next two important variables were *CFRACPOR* and *CMTRXPOR*, with transport tending to decrease as these variables increase. These negative effects result because increasing these variables increases the flux of U-234 into the matrix and thus slows transport. In the fully mined case, the next two important variables are *CFRACPOR* and *CCLIMSF*. As in the partially mined case, *CFRACPOR* produces a negative effect. The positive effect of *CCLIMSF* results because increasing this variable uniformly increases the groundwater flow velocity field and, therefore, the rate of transport. Note that the final regression models have R^2 values of only 0.47 and 0.63. Thus, these models are less effective in accounting for the uncertainty in the analysis outcomes. This lack of resolution is due to the large number of sample elements that have no release. Note that in the CCA, a meaningful regression analysis of conditional releases across the land withdrawal boundary could not be completed because of the fact that only one LHS element produced releases (WPO #42912).

Table 5.3.1. Stepwise Regression Analysis with Rank-Transformed Data for Cumulative Conditional U-234 Releases Across the Land Withdrawal Boundary over 10000 years

	Releases Under Partially Mined Conditions			Releases Under Fully Mined Conditions		
Step [a]	Variable [b]	SRRC [c]	R^2 [d]	Variable	SRRC	R^2
1	WOXYSTAT	0.65	0.45	WOXYSTAT	0.59	0.36
2	CMKDU6	-0.36	0.58	CMKDU6	-0.30	0.45
3	CFRACPOR	-0.19	0.62	CFRACPOR	-0.10	0.46
4	CMTRXPOR	-0.10	0.63	CCLIMSF	0.10	0.47

[a] Steps in stepwise regression analysis.
[b] Variables listed in order of selection of regression analysis.
[c] Standardized regression coefficients in final regression model with *ANHCOMP* and *HALCOMP* excluded from entry into regression model.
[d] Cumulative R^2 value with entry of each variable into regression model.

5.4 Release From the Culebra: CCDFs

As noted in Section 5.2, the CCDFs for releases to the Culebra (Figs. 5.2.5 through 5.2.8) are an interim step in the calculation of releases to the accessible environment. CCDFs for total releases from the Culebra to the accessible environment are constructed by using the releases to the Culebra for each isotope for each of 10,000 randomly-sampled futures in conjunction with the Culebra transport results. This approach produces 100 CCDFs for total releases from the Culebra for each of the three replicates. The outcomes are distributions of CCDFs for each LHS element in each replicate that fall far below the limit specified in 40 CFR 191 (Figs. 5.4.1, 5.4.2, 5.4.3). The overall mean CCDF constructed by pooling all three replicates is shown in Fig. 5.4.4. Note that only a few elements in each replicate actually produced releases to the accessible environment: 9 realizations in replicate 1 (Fig. 5.4.1); 7 realizations in replicate 2 (Fig. 5.4.2); and 4 realizations in replicate 3 (Fig. 5.4.3). In the CCA, no LHS elements produced releases to the accessible environment. Finally, because of the small number of nonzero outcomes a meaningful regression analysis of the CCDFs for total releases from the Culebra could not be performed.

6.0 TOTAL NORMALIZED RELEASES TO THE ACCESSIBLE ENVIRONMENT

As described in previous reports (WPO #46674 and WPO #46702), the PAVT mean CCDF for total normalized releases to the accessible environment shifted to the right of the CCA mean CCDF by a factor of 2 or 3 for all probabilities of exceedance and does not exceed or come within an order of magnitude of the EPA Limit. This increase is primarily due to the increase in cuttings and cavings releases, and to a lesser extent to increased spallings releases. Analysis of all three PAVT replicates showed CCDFs for total normalized releases to the accessible environment to exhibit only small variations across the three replicates. Releases due to cuttings, spallings, direct brine release, and Culebra transport showed similar small variations across replicates.

6.1 Total Release: CCDFs

The CCDFs for total release can be reduced to expected values (Fig. 6.1.1). Comparison of expected values for cuttings and cavings, spallings, direct brine release, Culebra, and total releases shows that the total release is dominated by cuttings and cavings and by spallings. Direct brine release makes a smaller contribution to the total release, while releases from the Culebra were negligible. There were no contributions to total release from the Salado interbeds or from the Dewey Lake across the LWB.

Stepwise regression analysis can be used to determine the dominant contributors to the expected value for total release due to cuttings, spallings and direct brine release (Table 6.1.1). The two dominant variables with respect to uncertainty in the expected total release are *WTAUFAIL* and *BHPRM*, with the size of the expected release tending to decrease as these variables increase. The negative effect for *WTAUFAIL* results from its influence on the size of the cuttings release, as *WTAUFAIL* increases cuttings releases decrease. The negative effect for *BHPRM* results from its influence on repository pressure, as *BHPRM* decreases repository pressures increase. Recall that the primary determinant of the uncertainty in the CCDFs for spallings is the pressure conditions in repository, with no spallings releases taking place at pressures less than 8 MPa. As a further reminder, the total release is completely dominated by cuttings and spallings, with *WTAUFAIL* and *BHPRM* being the dominant contributors to the uncertainty in these two release models (see Section 3). The positive effects for *VOLSPALL* and *WMICDFLG* results from their influence on the size of the spallings release. The remaining variables in the regression model (i.e., *DRZPRM*, *HALPOR*, and *PBRINE*) also appear primarily because of their effects on the spallings release.

These PAVT sensitivity results for total releases are similar to the CCA. The primary differences are that *WTAUFAIL* and *BHPRM* increased in importance relative to the CCA, while *WMICDFLG* decreased in importance. *VOLSPALL*, a new PAVT variable important to spallings releases, also is an important variable for total releases to the accessible environment in the PAVT.

Table 6.1.1. Stepwise Regression Analysis with Rank-Transformed Data for Expected Normalized Release Associated with Individual CCDFs for Total Release Due to Cuttings, Spallings, and Direct Brine Release.

	Expected Normalized Release		
Step [a]	Variable [b]	SRRC [c]	R^2 [d]
1	WTAUFAIL	-0.61	0.39
2	BHPRM	-0.40	0.56
3	VOLSPALL	0.33	0.66
4	WMICDFLG	0.27	0.74
5	HALPOR	0.13	0.76
6	DRZPRM	0.12	0.78
7	PBRINE	0.12	0.79

[a] Steps in stepwise regression analysis.
[b] Variables listed in order of selection of regression analysis.
[c] Standardized regression coefficients in final regression model with *ANHCOMP* and *HALCOMP* excluded from entry into regression model.
[d] Cumulative R^2 value with entry of each variable into regression model.

[Corresponding Figure From CCA: 8.2.3]
[Corresponding Table From CCA: 8.2.1]

7.0 REFERENCES

Summary of EPA-Mandated Performance Assessment Verification Test (Replicate 1) and Comparison With the Compliance Certification Application Calculations, WPO # 46674.

Supplemental Summary of EPA-Mandated Performance Assessment Verification Test (All Replicates) and Comparison With the Compliance Certification Application Calculations, WPO # 46702.

Memo: Preliminary Summary of Uncertainty and Sensitivity Analysis Results Obtained in Support of the 1996 Compliance Certification Application for the Waste Isolation Pilot Plant, WPO # 42912.

APPENDIX A

DESCRIPTIONS OF VARIABLES

The following sampled variables are referenced in this report. A complete listing of all variables sampled in the CCA is provided in WPO #42912. Changes to sampled variables for the PAVT are described in WPO #46674.

ANHCOMP	Bulk compressibility of anhydrite (Pa^{-1}).
ANHPRM	Logarithm of anhydrite permeability (m^2).
BHPRM	Logarithm of borehole permeability (m^2).
BPCOMP	Logarithm of bulk compressibility of brine pocket (Pa^{-1}).
BPINTPRS	Initial pressure in brine pocket (Pa). Also equal to brine pocket pressure at time of first intrusion.
CCLIMSF	Climate scale factor for Culebra flow field (dimensionless).
CFRACPOR	Culebra fracture (i.e., advective) porosity (dimensionless).
CMKDU6	Culebra matrix distribution coefficient (m^3/kg) for uranium in +6 oxidation state.
CMTRXPOR	Culebra matrix (i.e., diffusive) porosity (dimensionless).
DOMEGA	Drill string angular velocity (rad/s).
DRZPRM	Logarithm of DRZ permeability (m^2). Sampled in PAVT only.
HALCOMP	Bulk compressibilty of anhydrite (Pa^{-1}).
HALPOR	Halite porosity (dimensionless).
HALPRM	Logarithm of halite permeability (m^2).
PBRINE	Probability that a Castile brine reservoir will be penetrated (dimensionless).
SALPRES	Initial brine pressure at the elevation of the midpoint of MB139 (Pa).
VOLSPALL	Spallings volume released if repository pressure is above 8 MPa. PAVT variable only.
WASTWICK	Increase in brine saturation of waste due to capillary forces (dimensionless).
WGRCOR	Corrosion rate for steel under inundated conditions in the absence of CO_2 (m/s).
WGRMICI	Microbial degradation rate for cellulose under inundated conditions (mol/kg·s).
WMICDFLG	Pointer variable for microbial degradation of cellulose.
WPRTDIAM	Waste particle diameter (m). Sampled in CCA only.

WOXYSTAT Pointer variable for elemental oxidation states (dimensionless).

WRBRNSAT Residual brine saturation in waste (dimensionless).

WRGSSAT Residual gas saturation in waste (dimensionless).

WSOLAM3C Logarithm of scale factor used to define solubility in Castile brine of americium in oxidation state III (dimensionless).

WSOLPU4C Same as WSOLAM3C but for plutonium in oxidation state IV.

WSOLU6C Same as WSOLAM3C but for uranium in oxidation state VI.

WTAUFAIL Shear strength of waste (Pa).

APPENDIX B

CODES USED IN UNCERTAINTY AND SENSITIVITY ANALYSIS

The following codes were used to perform and present the uncertainty and sensitivity analyses presented in this report.

Code	Version	Executable	Location	Software Problem Reports (SPRs)
STEPWISE	2.21	stepwise_pa96_2.exe	wp$prodroot:[stp.exe]	none
NUCPLOT	1.19	nucplot_pa96.exe	wp$prodroot:[npl.exe]	none
PCCSRC	2.21	pccsrc_pa96.exe	wp$prodroot:[pcc.exe]	none

SNL WIPP C97: BRAGFLO SIMULATIONS (C97 R1 S1)

Cumulative Brine Flow into DRZ from All Marker Beds

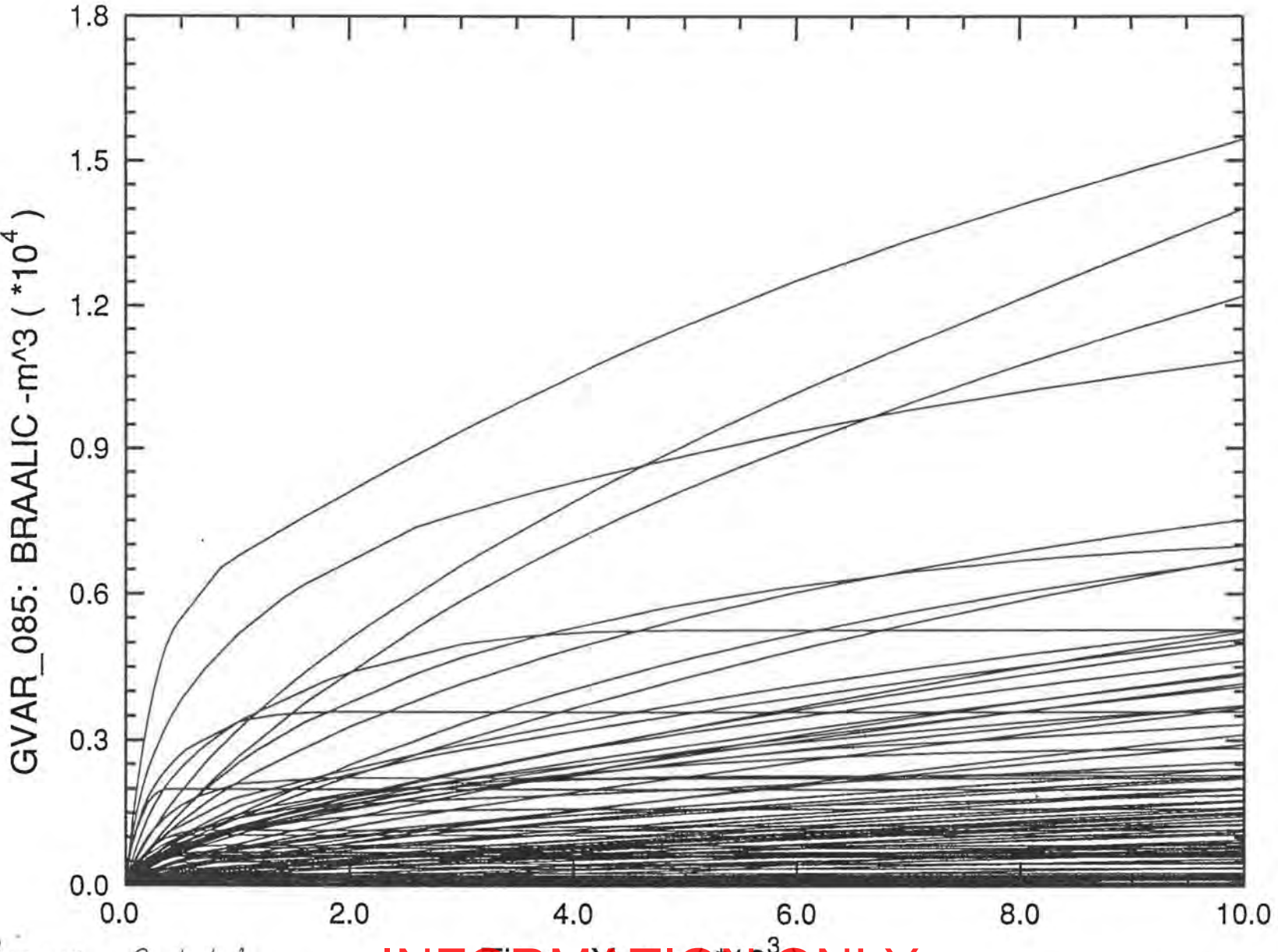

Figure 2.1.1.1

SNL WIPP C97: BRAGFLO SIMULATIONS (C97 R1 S1)

Cumulative Brine Flow into Repository

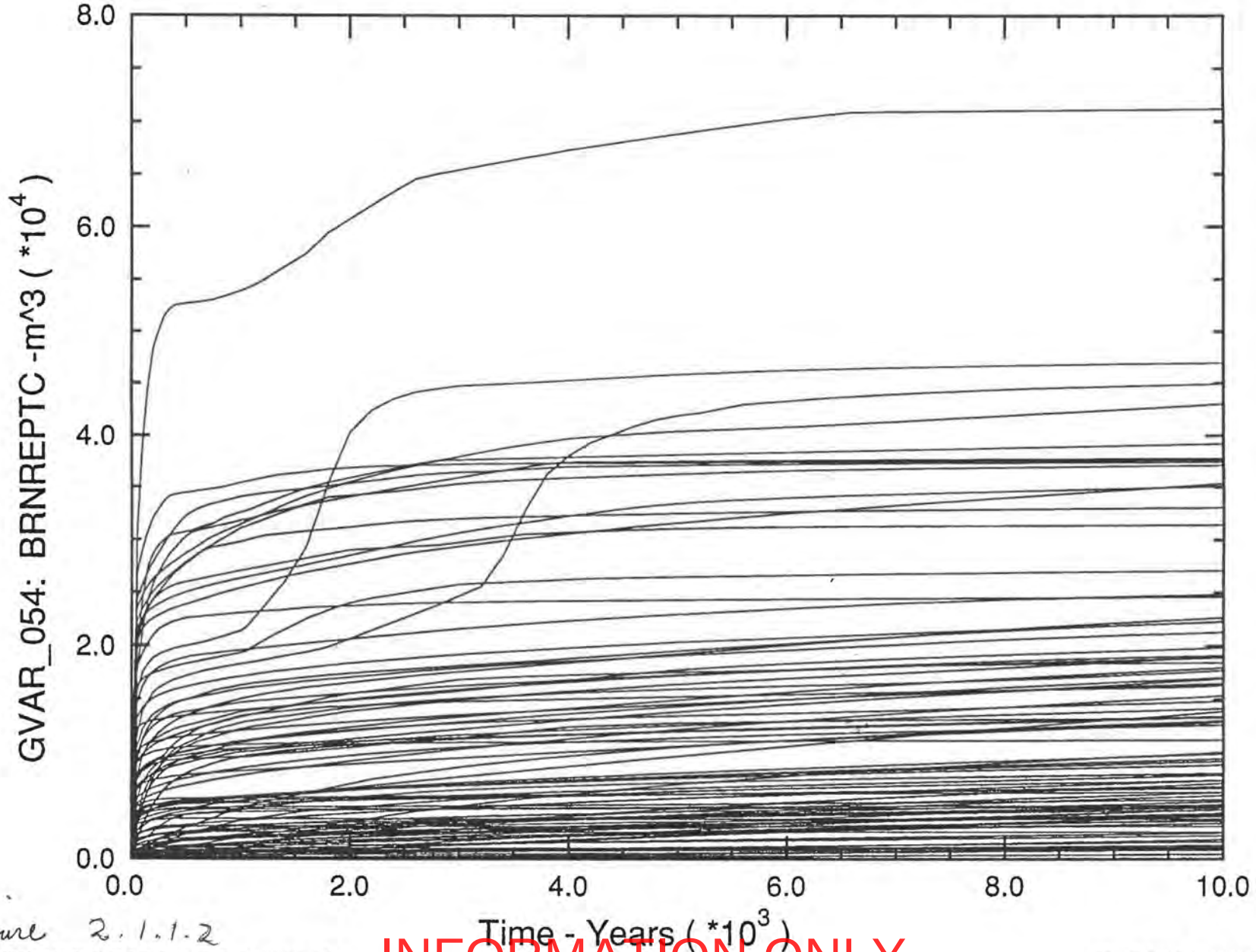

Figure 2.1.1.2

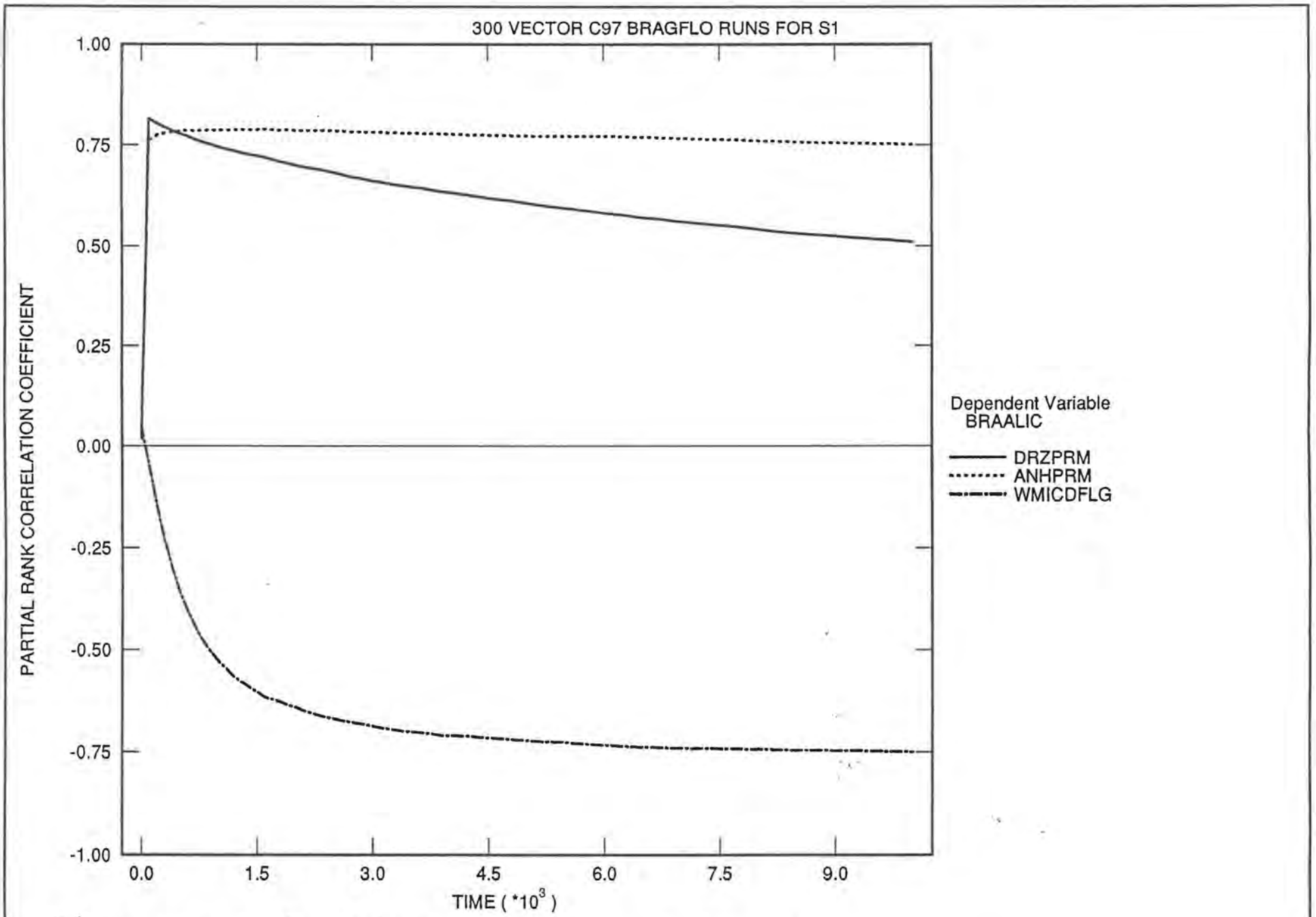

Figure 2.1.4.3 Cumulative Brine Flow From Marker Beds

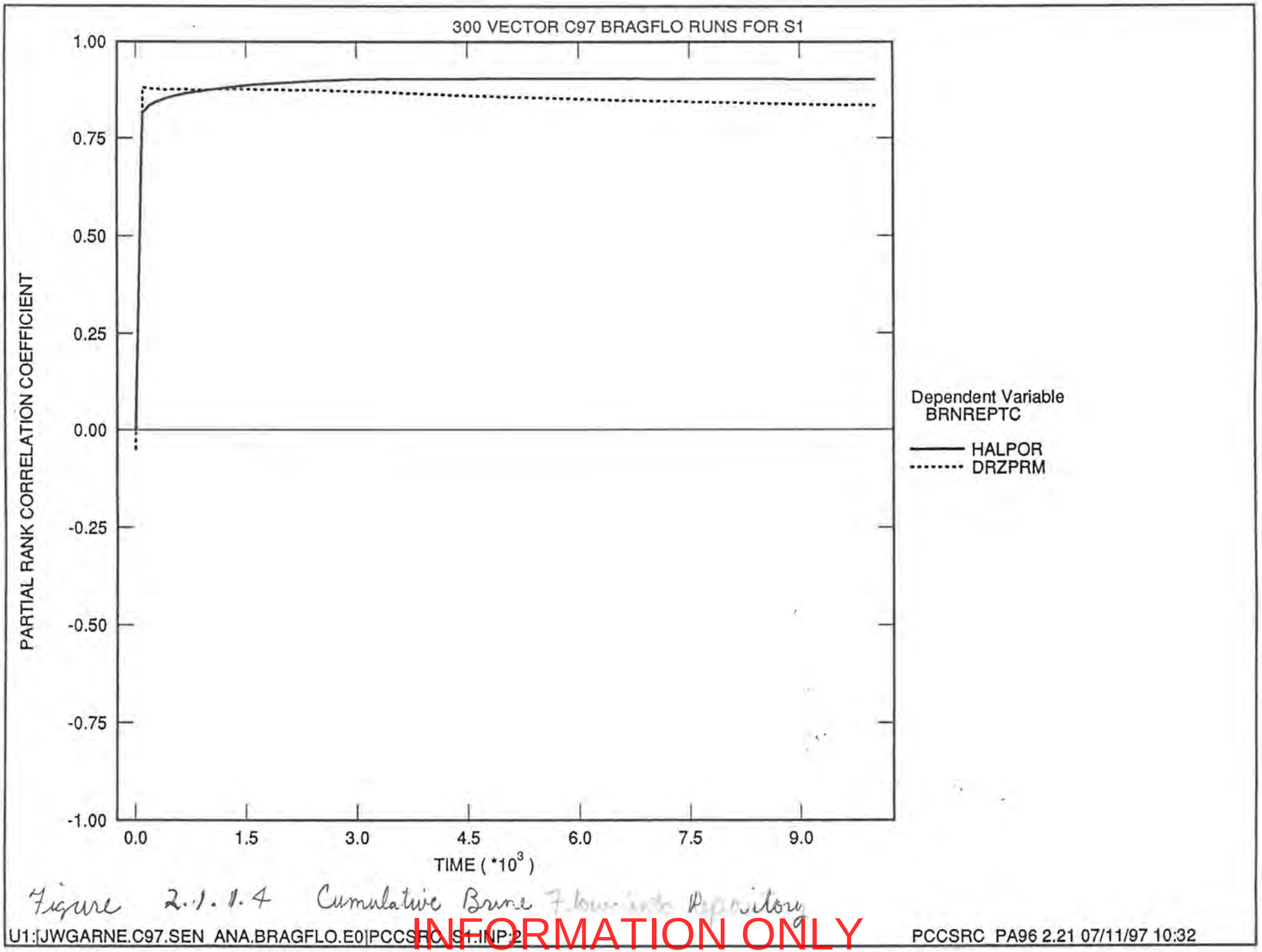

Figure 2.1.1.4 Cumulative Brine Flow into Repository

SNL WIPP C97: BRAGFLO SIMULATIONS (C97 R1 S1)

Cumulative Gas Generated by Corrosion

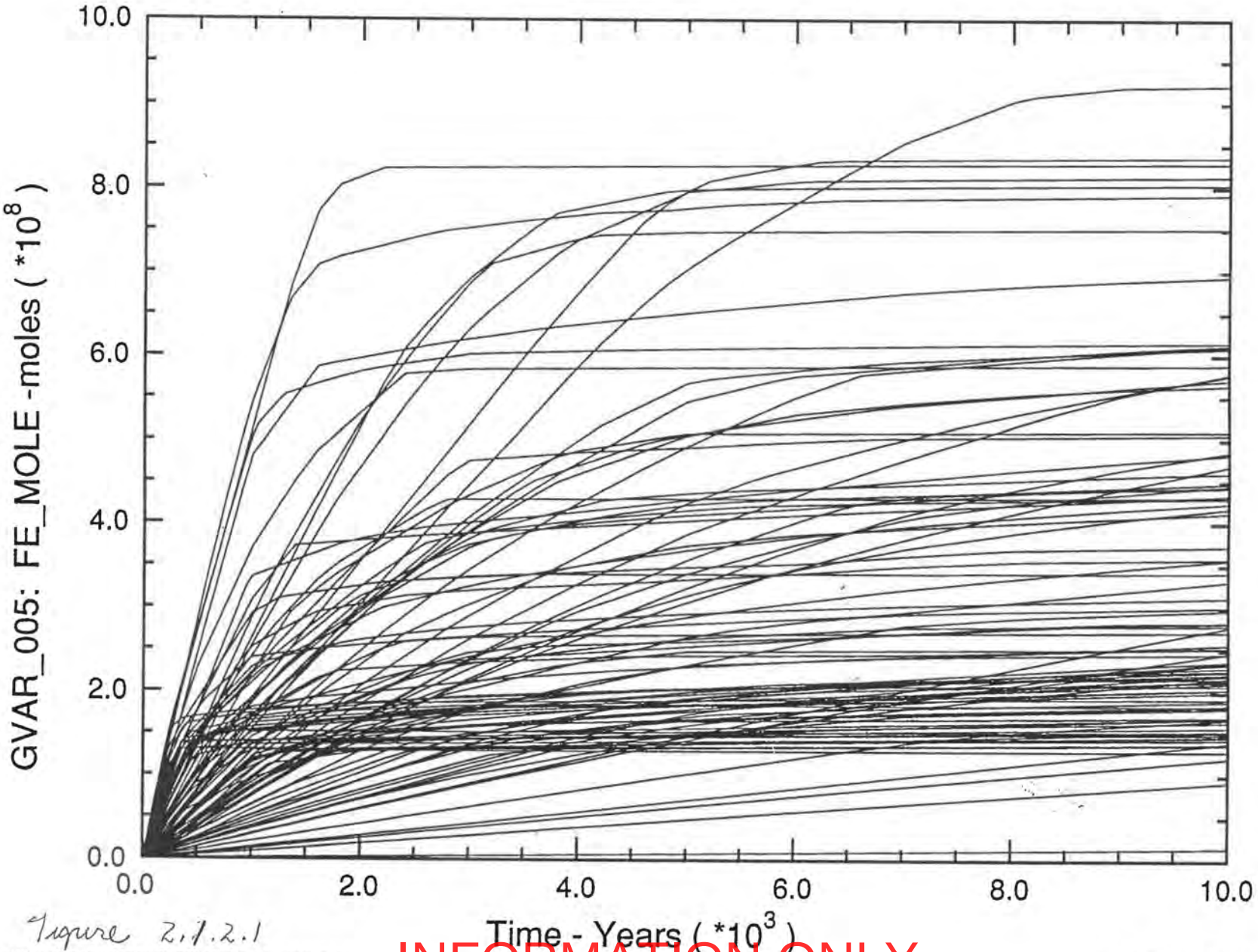

Figure 2.1.2.1

1DRA1:[JEBEAN.C97.SUMMZ.R1S1]SPLAT_R1_S1_H005.INP;1

SPLAT_PA96_2 1.02 05/27/97 08:06:36

SNL WIPP C97: BRAGFLO SIMULATIONS (C97 R1 S1)

Total Microbial Gas Generation

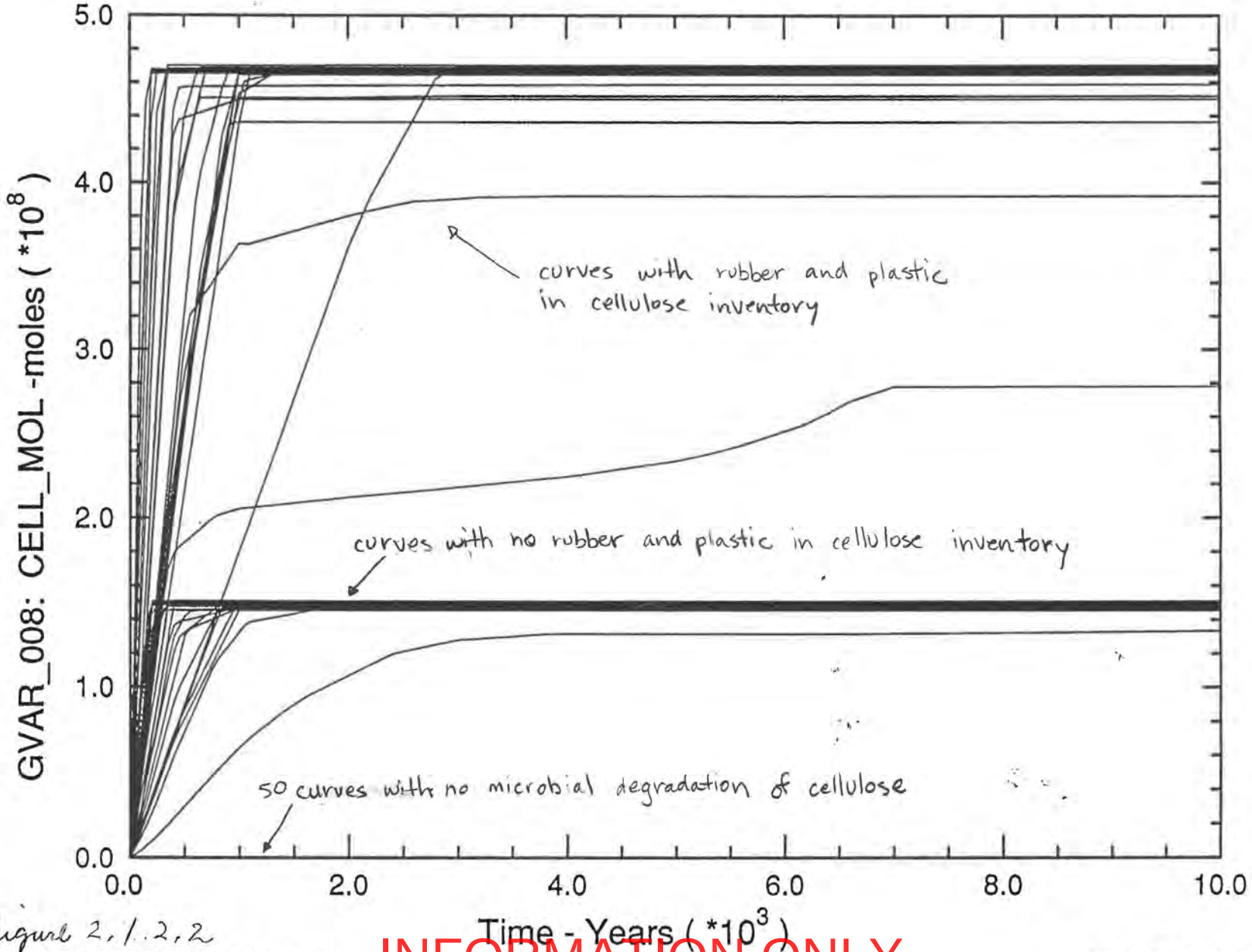

Figure 2.1.2.2

SNL WIPP C97: BRAGFLO SIMULATIONS (C97 R1 S1)

Total Gas Generated

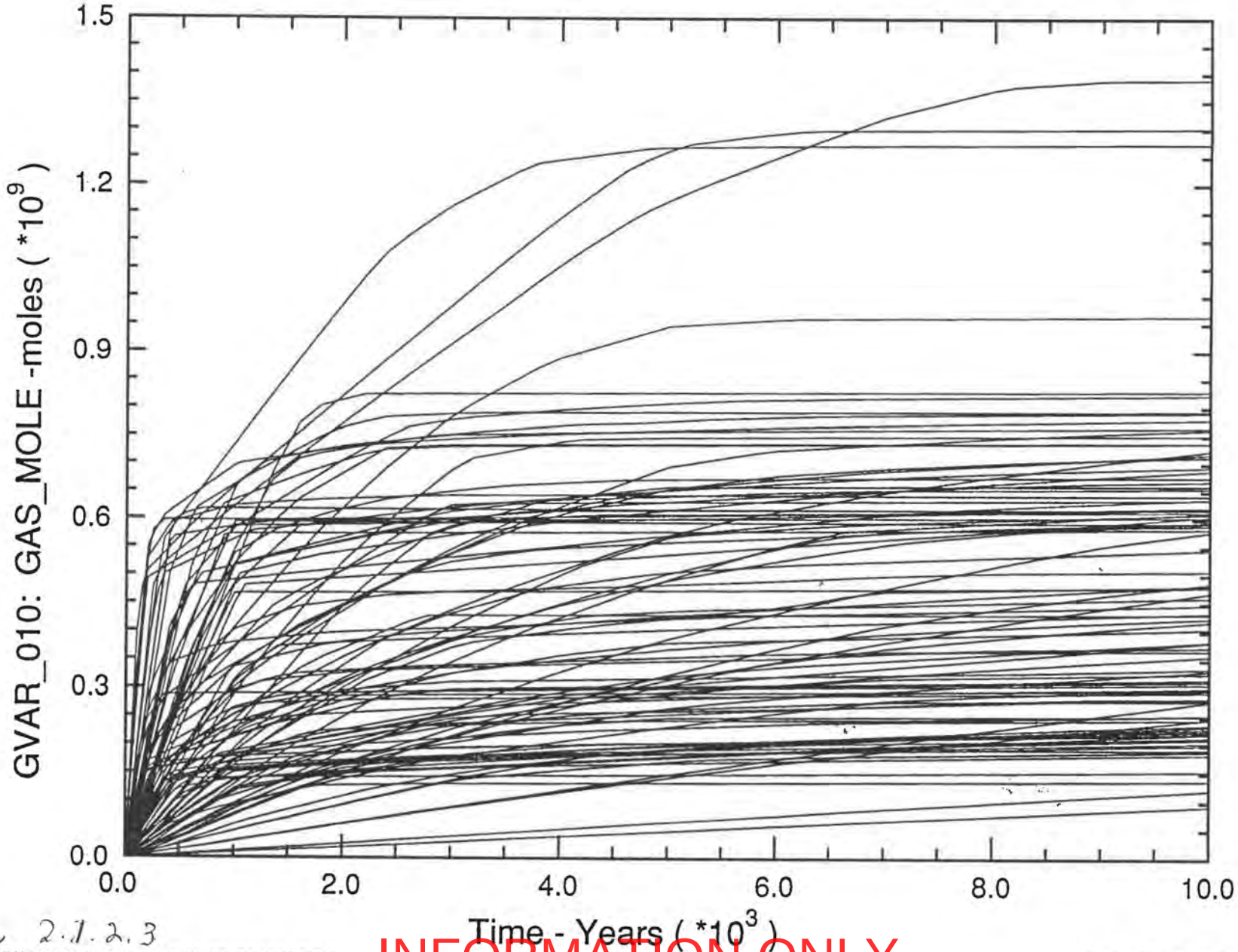

Figure 2.1.2.3

1DRA1:[JEBEAN.C97.SUMMZ.R1S1]SPLAT_R1_S1_H010.INP;1

SPLAT_PA96_2 1.02 05/27/97 08:25:19

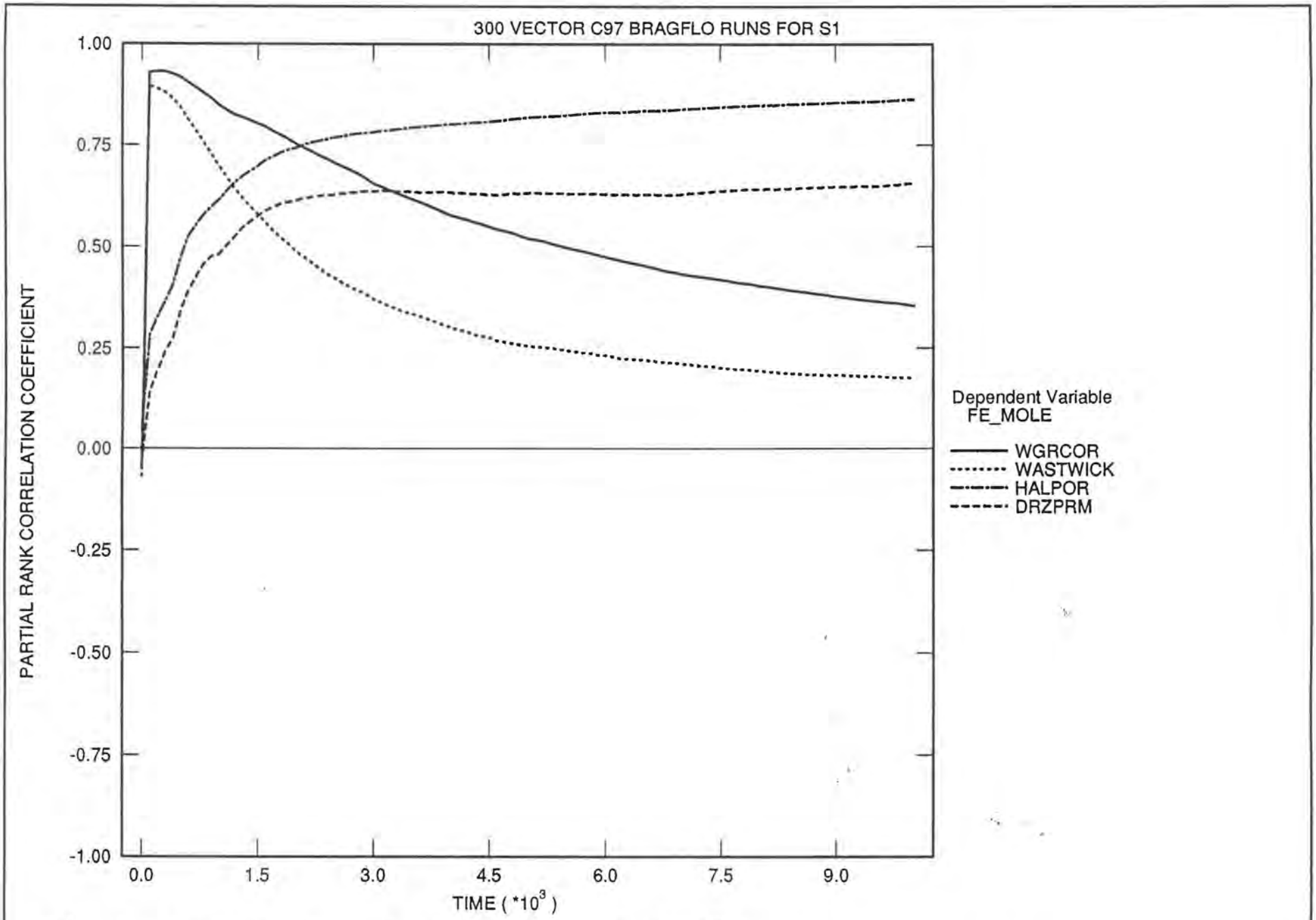

Figure 2.1.2.4 Gas Generation Due to Corrosion

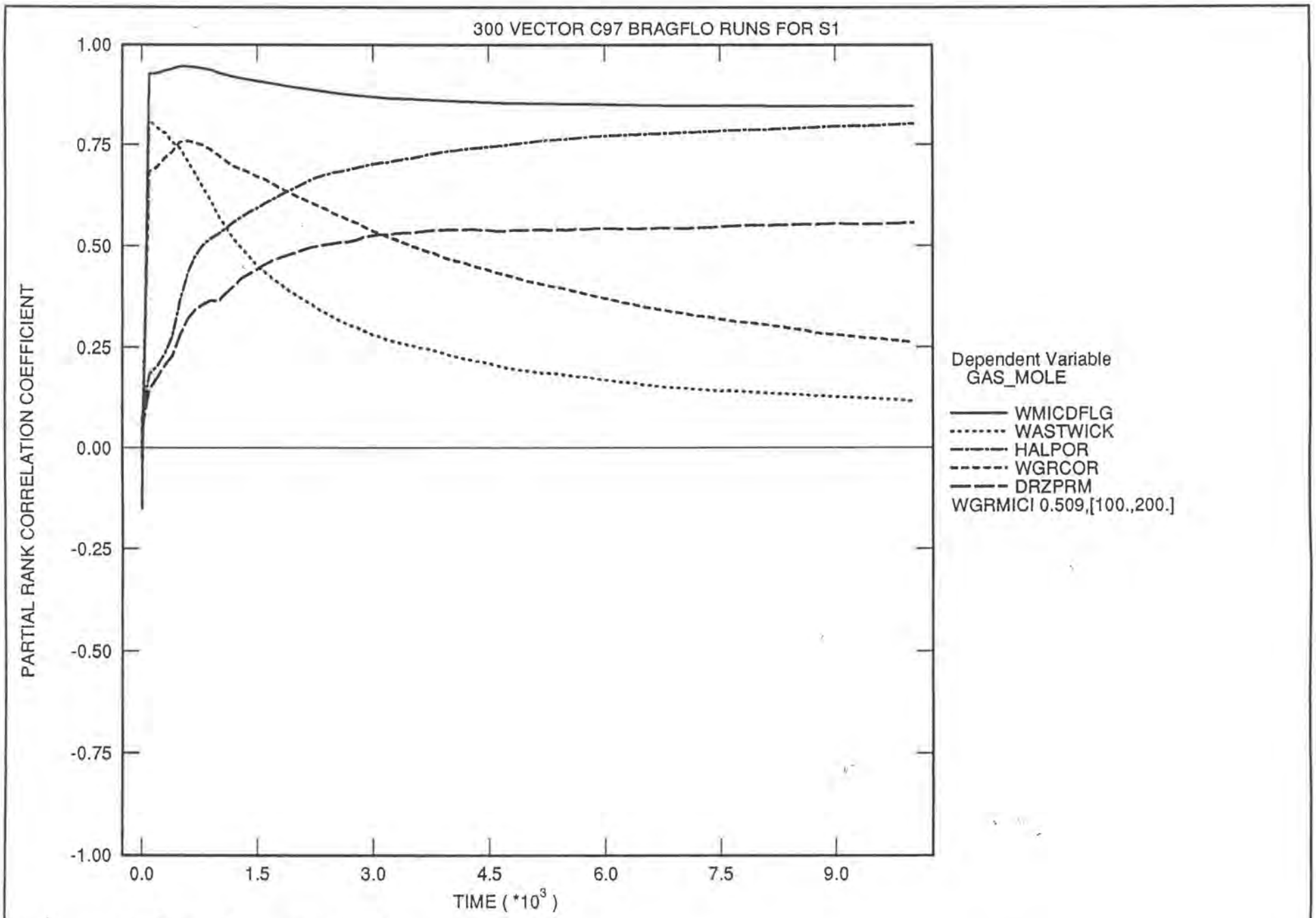

Figure 2.1.2.5 Total Gas Generation

SNL WIPP C97: BRAGFLO SIMULATIONS (C97 R1 S1)

Remaining Fraction of Steel Inventory in Rest of Repository (upper panels)

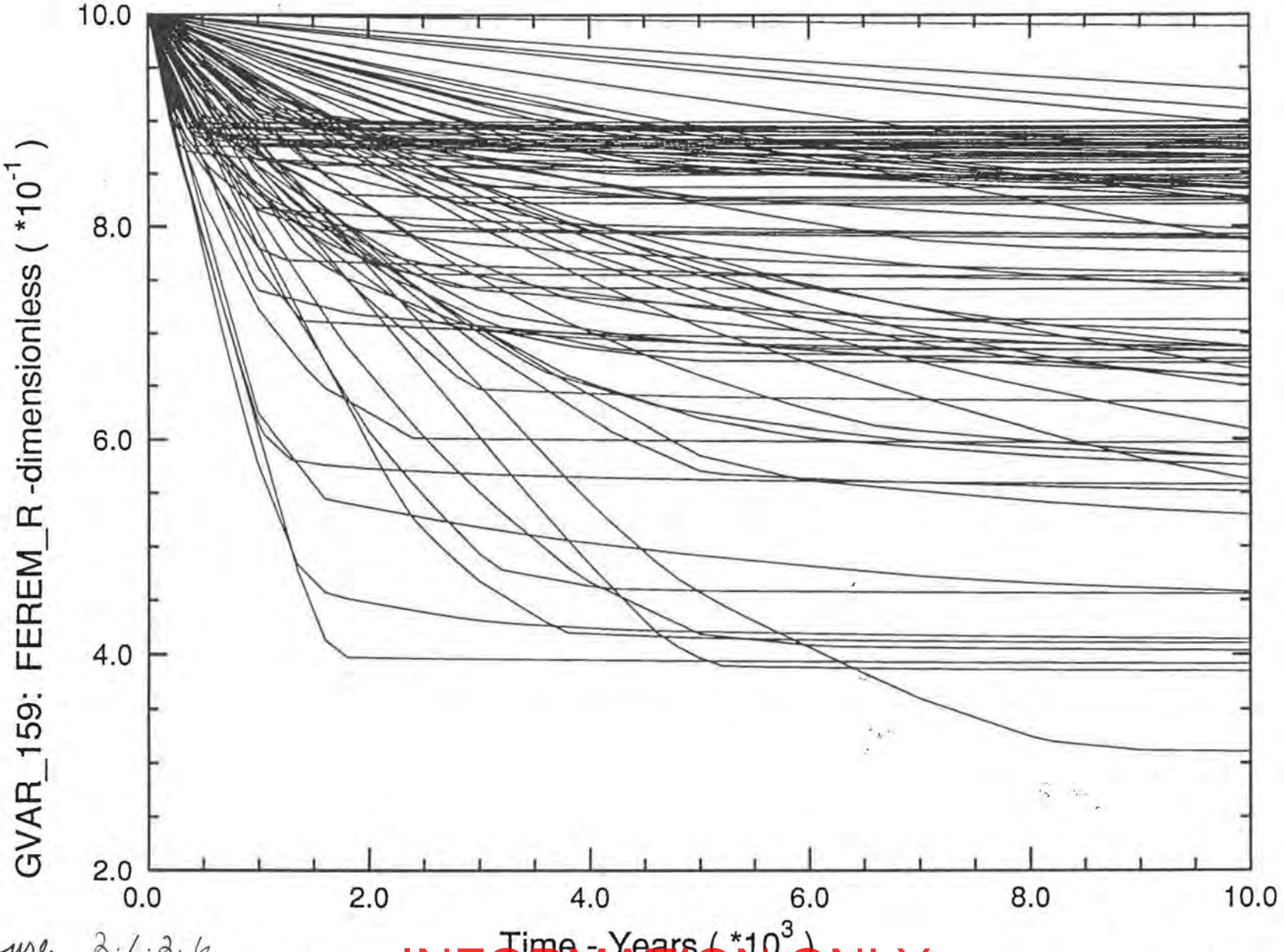

Figure 2.1.2.6

1DRA1:[JEBEAN.C97.SUMMZ.R1S1]SPLAT_R1_S1_H159.INP;1

SPLAT_PA96_2 1.02 05/28/97 10:55:33

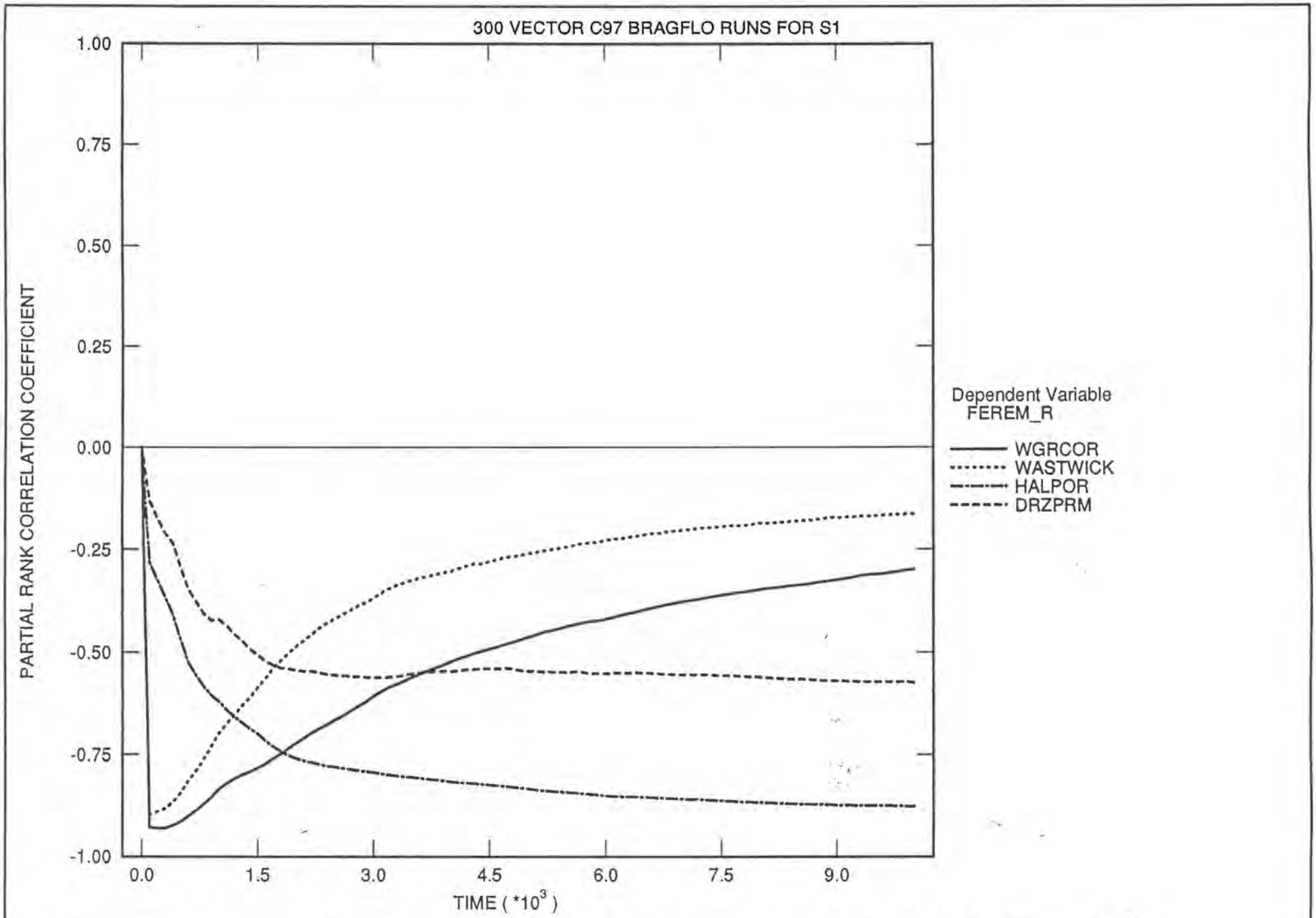

Figure 2.1.2.8 Fraction of Steel Remaining in Upper Panels (Rest of Repository)

SNL WIPP C97: BRAGFLO SIMULATIONS (C97 R1 S1)

Remaining Fraction of Steel Inventory in Waste Panel (Lower Panel)

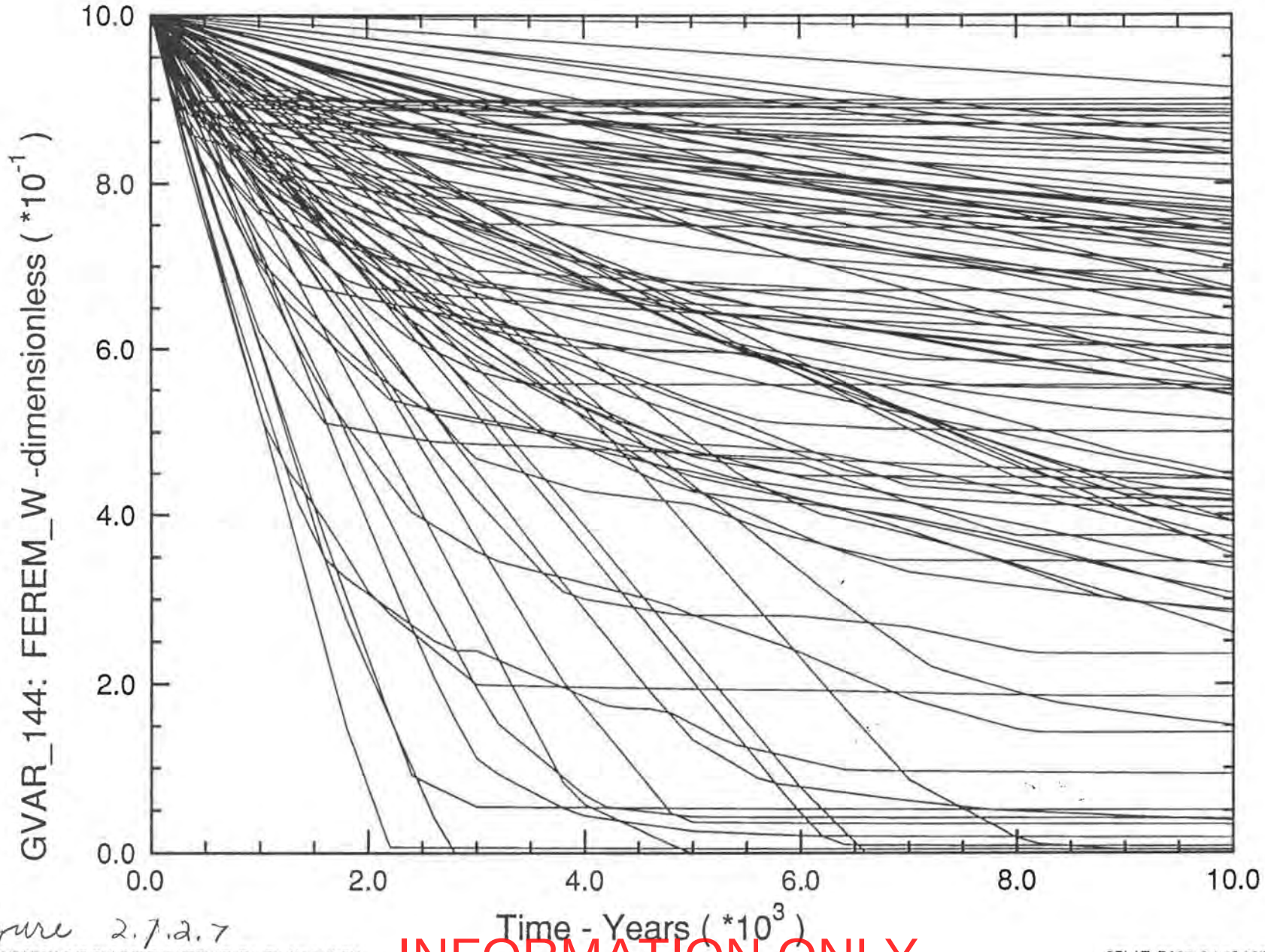

Figure 2.7.2.7

1DRA1:[JEBEAN.C97.SUMMZ.R1S1]SPLAT_R1_S1_H144.INP;1

SPLAT_PA96_2 1.02 05/28/97 10:07:16

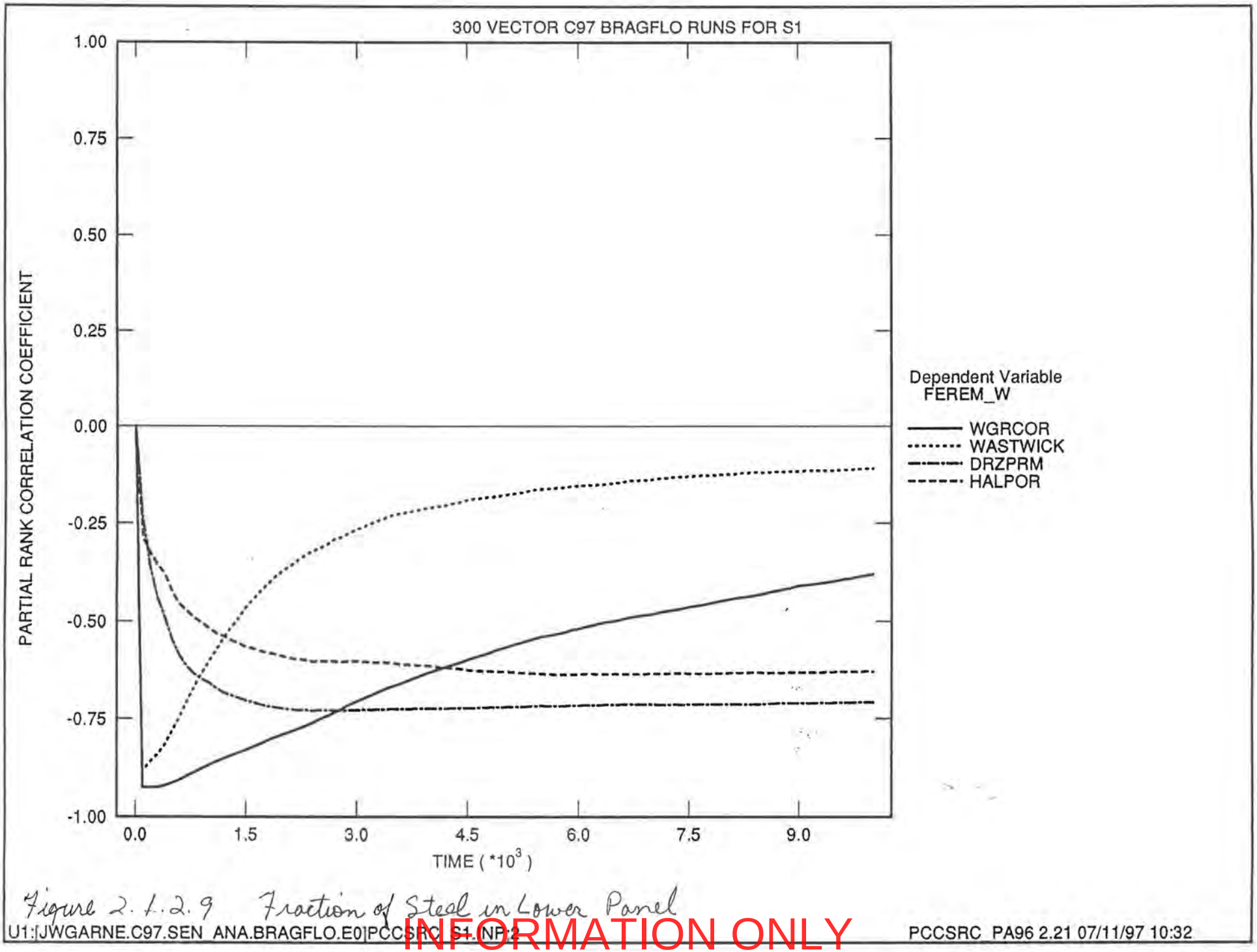

Figure 2.1.2.9 Fraction of Steel in Lower Panel

SNL WIPP C97: BRAGFLO SIMULATIONS (C97 R1 S1)

Volume-Averaged Pressure in Waste Panel

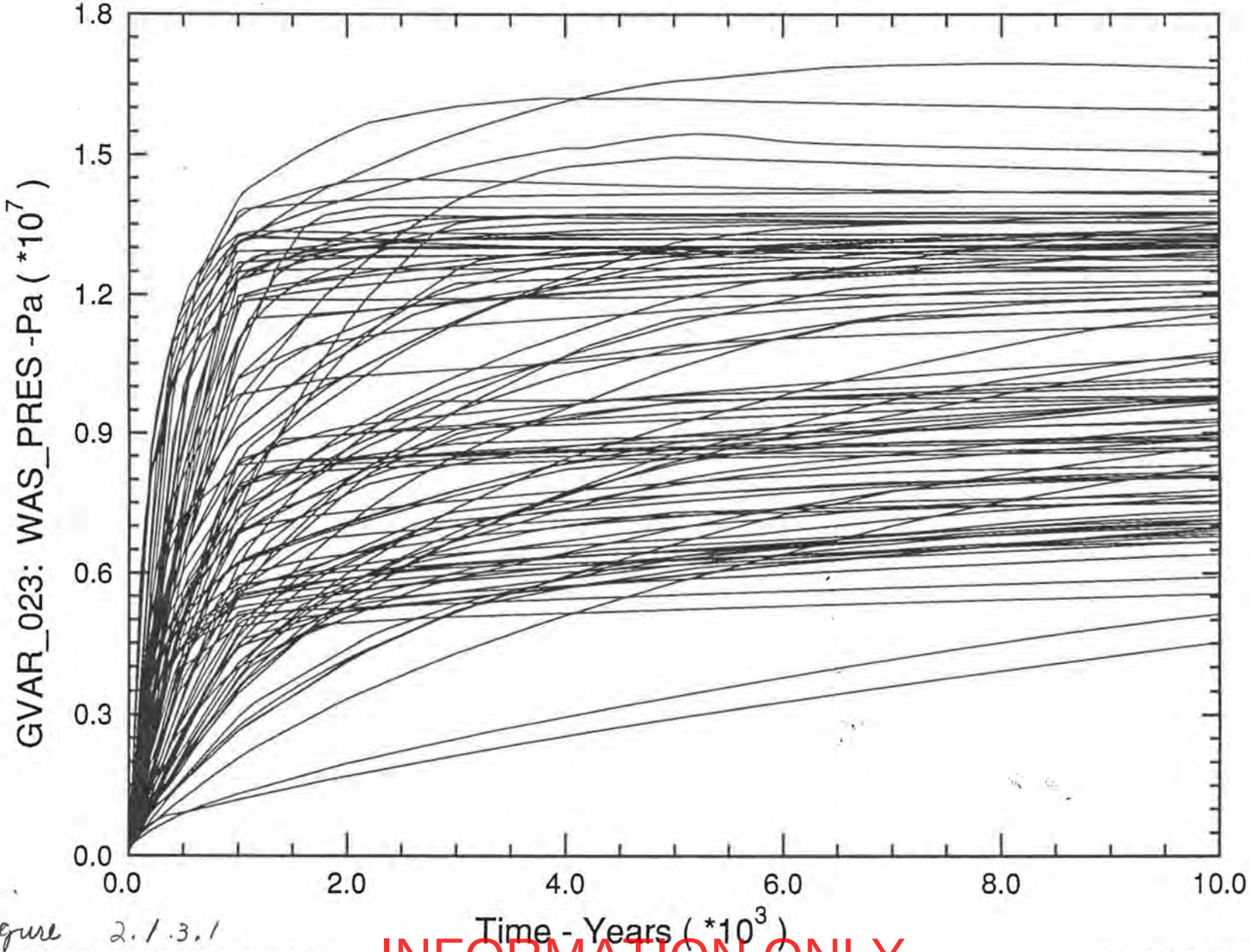

Figure 2.1.3.1

1DRA1:[JEBEAN.C97.SUMMZ.R1S1]SPLAT_R1_S1_H023.INP;1

INFORMATION ONLY

SPLAT_PA96_2 1.02 05/27/97 09:11:07

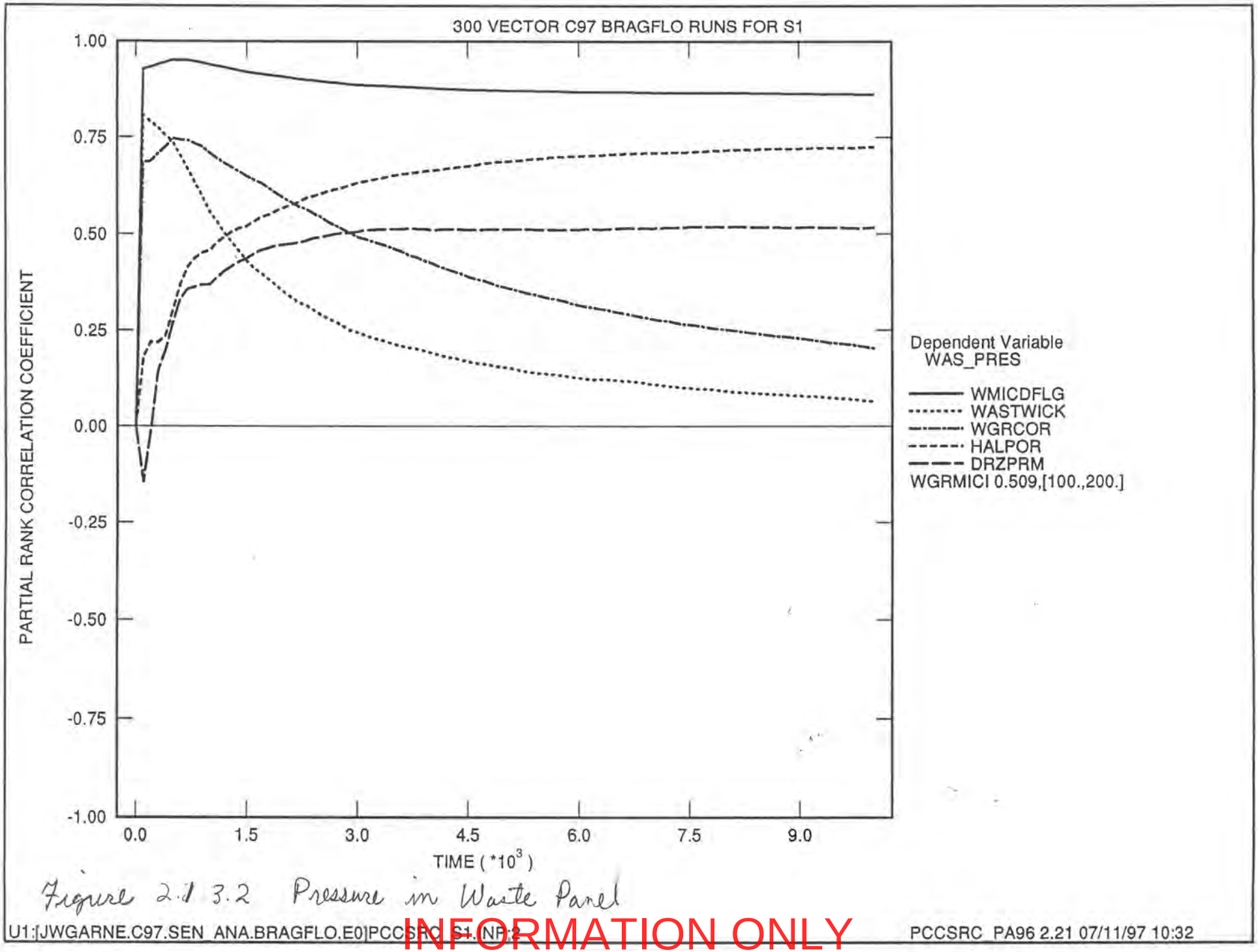

Figure 2.1 3.2 Pressure in Waste Panel

SNL WIPP C97: BRAGFLO SIMULATIONS (C97 R1 S1)

Volume-Averaged Brine Saturation in Rest of Repository

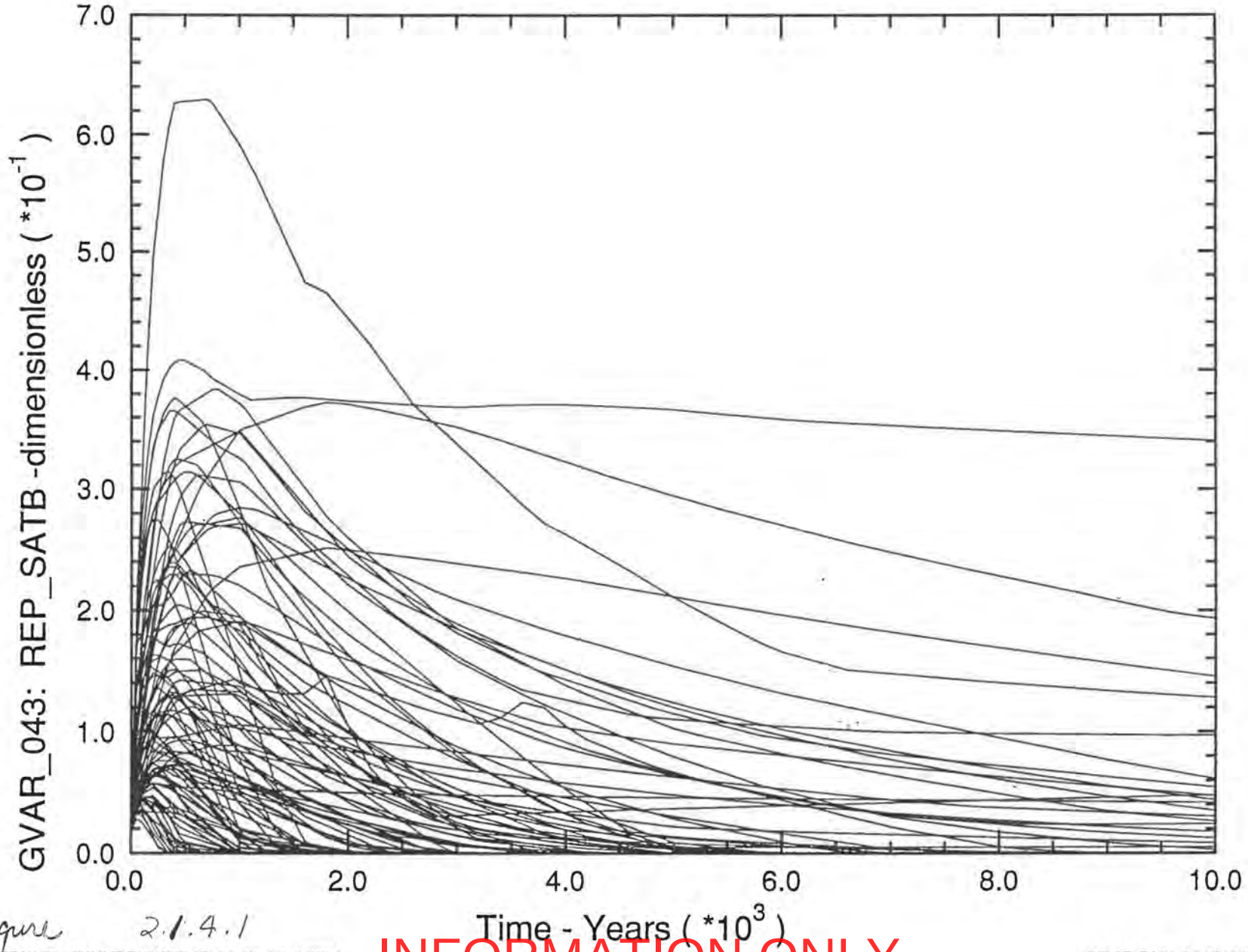

Figure 2.1.4.1

1DRA1:[JEBEAN.C97.SUMMZ.R1S1]SPLAT_R1_S1_H043.INP;1

SPLAT_PA96_2 1.02 05/27/97 10:22:58

SNL WIPP C97: BRAGFLO SIMULATIONS (C97 R1 S1)

Volume-Averaged Brine Saturation in Waste Panel

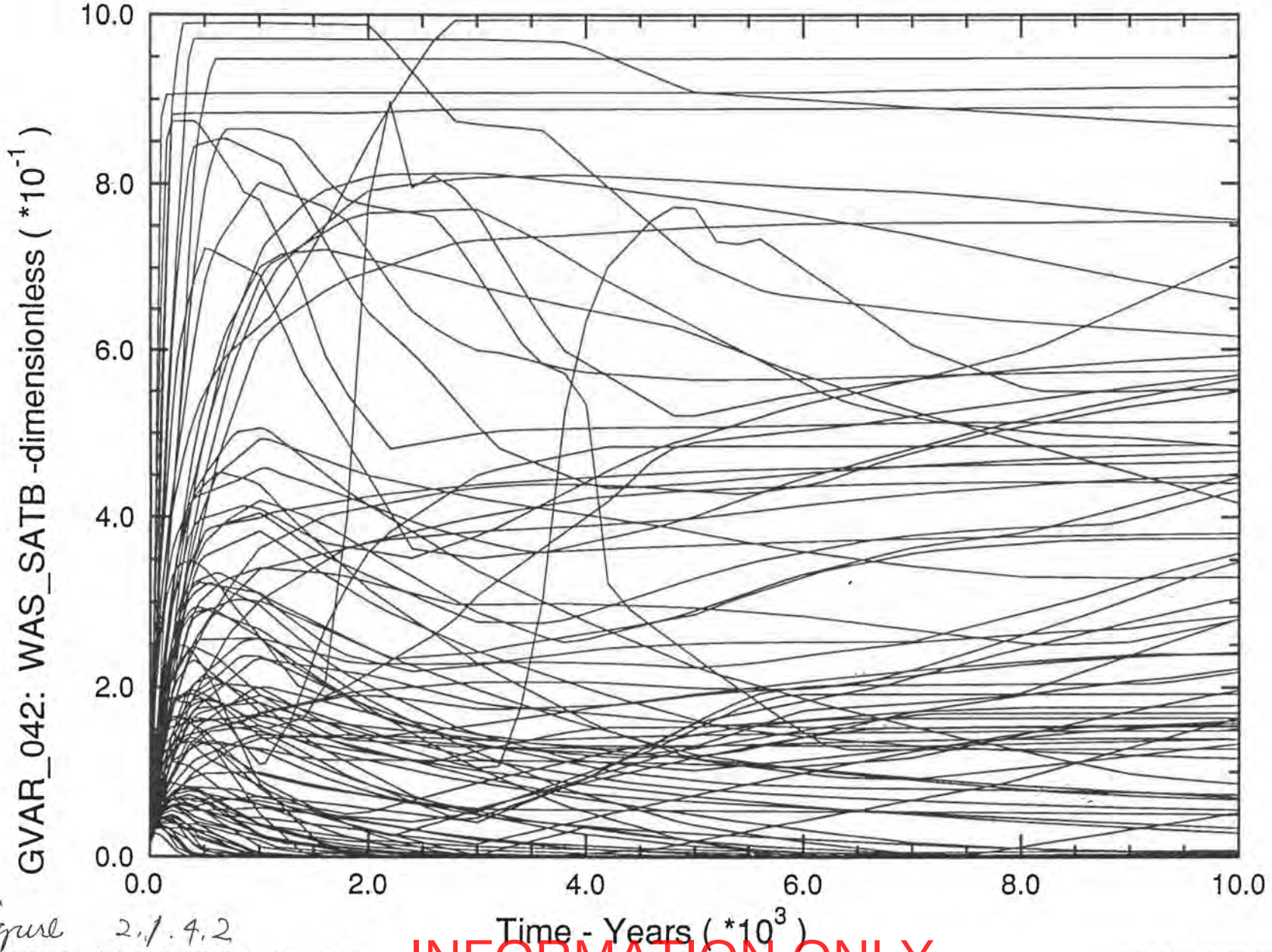

Figure 2.1.4.2

1DRA1:[JEBEAN.C97.SUMMZ.R1S1]SPLAT_R1_S1_H042.INP;1

SPLAT_PA96_2 1.02 05/27/97 10:19:03

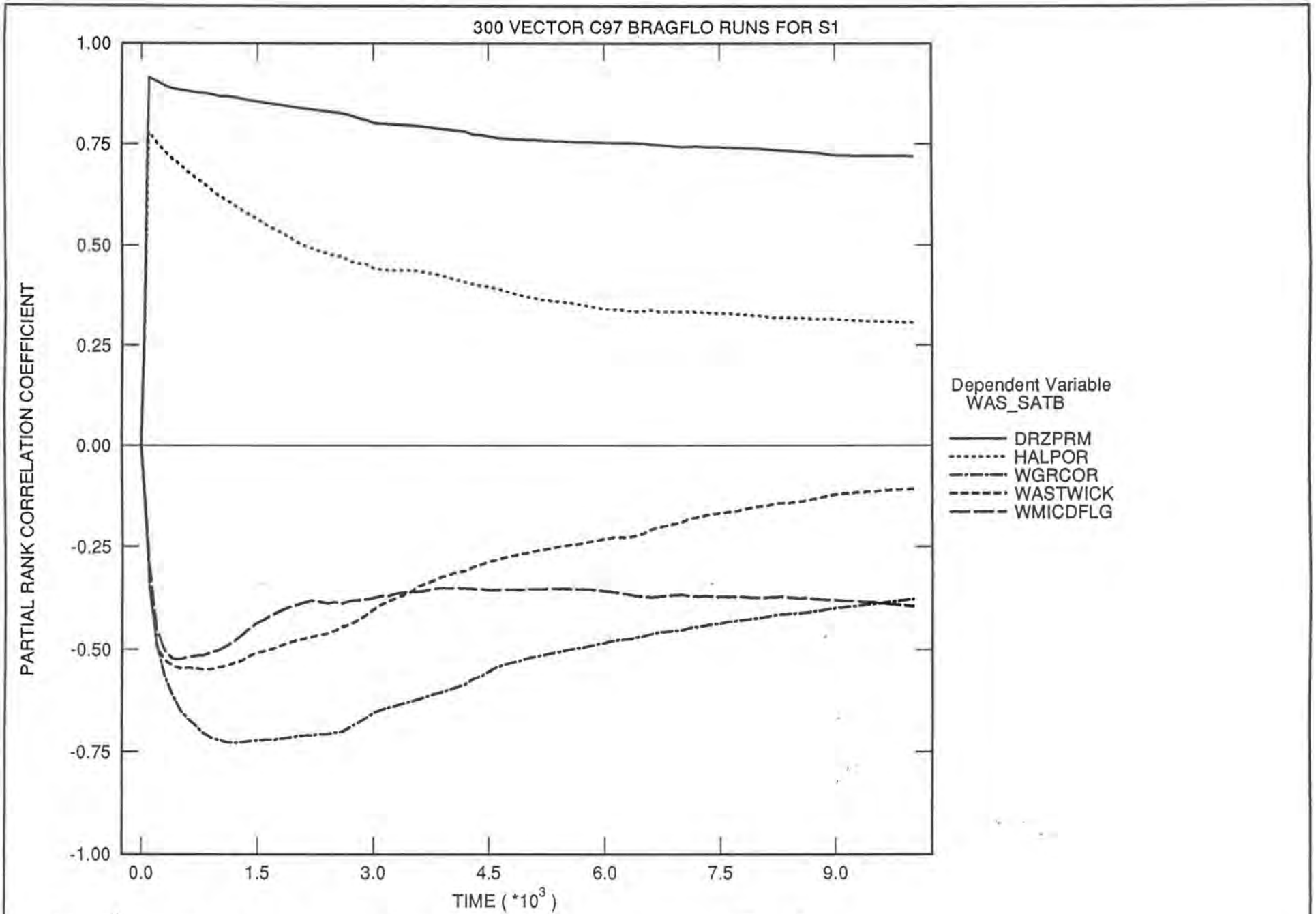

Figure 2.1.4.3 Brine Saturation in Lower Panel

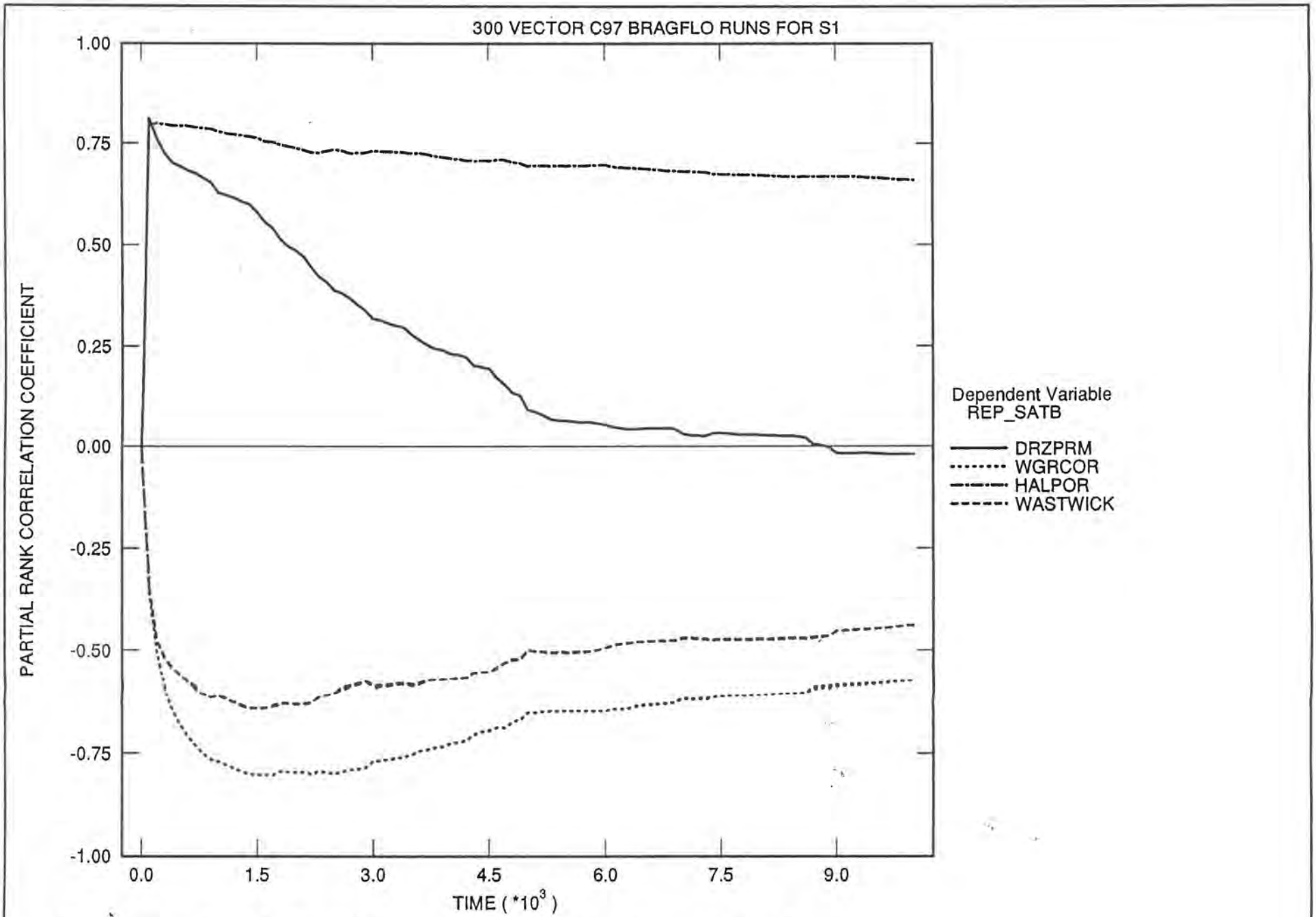

Figure 2.1.4.4 Brine Saturation in Upper Panels

SNL WIPP C97: BRAGFLO SIMULATIONS (C97 R1 S5)

Cumulative Brine Flow into DRZ from All Marker Beds

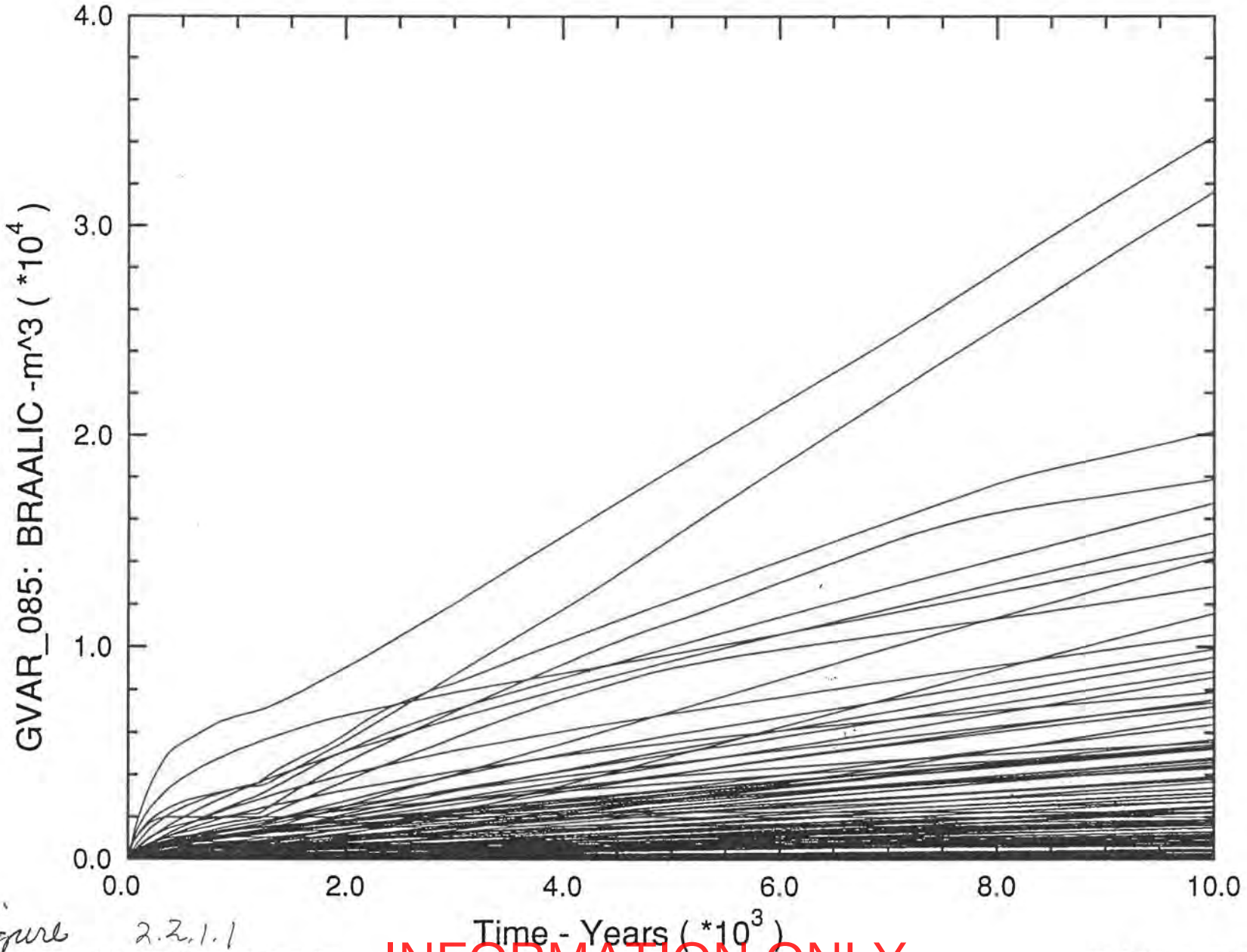

Figure 2.2.1.1

1DRA1:[JEBEAN.C97.SUMMZ.R1S5]SPLAT_R1_S5_H085.INP;1

SPLAT_PA96_2 1.02 05/27/97 13:06:56

SNL WIPP C97: BRAGFLO SIMULATIONS (C97 R1 S3)

Cumulative Brine Flow into DRZ from All Marker Beds

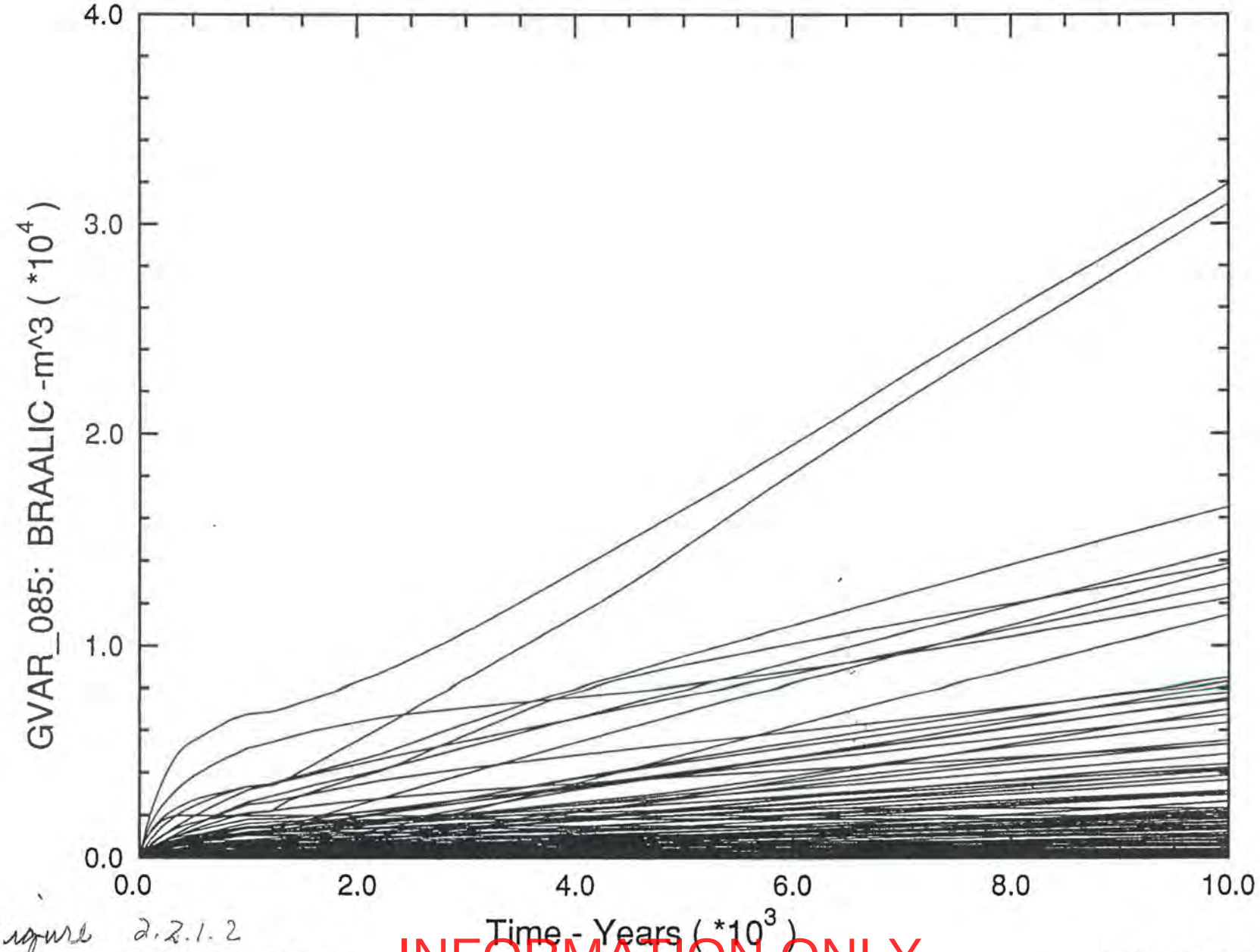

Figure 2.2.1.2

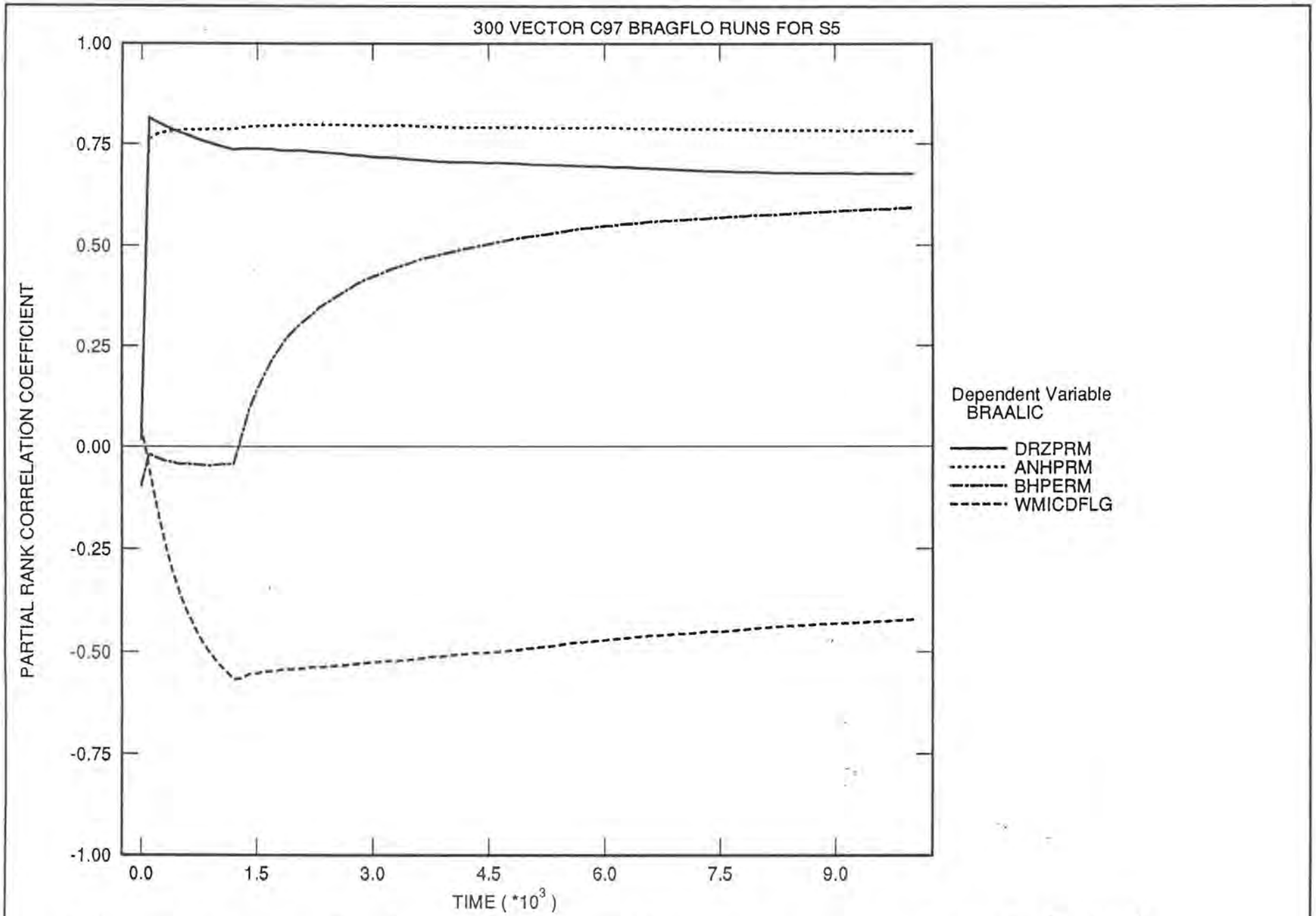

Figure 2.2.1.3 Cumulative Brine Flow into DRZ from all Marker Beds (S5)

U1:[JWGARNE.C97.SEN_ANA.BRAGFLO.E2]PCCSRC_S5.INP;2 PCCSRC PA96 2.21 08/06/97 10:26

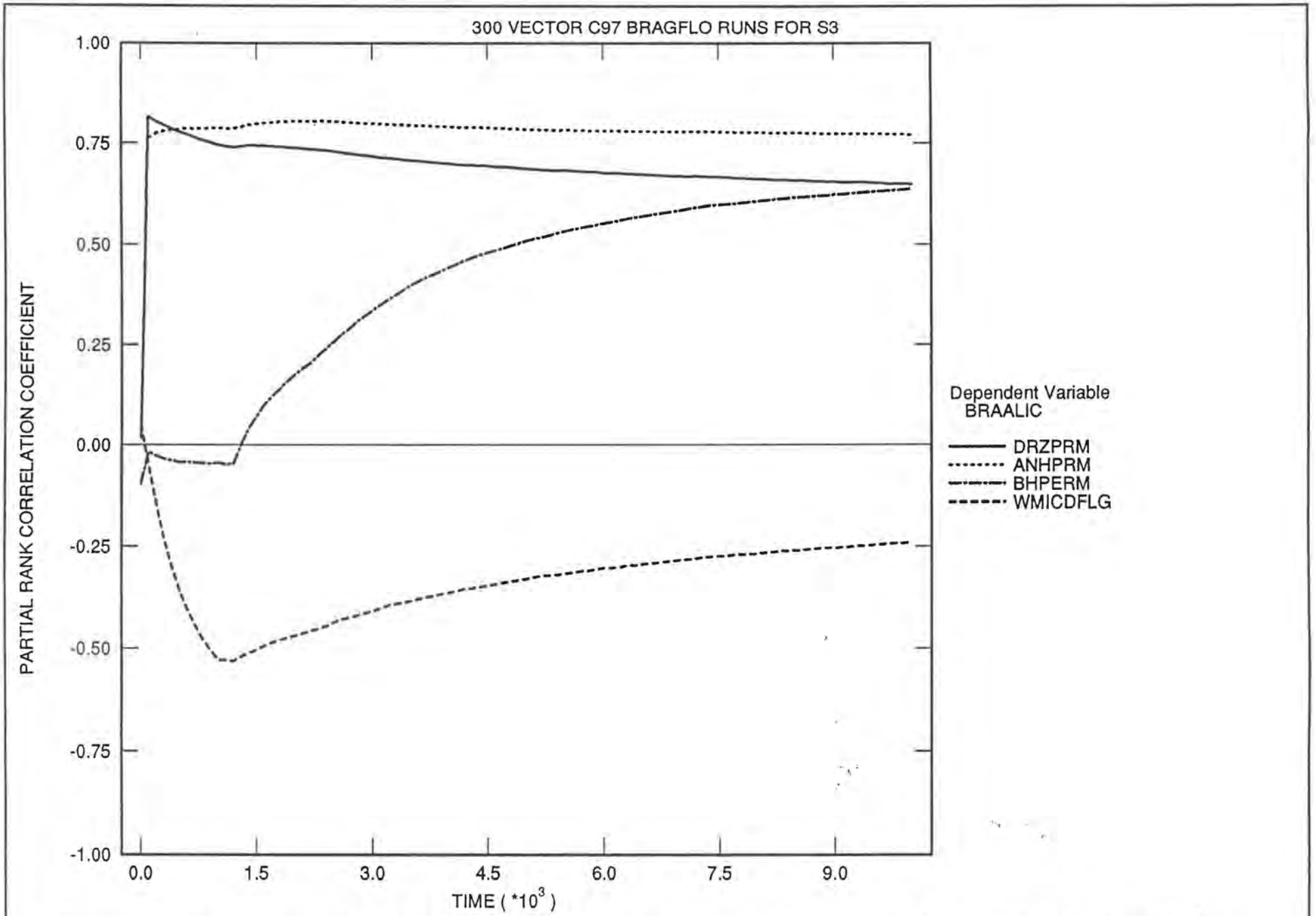

Figure 2.2.1.4 Cumulative Brine Flow into DRZ from all Marker Beds (S3)

SNL WIPP C97: BRAGFLO SIMULATIONS (C97 R1 S5)

Cumulative Brine Flow into Repository

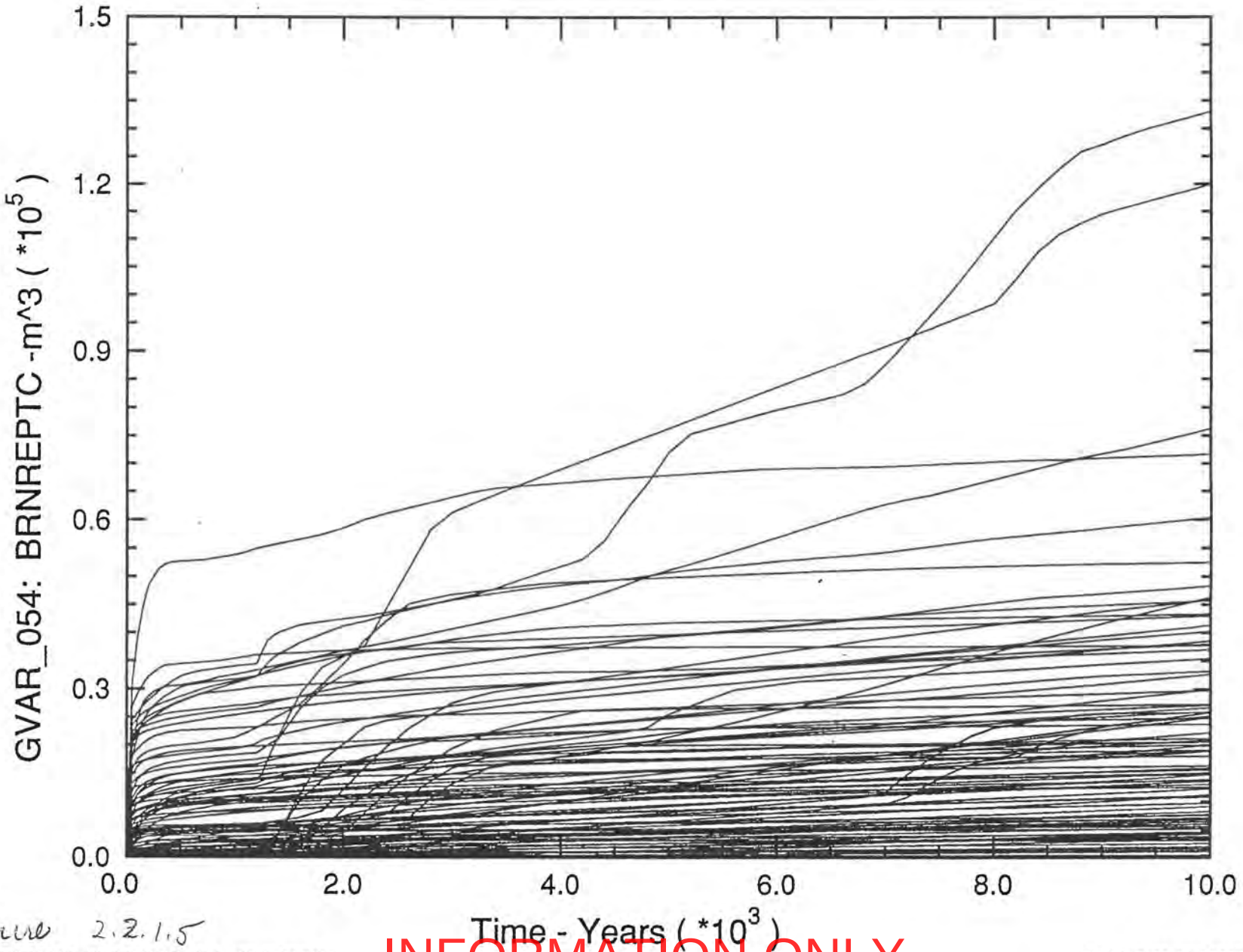

Figure 2.2.1.5

1DRA1:[JEBEAN.C97.SUMMZ.R1S5]SPLAT_R1_S5_H054.INP;1

SPLAT_PA96_2 1.02 05/27/97 11:08:22

SNL WIPP C97: BRAGFLO SIMULATIONS (C97 R1 S3)

Cumulative Brine Flow into Repository

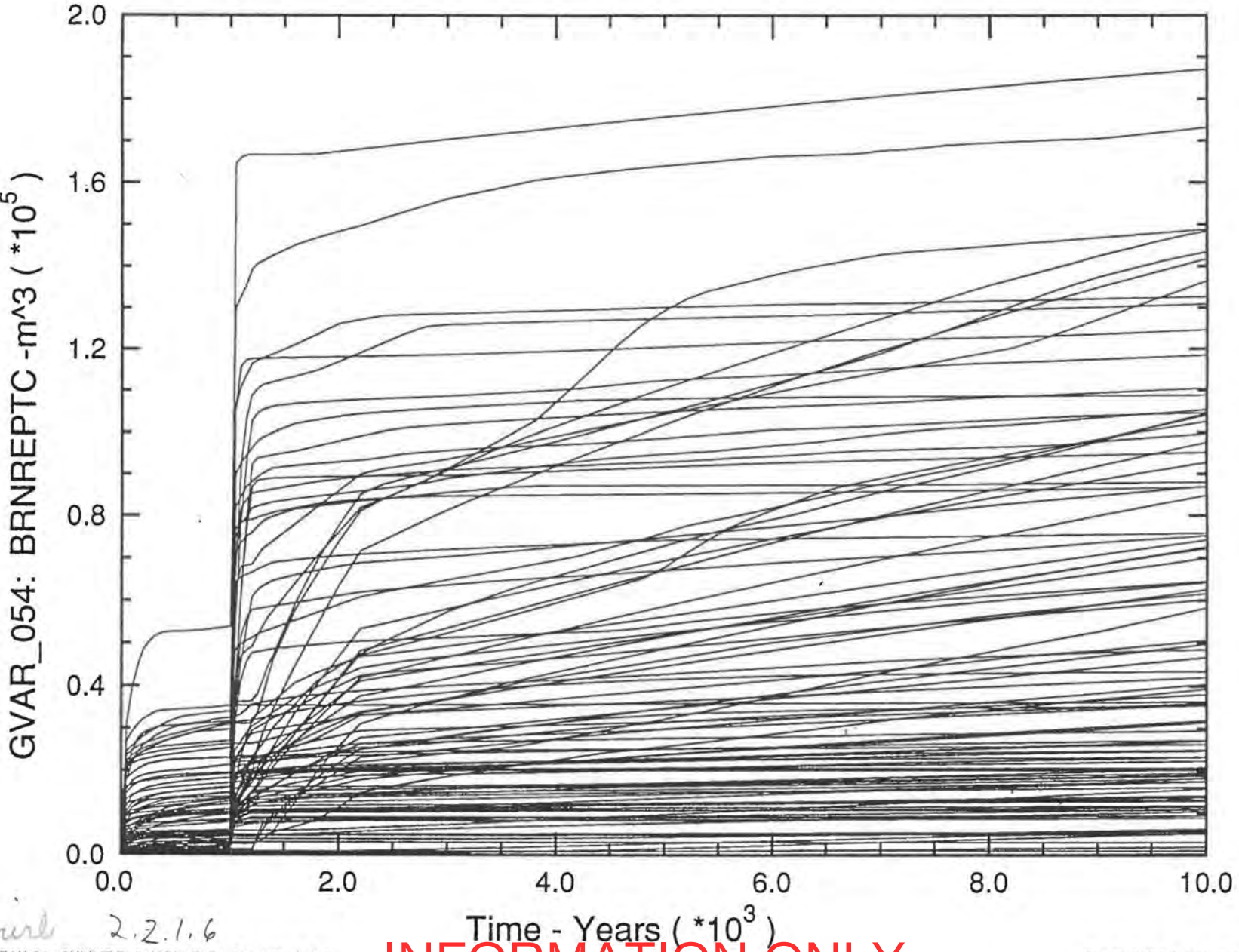

Figure 2.2.1.6

1DRA1:[JEBEAN.C97.SUMMZ.R1S3]SPLAT_R1_S3_H054.INP;1

SPLAT_PA96_2 1.02 05/27/97 10:12:24

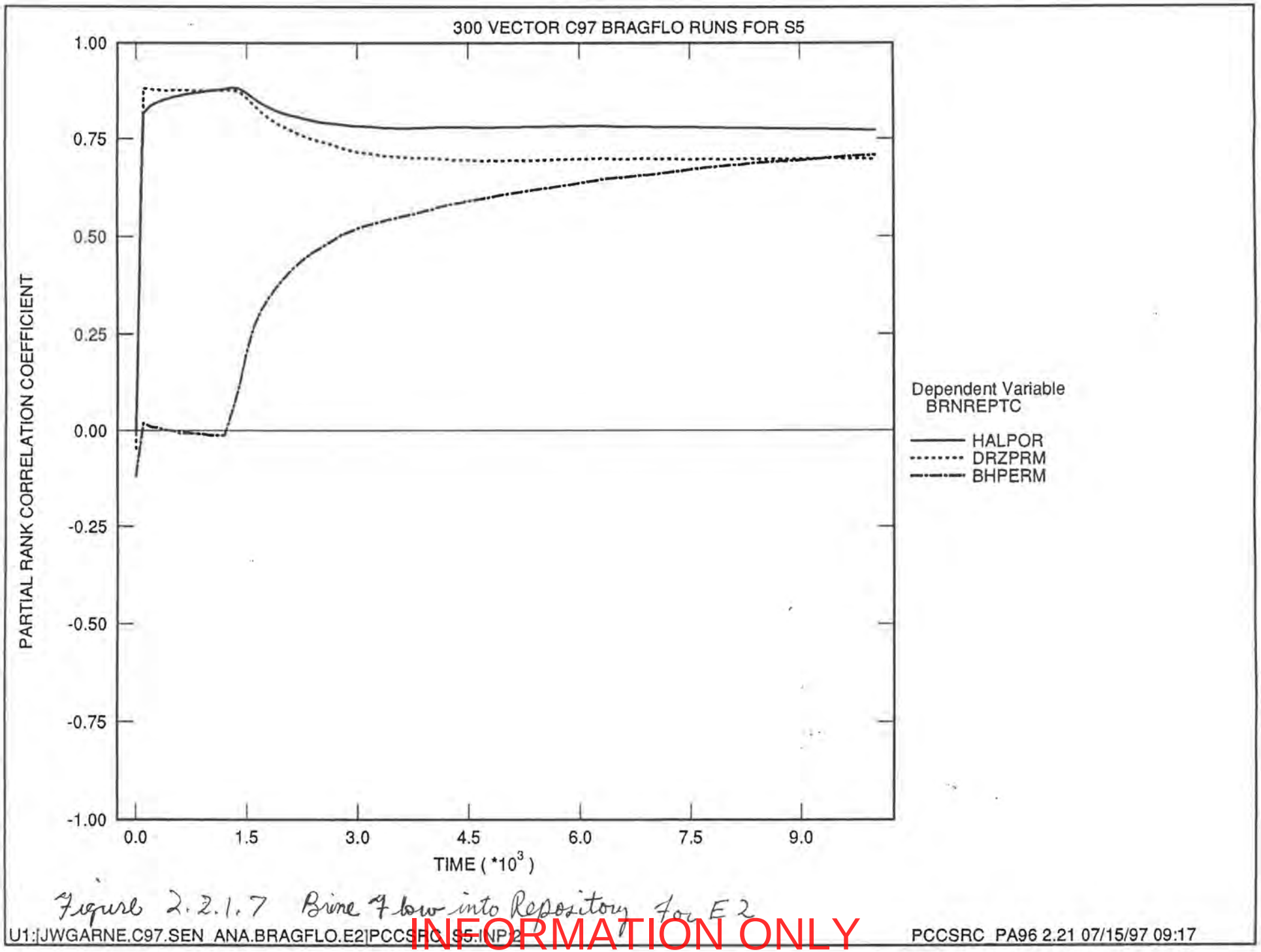

Figure 2.2.1.7 Brine flow into Repository for E2

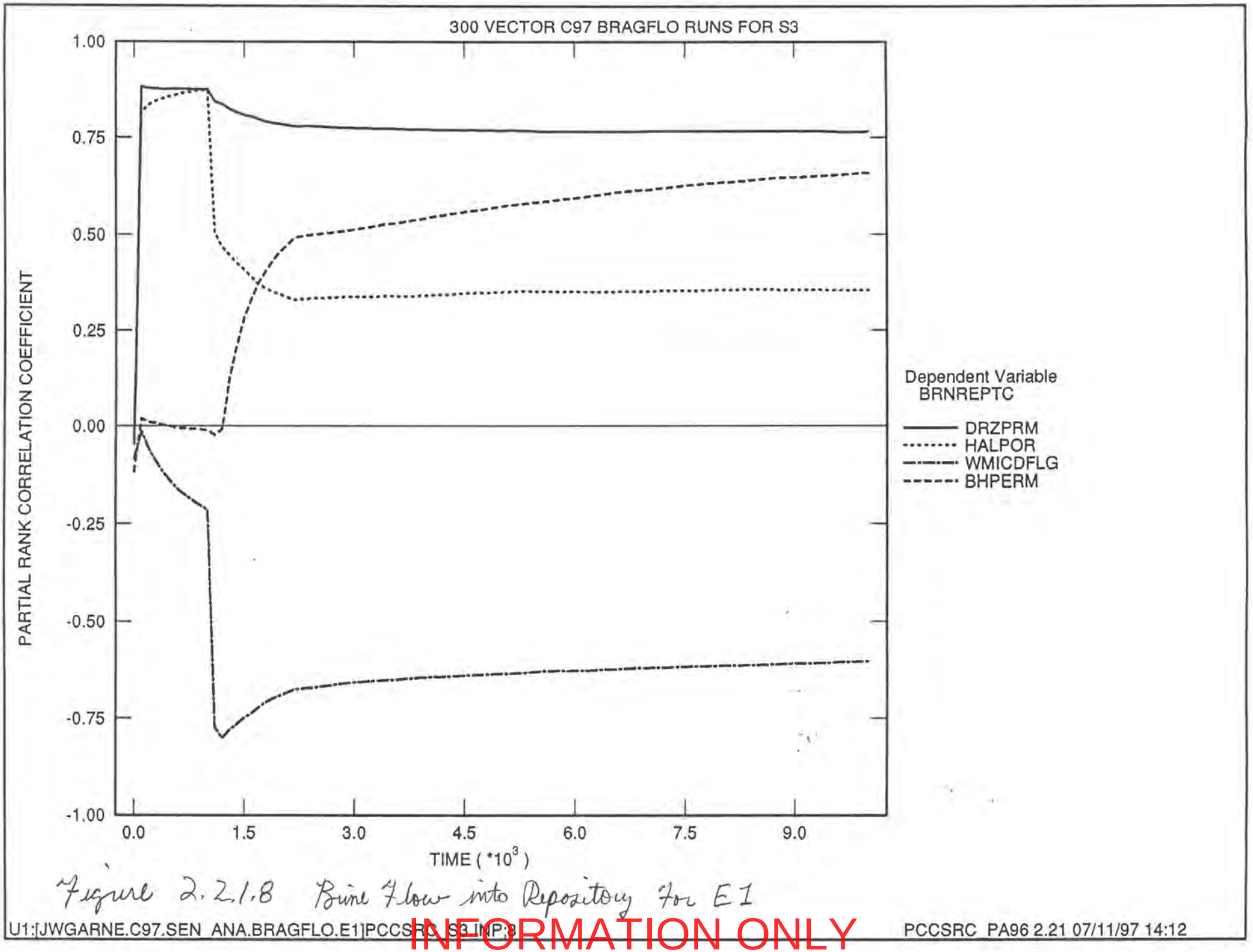

Figure 2.2.1.8 Brine Flow into Repository for E1

SNL WIPP C97: BRAGFLO SIMULATIONS (C97 R1 S5)

Cumulative Brine Flow Down Borehole at MB 138 (E:223)

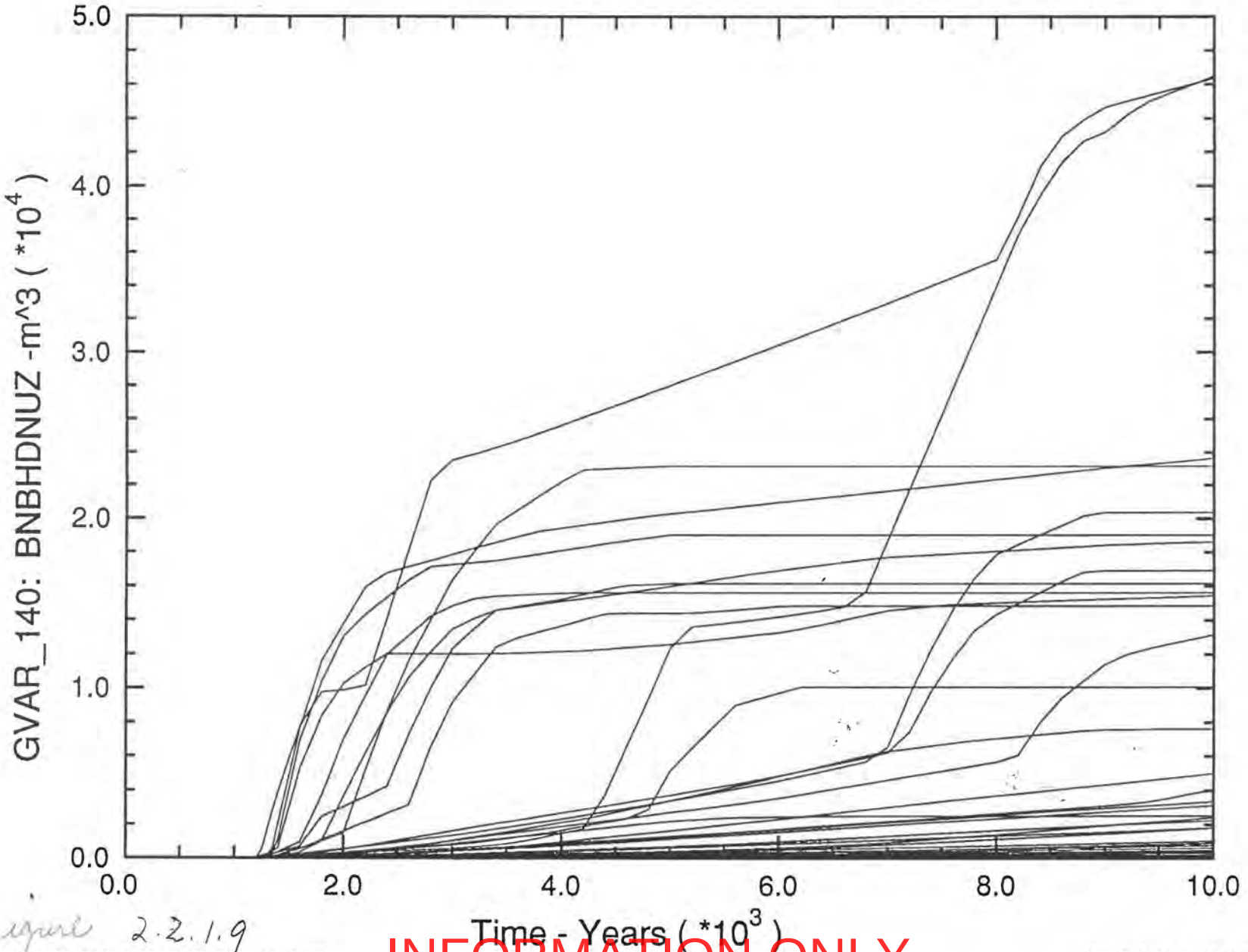

Figure 2.2.1.9

SNL WIPP C97: BRAGFLO SIMULATIONS (C97 R1 S3)

Cumulative Brine Flow Down Borehole at MB 138 (E:223)

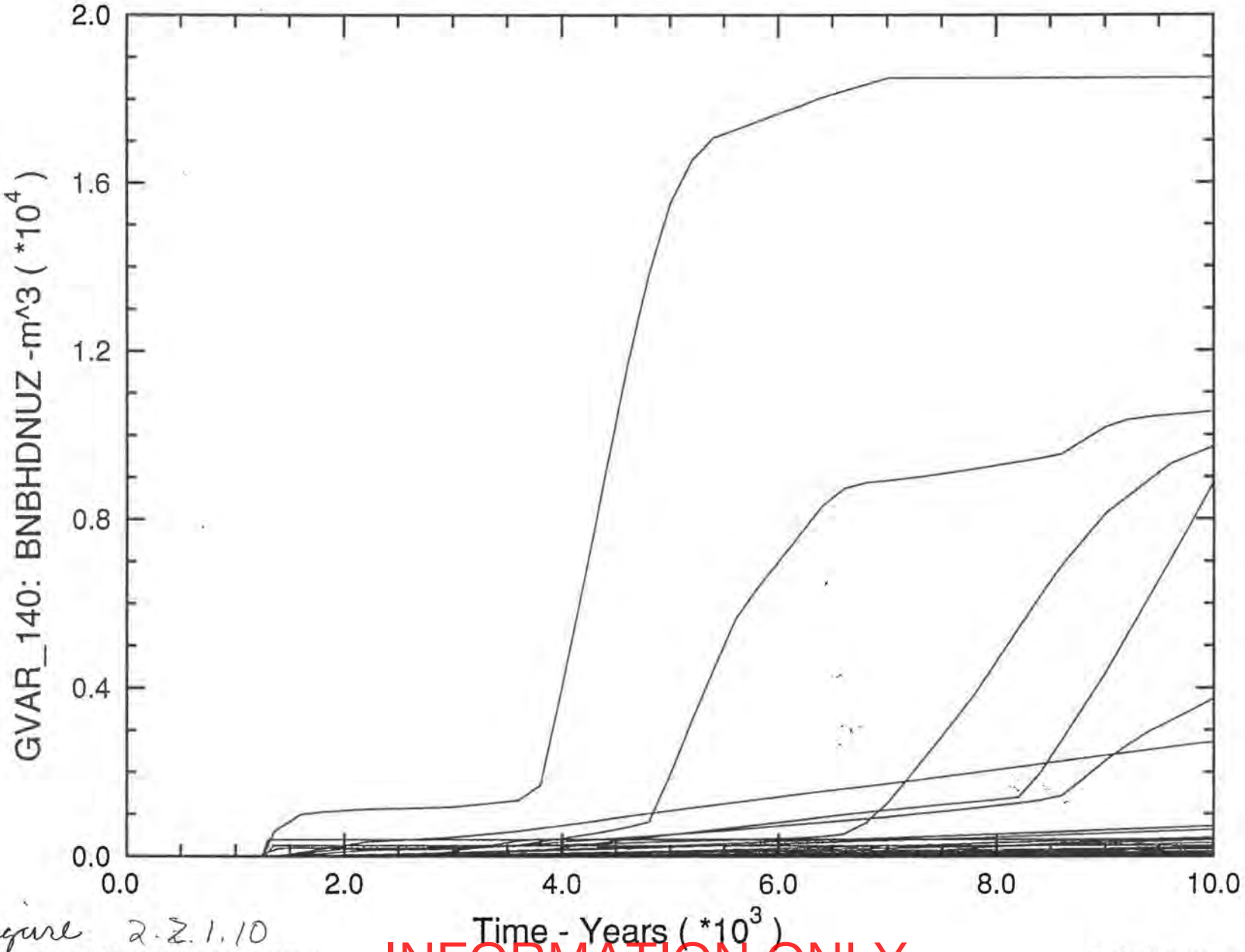

Figure 2.2.1.10

1DRA1:[JEBEAN.C97.SUMMZ.R1S3]SPLAT_R1_S3_H140.INP;1

SPLAT_PA96_2 1.02 05/27/97 14:02:22

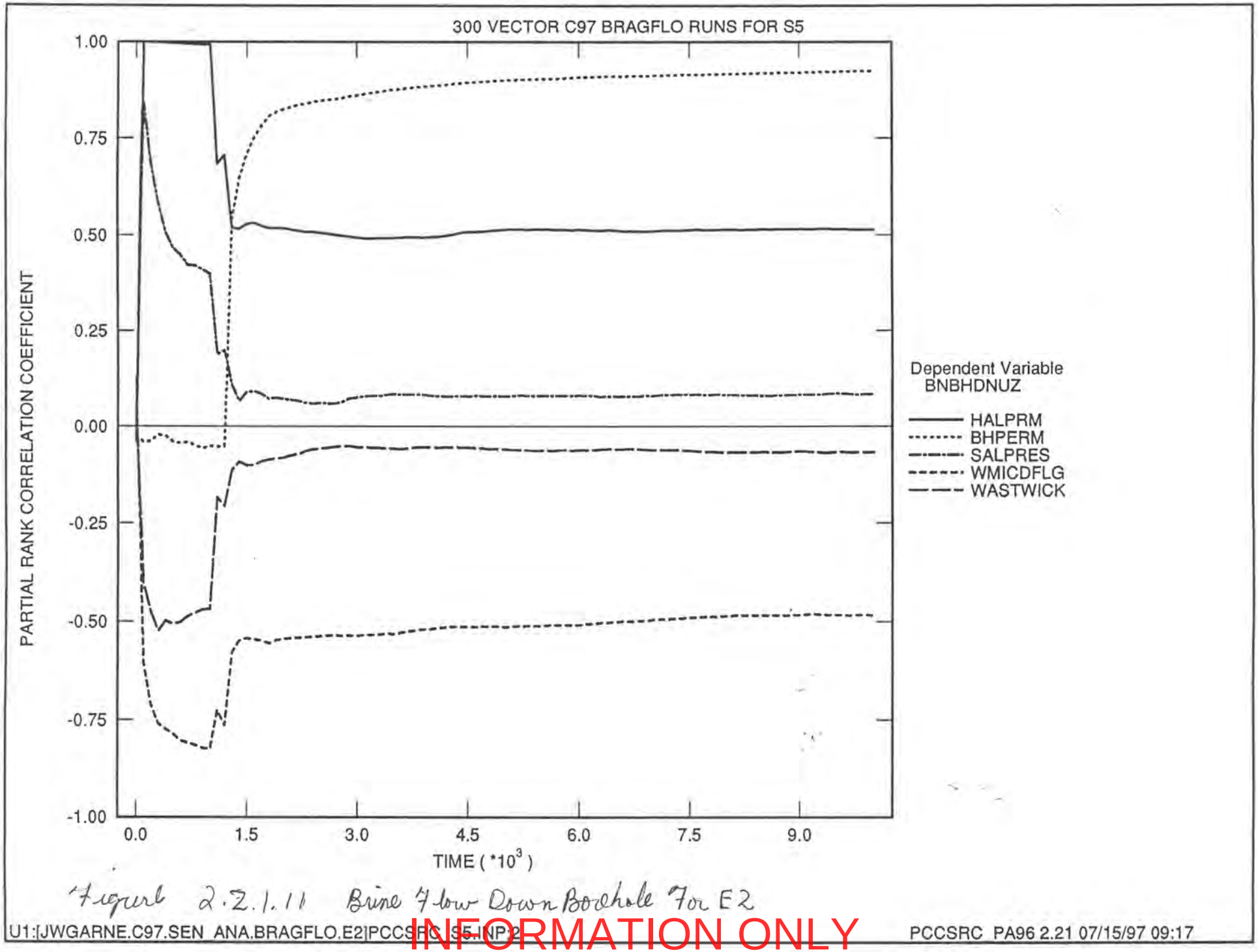

Figure 2.2.1.11 Brine Flow Down Borehole for E2

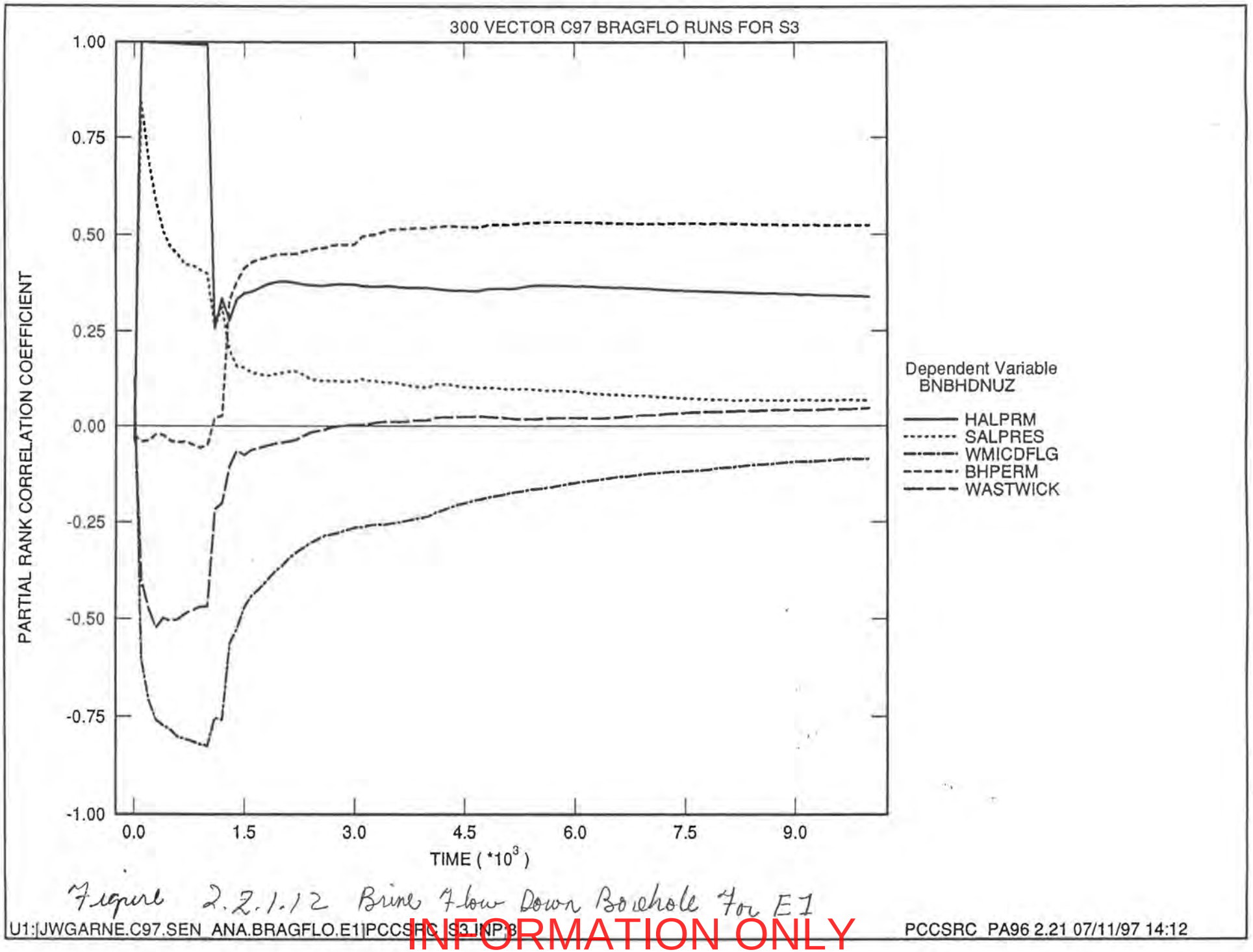

Figure 2.2.1.12 Brine Flow Down Borehole for E1

SNL WIPP C97: BRAGFLO SIMULATIONS (C97 R1 S3)

Cumulative Brine Flow up Borehole into Bottom of Lower DRZ (E:439)

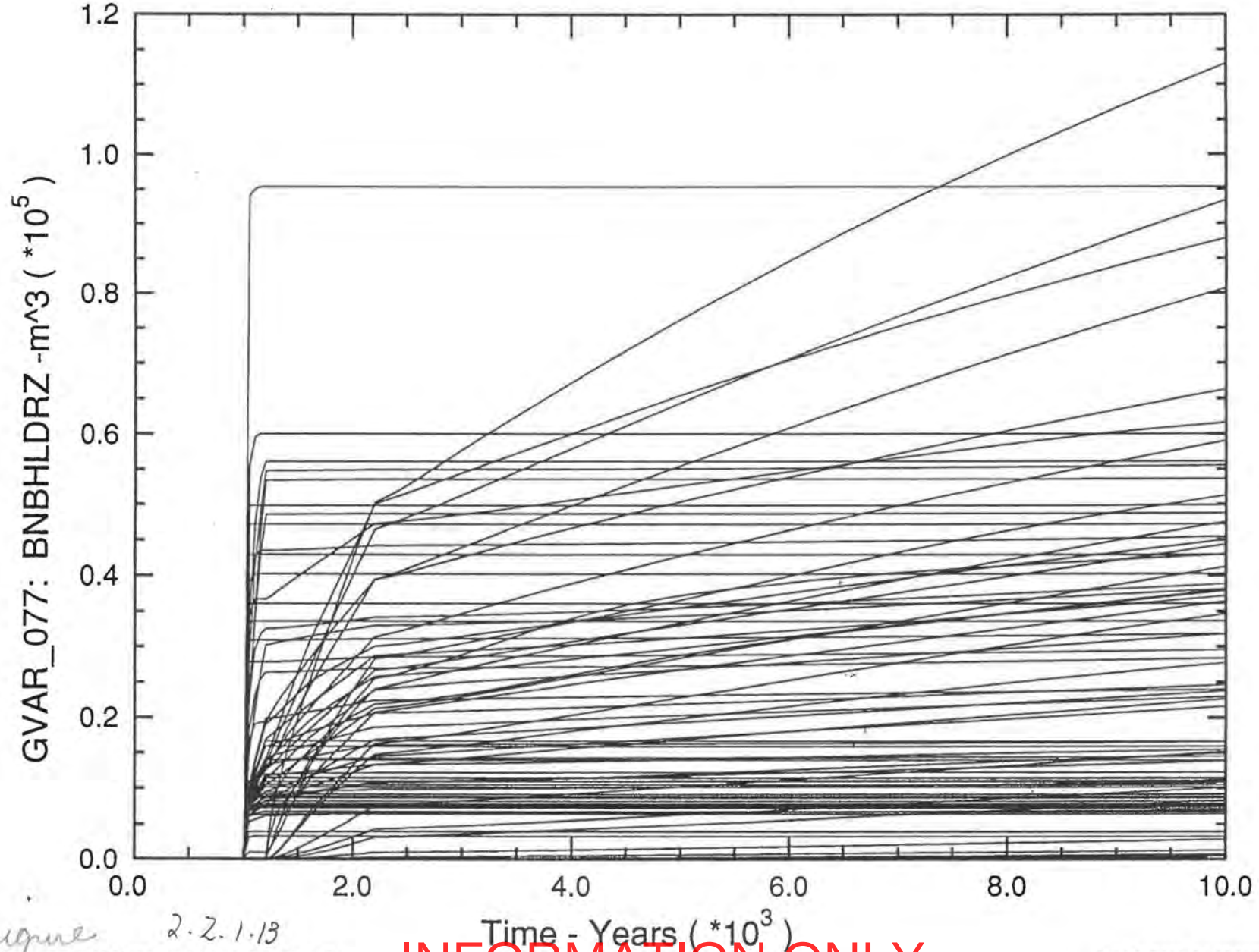

Figure 2.2.1.13

1DRA1:[JEBEAN.C97.SUMMZ.R1S3]SPLAT_R1_S3_H077.INP;1

SPLAT_PA96_2 1.02 05/27/97 11:14:54

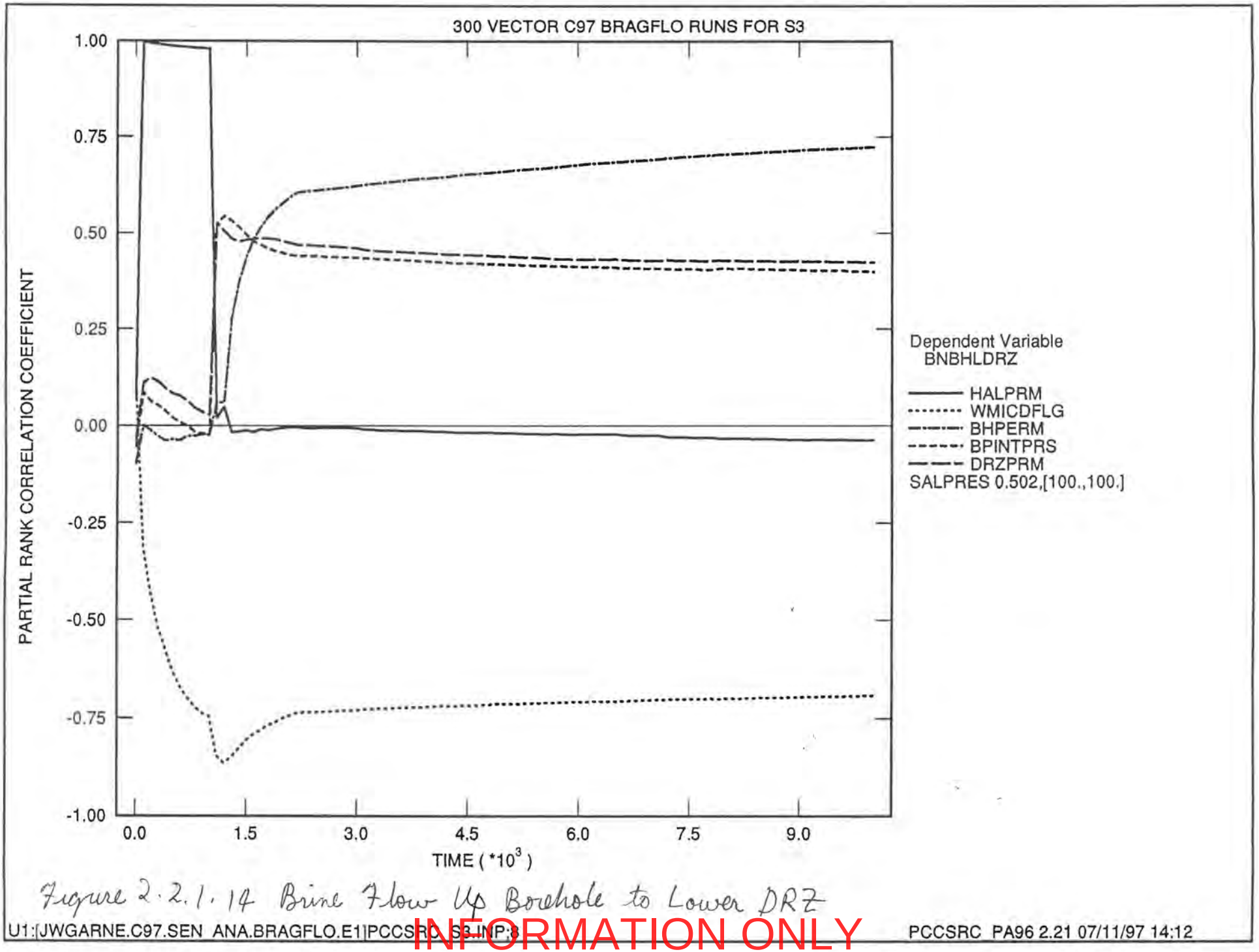

Figure 2.2.1.14 Brine Flow Up Borehole to Lower DRZ

SNL WIPP C97: BRAGFLO SIMULATIONS (C97 R1 S5)

Cumulative Gas Generated by Corrosion

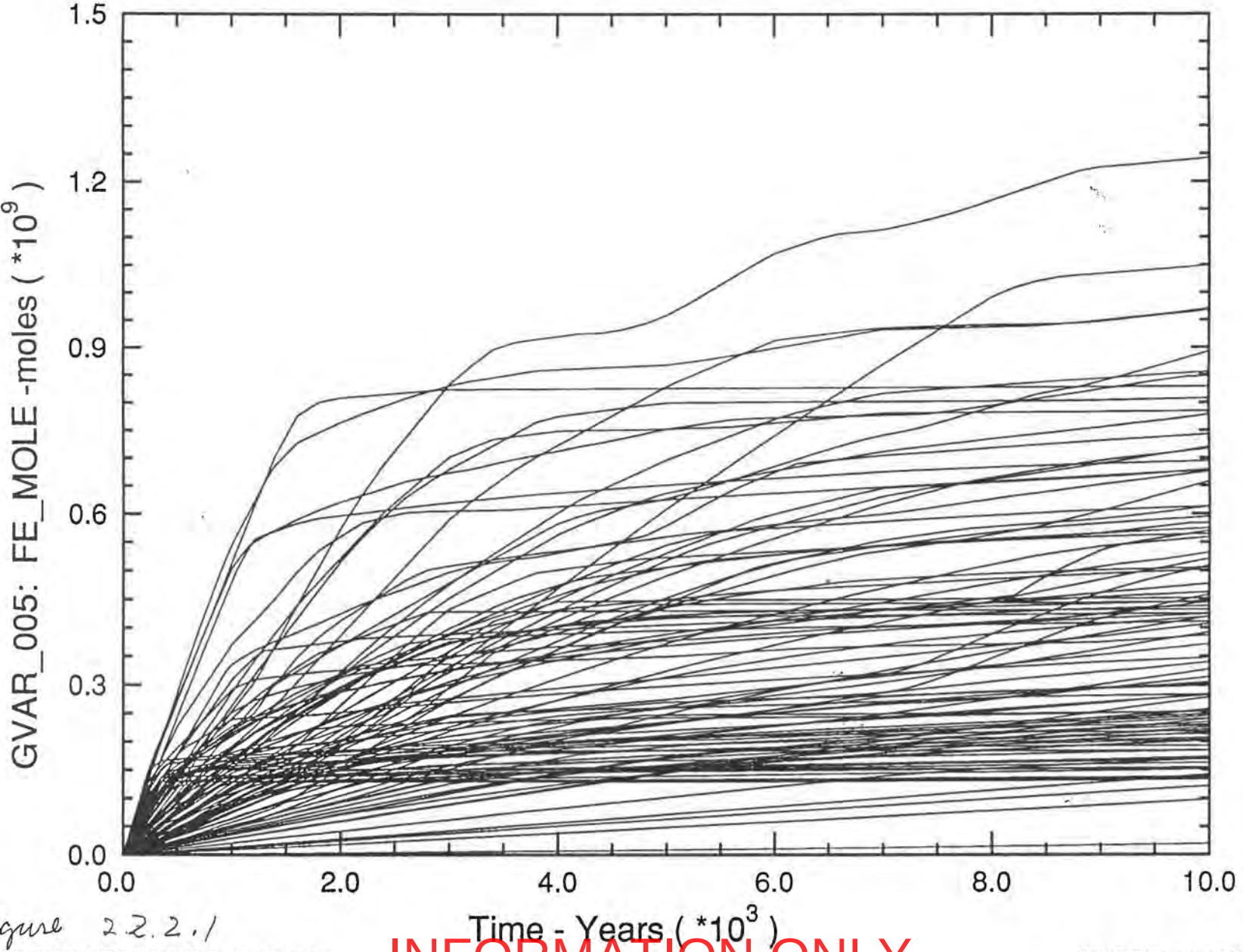

Figure 22.2.1

1DRA1:[JEBEAN.C97.SUMMZ.R1S5]SPLAT_R1_S5_H005.INP;1

SPLAT_PA96_2 1.02 05/27/97 08:07:57

SNL WIPP C97: BRAGFLO SIMULATIONS (C97 R1 S3)

Cumulative Gas Generated by Corrosion

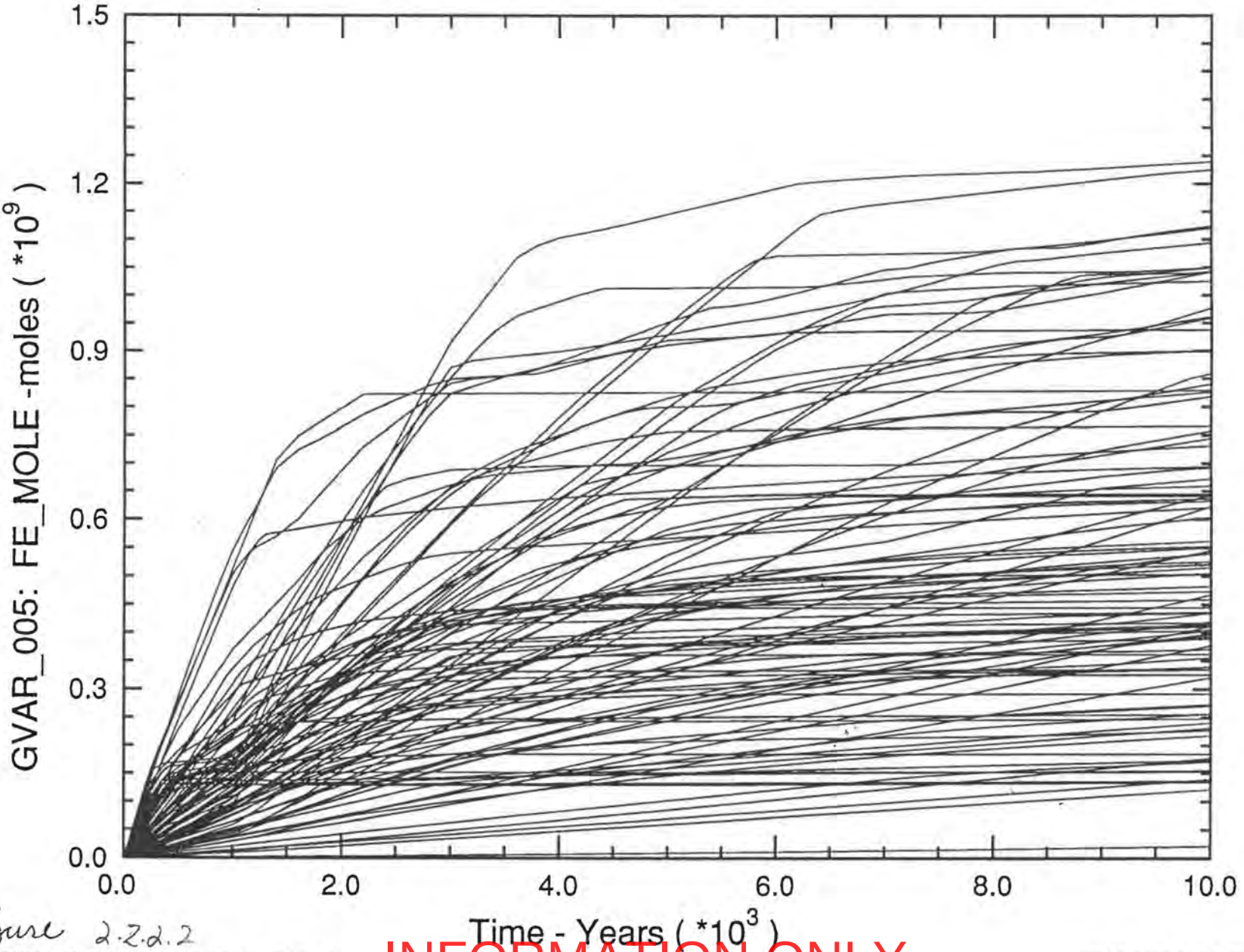

Figure 2.2.2.2

1DRA1:[JEBEAN.C97.SUMMZ.R1S3]SPLAT_R1_S3_H005.INP;1

SPLAT_PA96_2 1.02 05/27/97 08:02:09

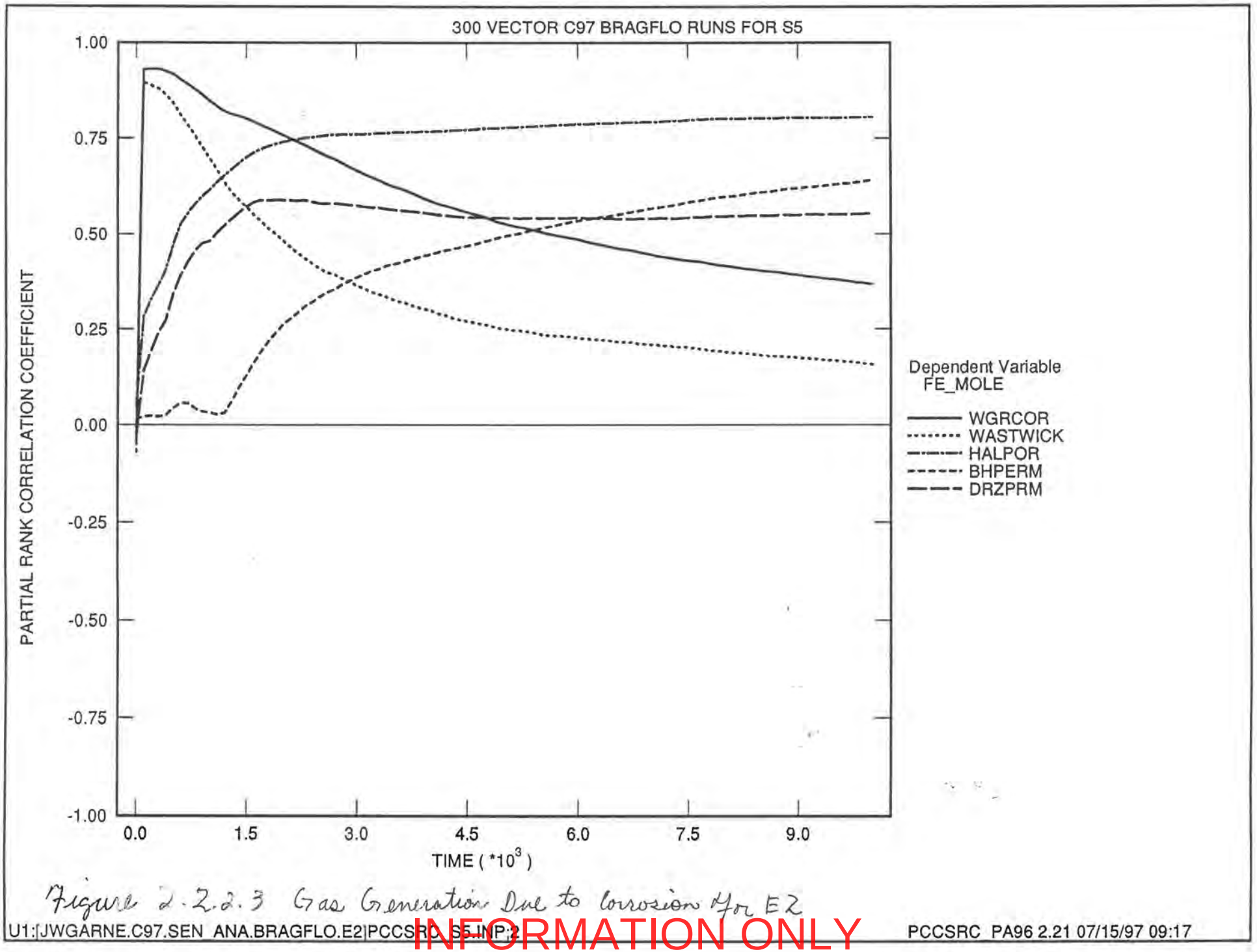

Figure 2.2.2.3 Gas Generation Due to Corrosion for E2

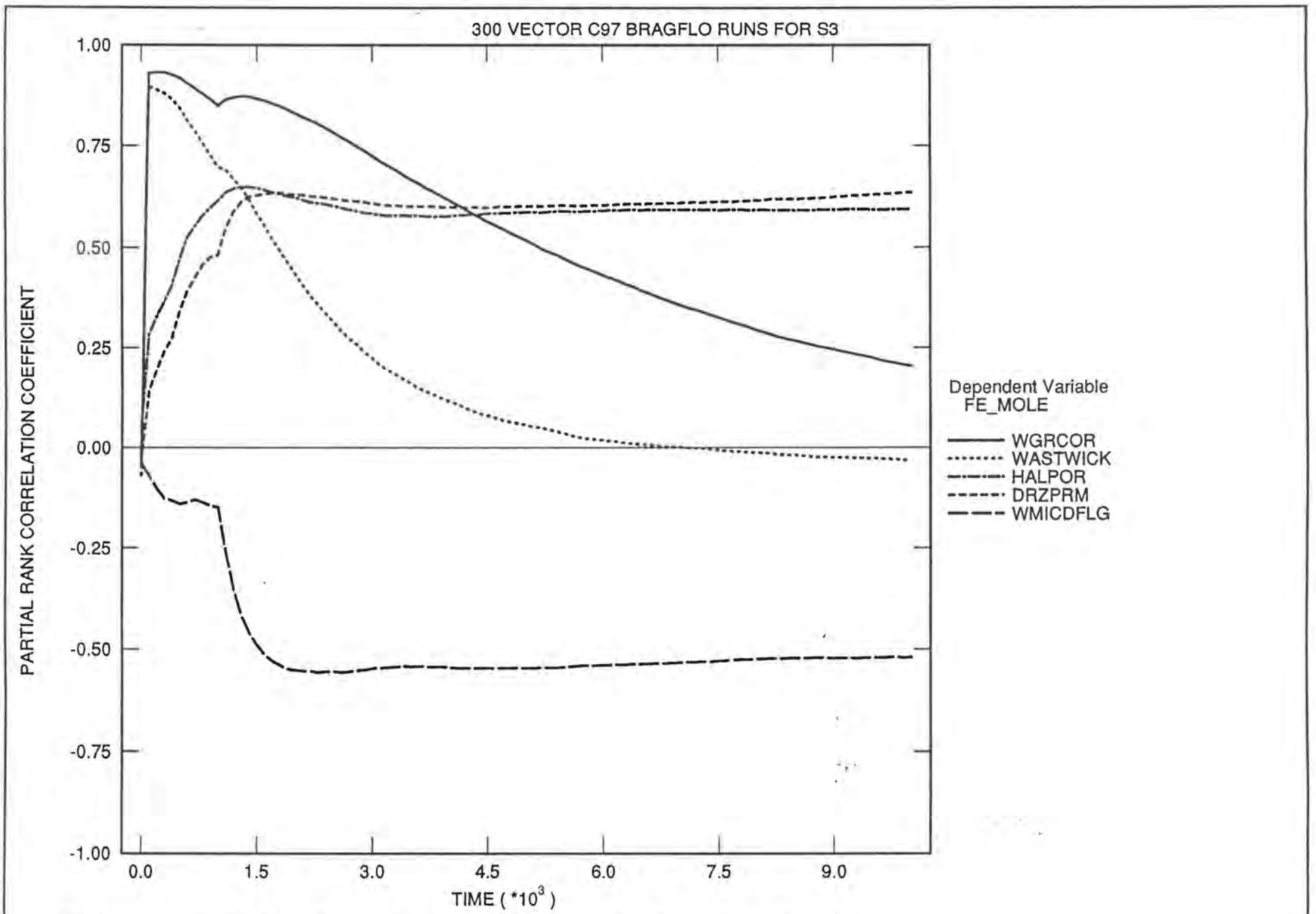

Figure 2.2.2.4 Gas Generation Due to Corrosion For E1

SNL WIPP C97: BRAGFLO SIMULATIONS (C97 R1 S5)

Total Gas Generated

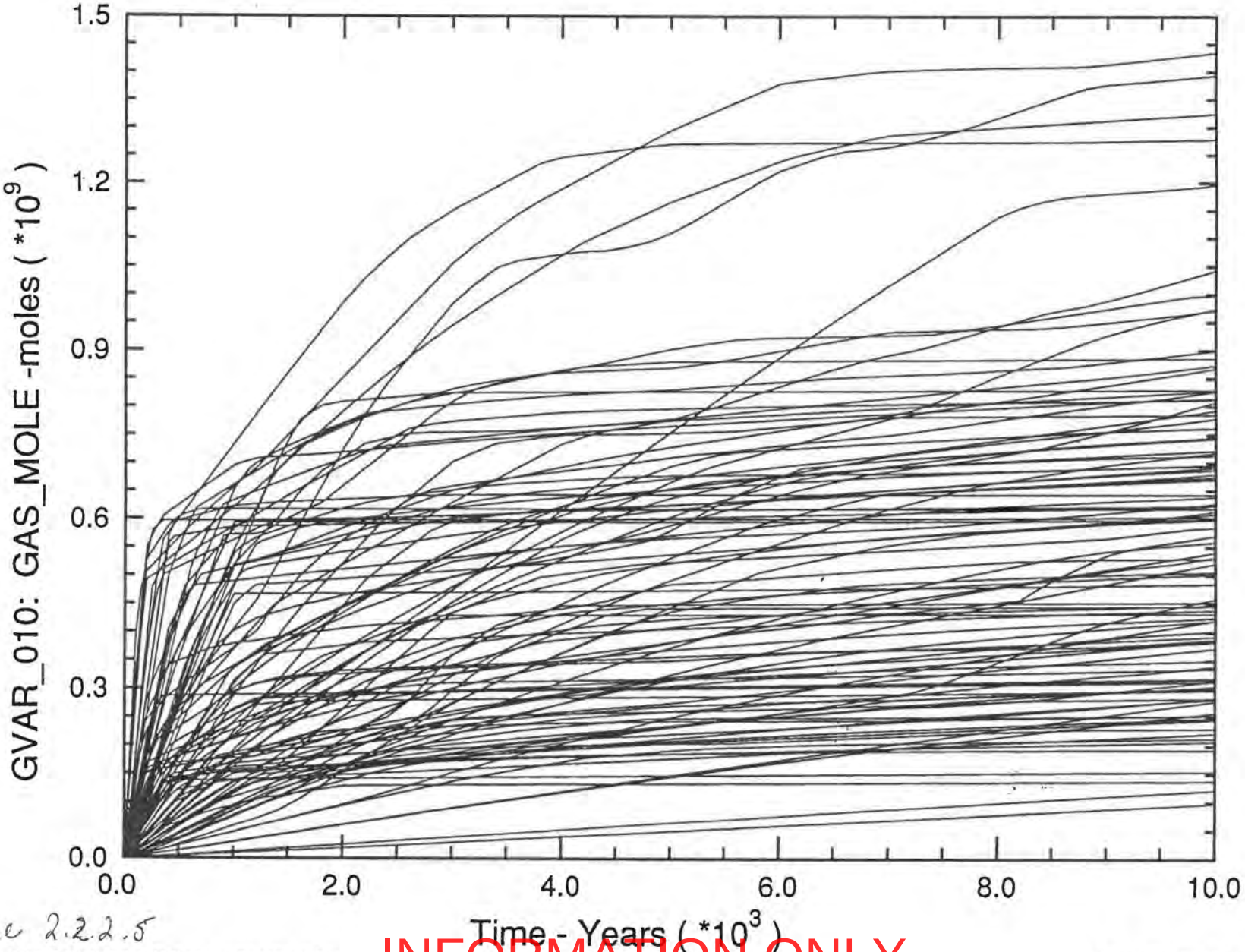

Figure 2.2.2.5

1DRA1:[JEBEAN.C97.SUMMZ.R1S5]SPLAT_R1_S5_H010.INP;1

SPLAT_PA96_2 1.02 05/27/97 08:27:13

SNL WIPP C97: BRAGFLO SIMULATIONS (C97 R1 S3)

Total Gas Generated

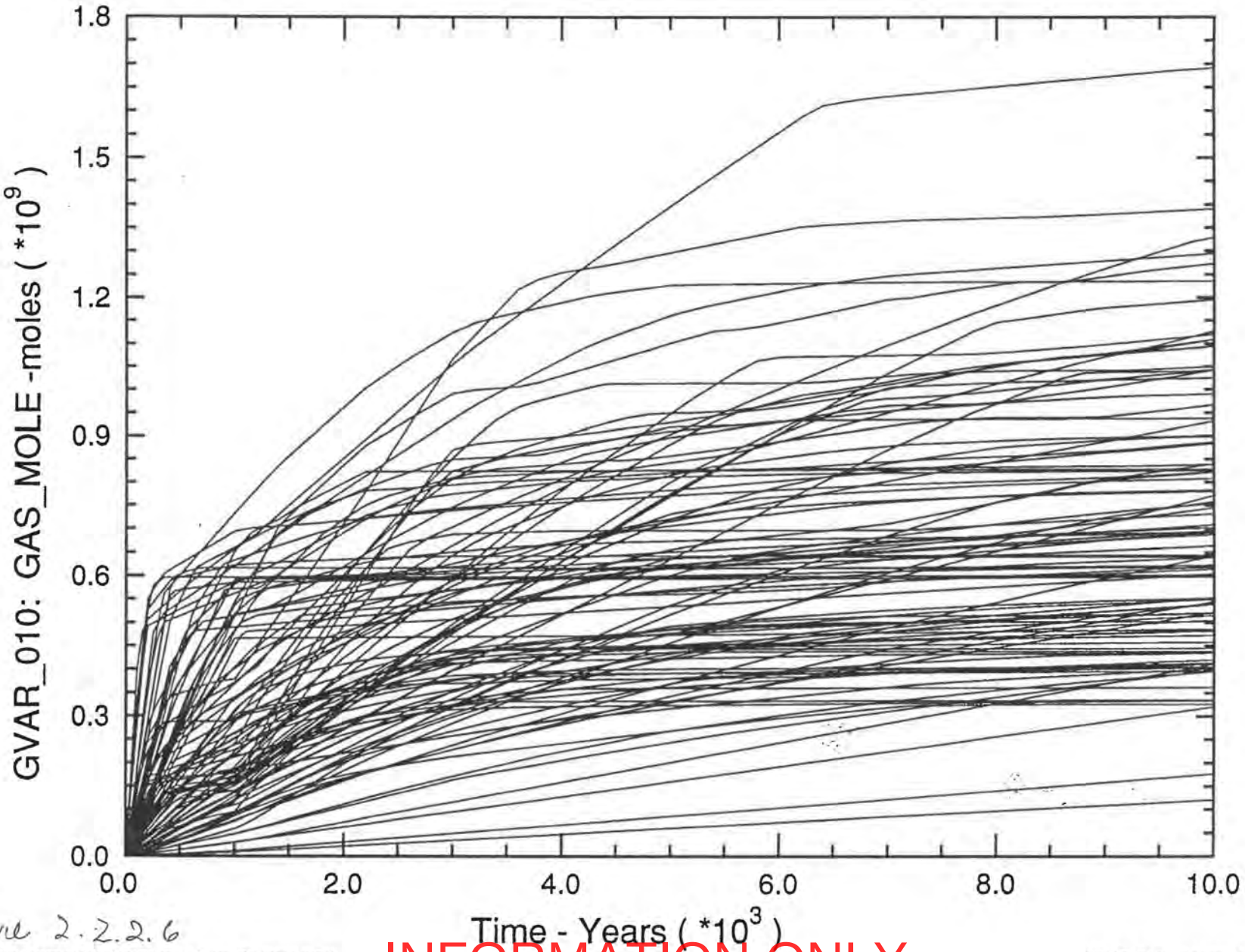

Figure 2.2.2.6

1DRA1:[JEBEAN.C97.SUMMZ.R1S3]SPLAT_R1_S3_H010.INP;1

SPLAT_PA96_2 1.02 05/27/97 08:15:04

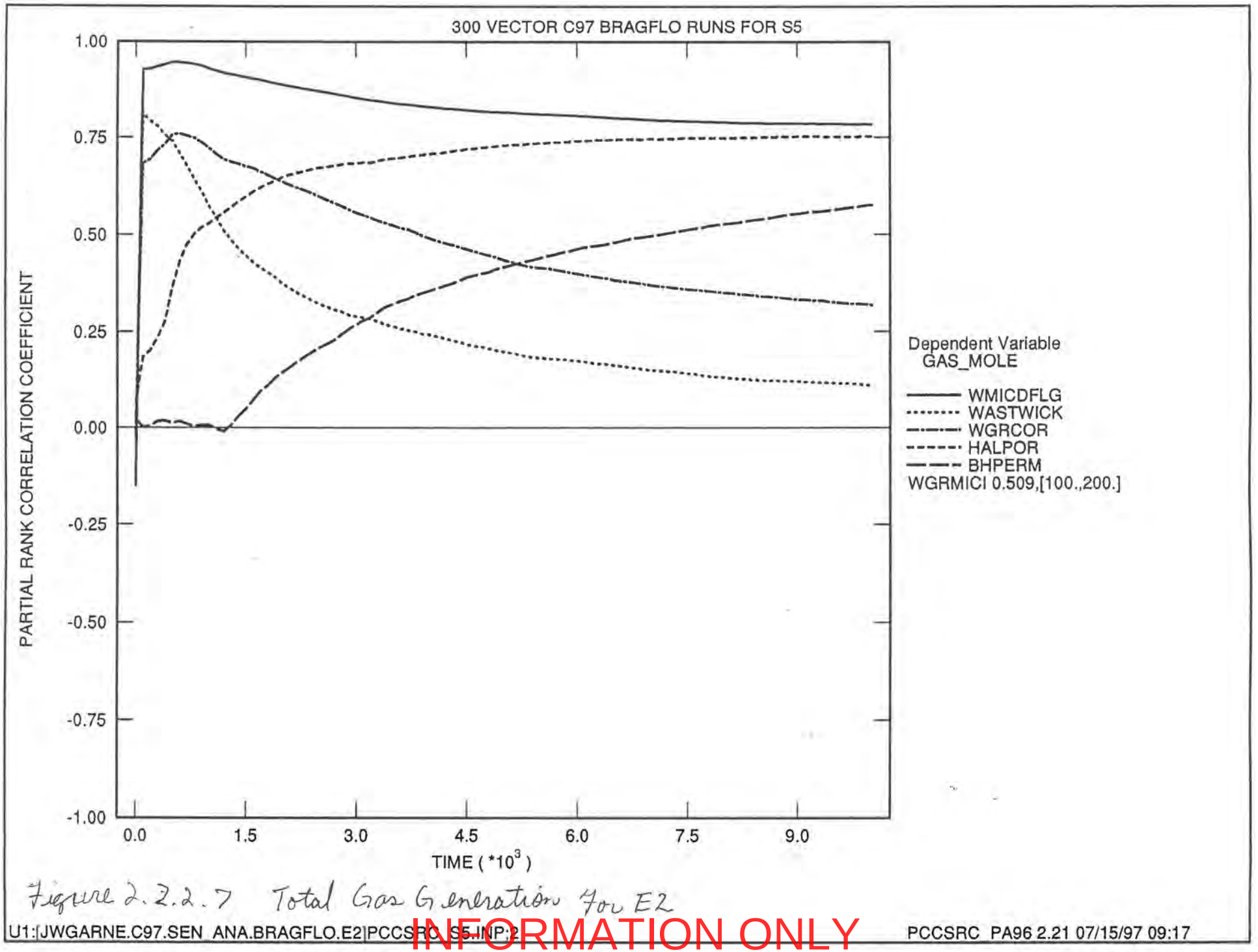

Figure 2.2.2.7 Total Gas Generation for E2

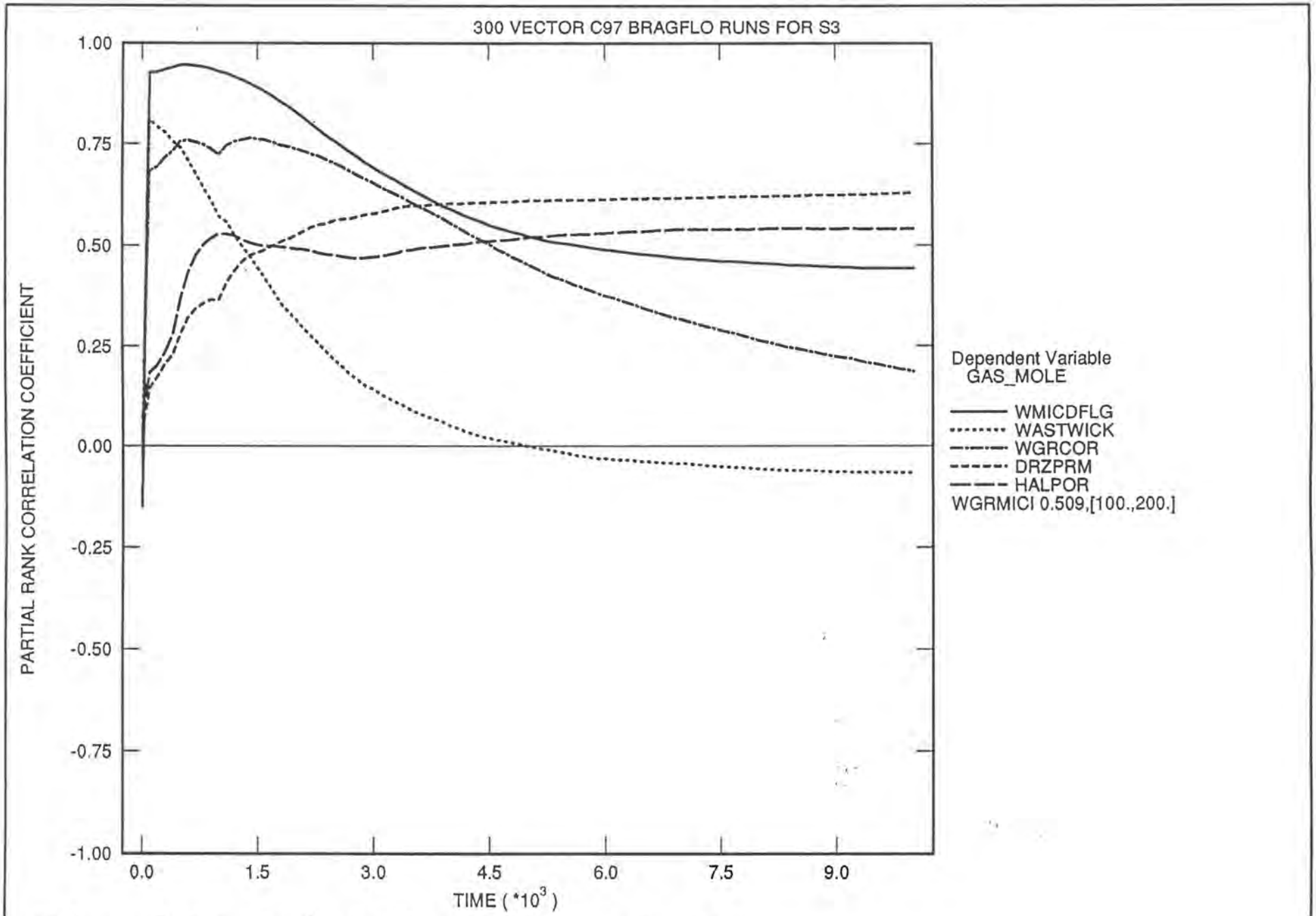

Figure 2.2.2.8 Total Gas Generation for E1

SNL WIPP C97: BRAGFLO SIMULATIONS (C97 R1 S5)

Remaining Fraction of Steel Inventory in Waste Panel

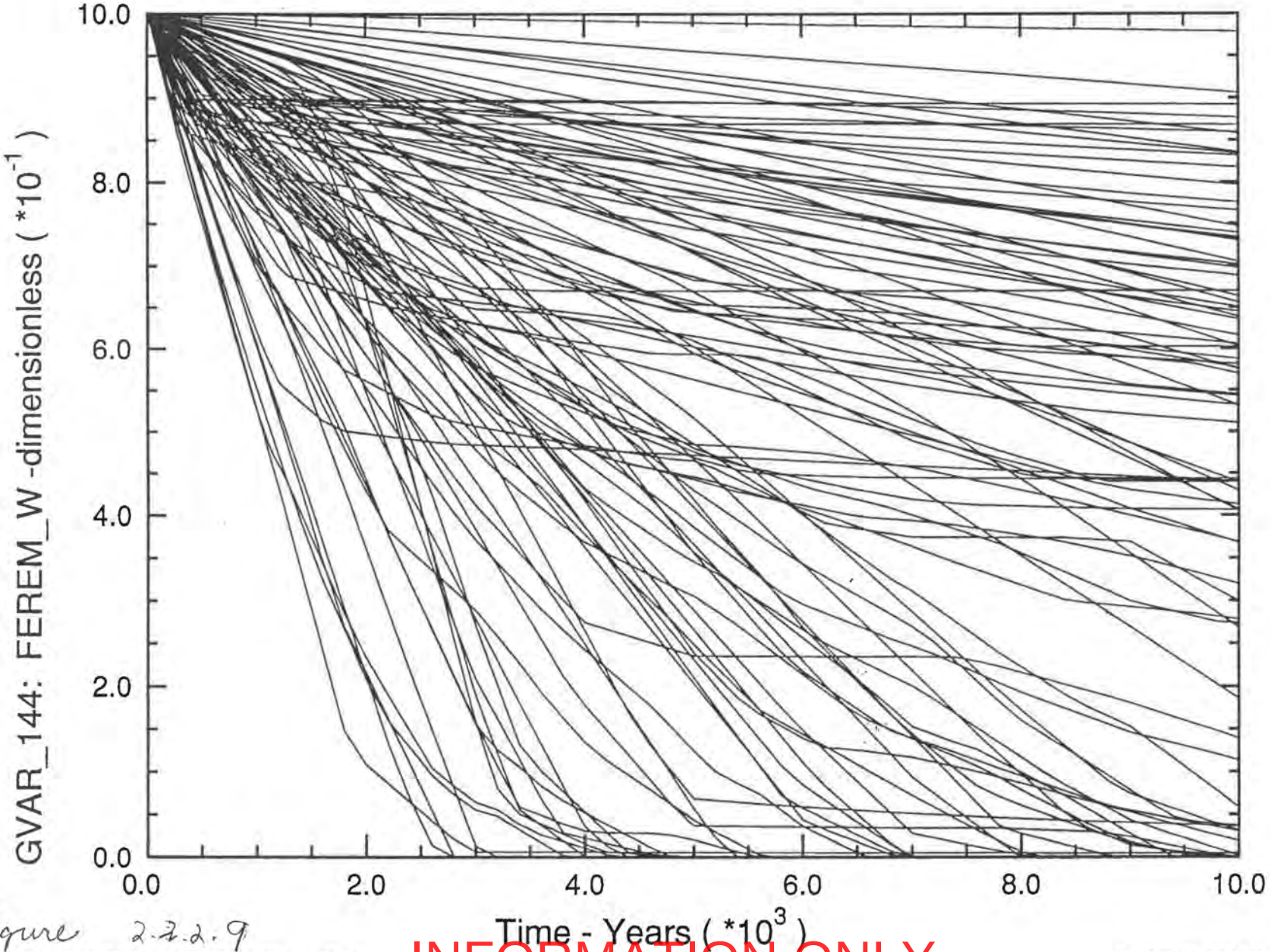

Figure 2.7.2.9

1DRA1:[JEBEAN.C97.SUMMZ.R1S5]SPLAT_R1_S5_H144.INP;1

SPLAT_PA96_2 1.02 05/28/97 10:24:58

SNL WIPP C97: BRAGFLO SIMULATIONS (C97 R1 S3)

Remaining Fraction of Steel Inventory in Waste Panel

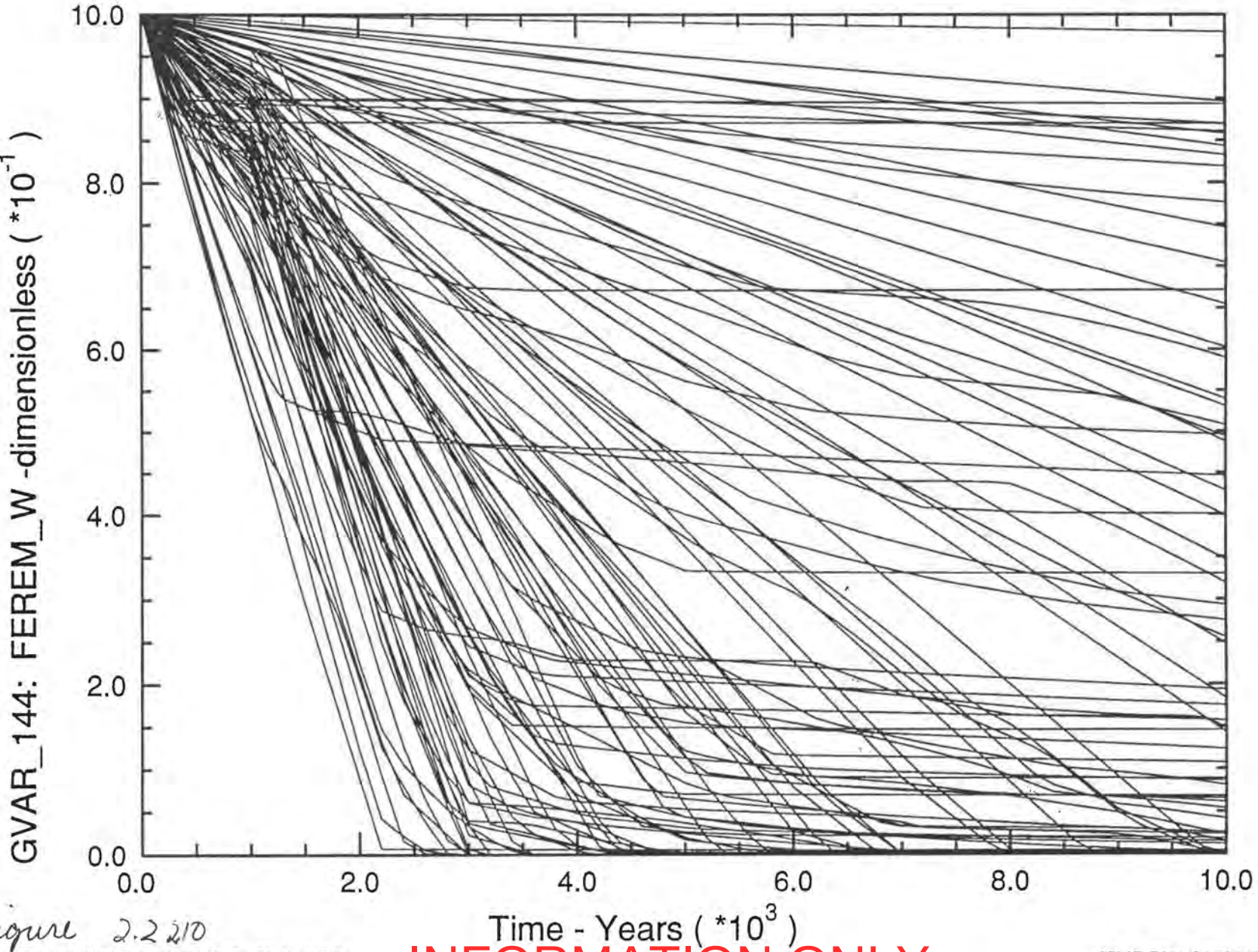

Figure 2.2.2.10

1DRA1:[JEBEAN.C97.SUMMZ.R1S3]SPLAT_R1_S3_H144.INP;1

INFORMATION ONLY

SPLAT_PA96_2 1.02 05/27/97 14:13:01

SNL WIPP C97: BRAGFLO SIMULATIONS (C97 R1 S5)

Remaining Fraction of Steel Inventory in Rest of Repository

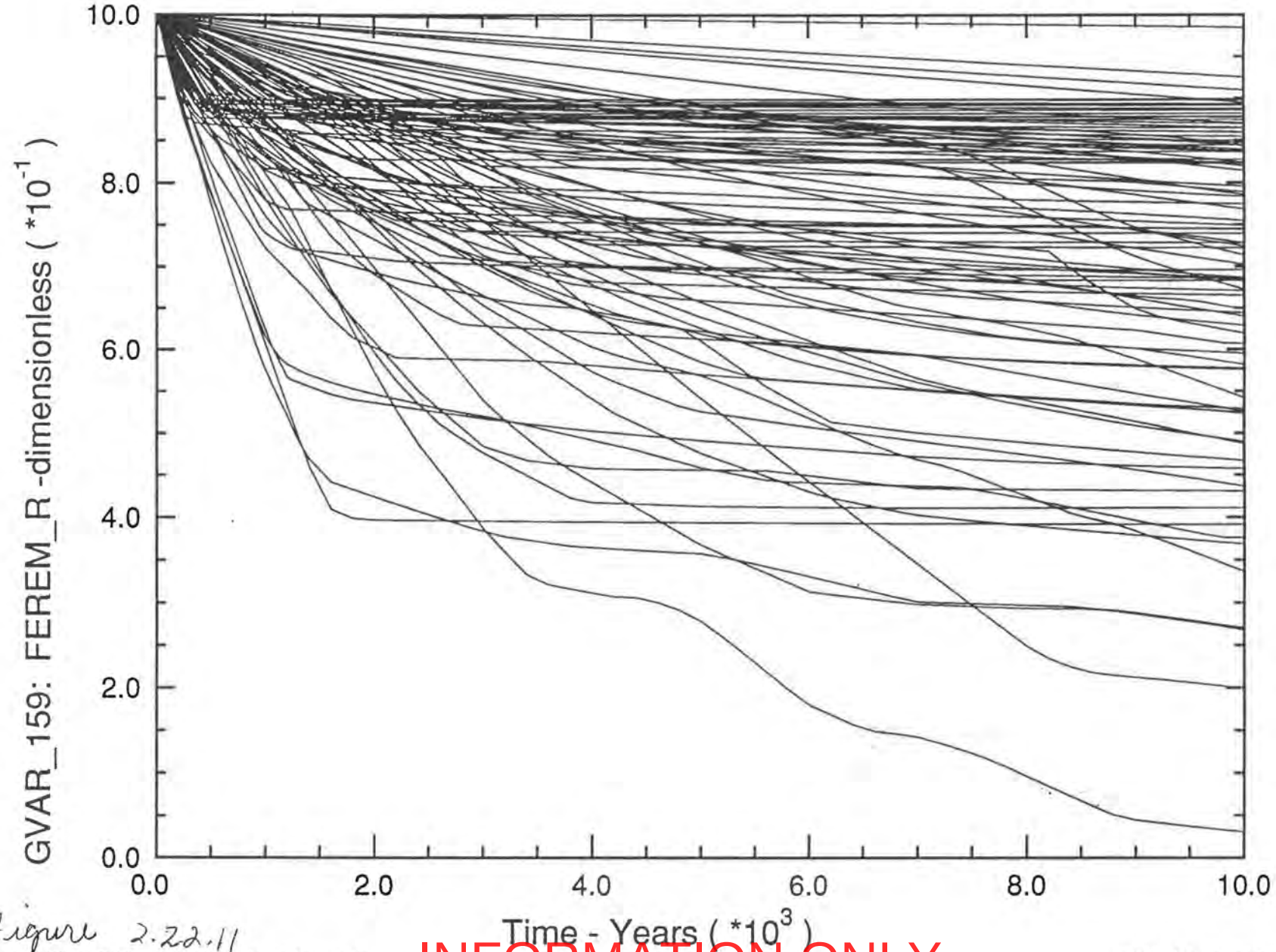

Figure 2.22.11

1DRA1:[JEBEAN.C97.SUMMZ.R1S5]SPLAT_R1_S5_H159.INP;1

SPLAT_PA96_2 1.02 05/28/97 11:03:58

SNL WIPP C97: BRAGFLO SIMULATIONS (C97 R1 S3)

Remaining Fraction of Steel Inventory in Rest of Repository

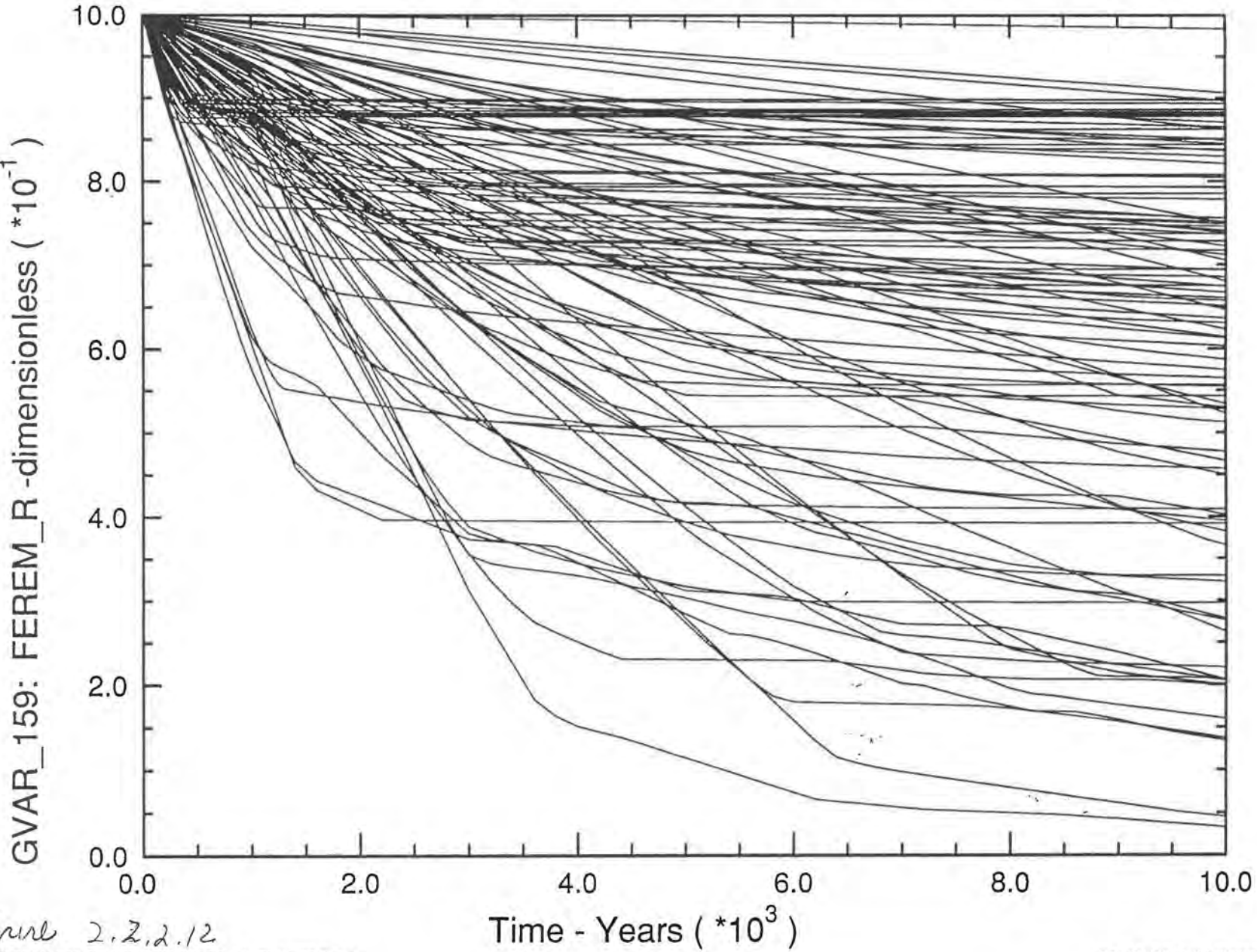

Figure 2.2.2.12

1DRA1:[JEBEAN.C97.SUMMZ.R1S3]SPLAT_R1_S3_H159.INP;1

INFORMATION ONLY

SPLAT_PA96_2 1.02 05/27/97 14:52:46

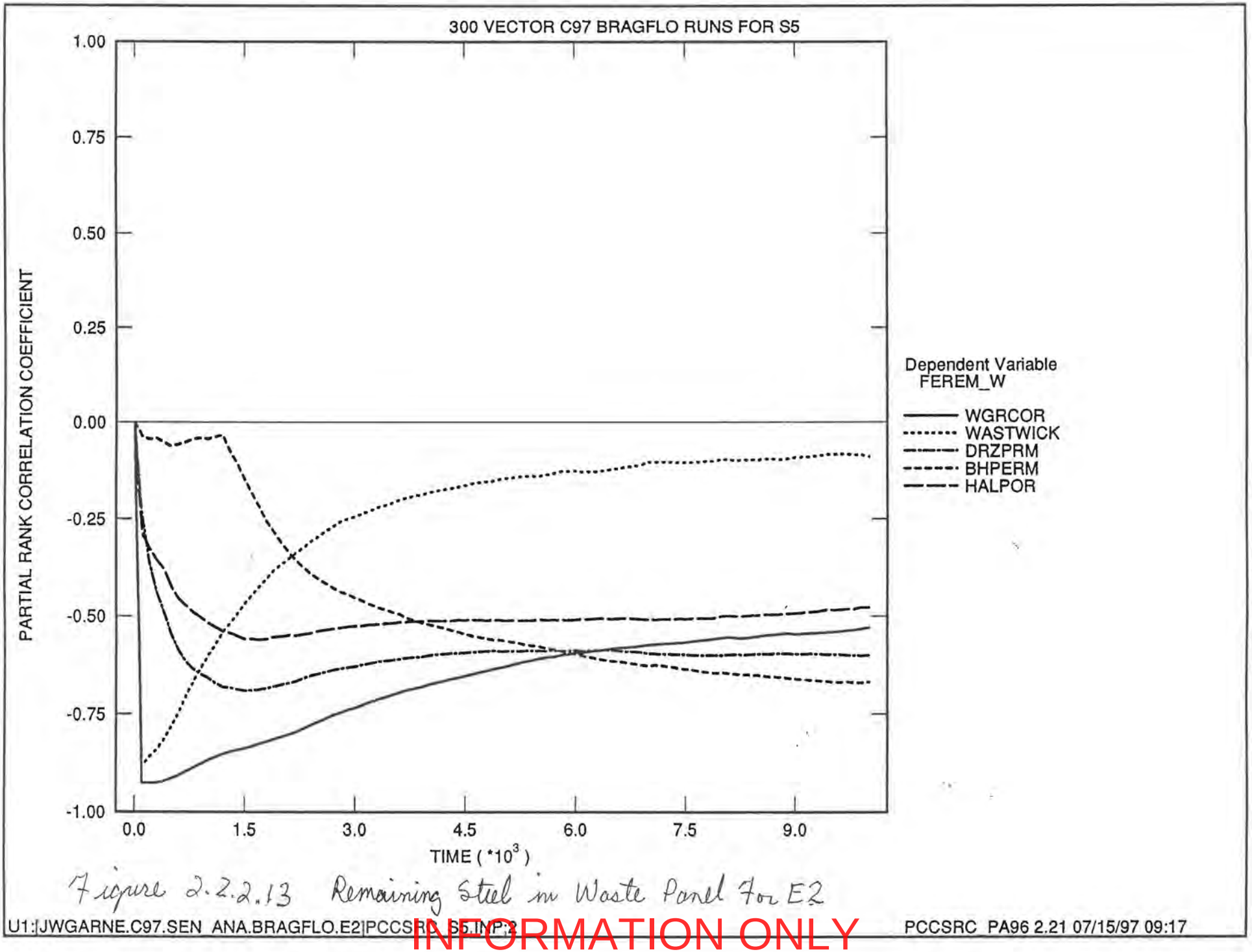

Figure 2.2.2.13 Remaining Steel in Waste Panel for E2

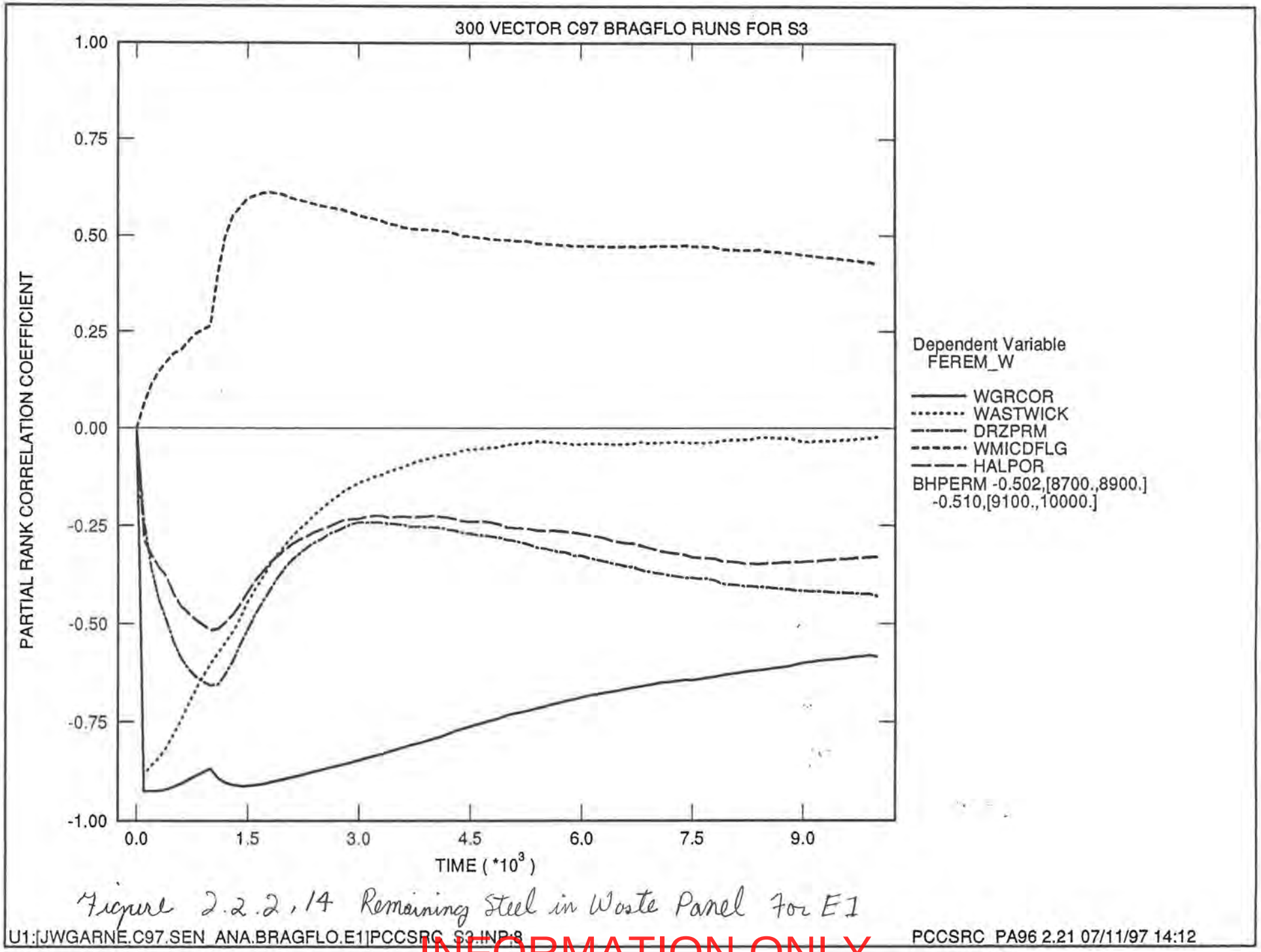

Figure 2.2.2.14 Remaining Steel in Waste Panel for E1

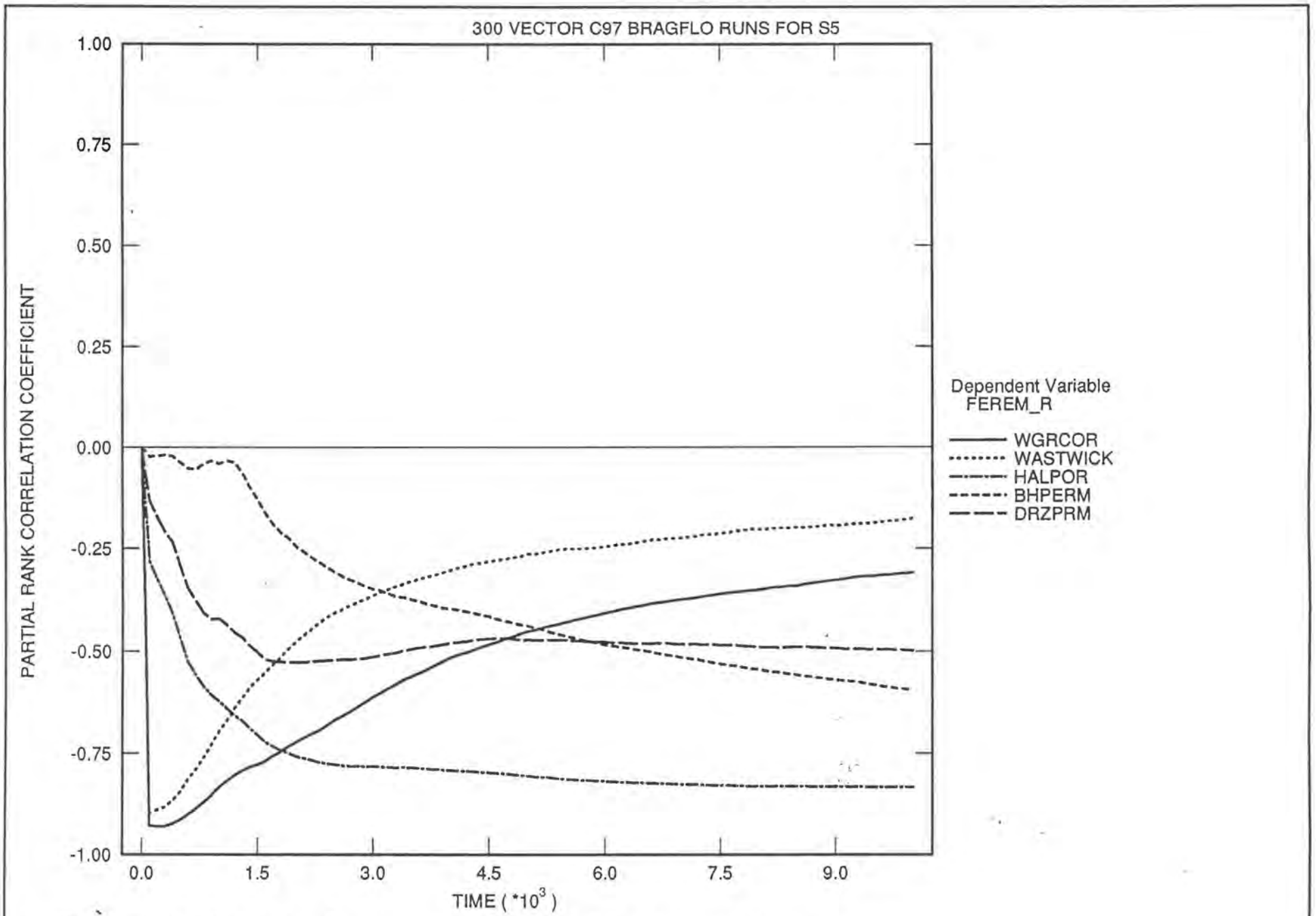

Figure 2.2.2.15 Remaining Steel in Rest of Repository for E2

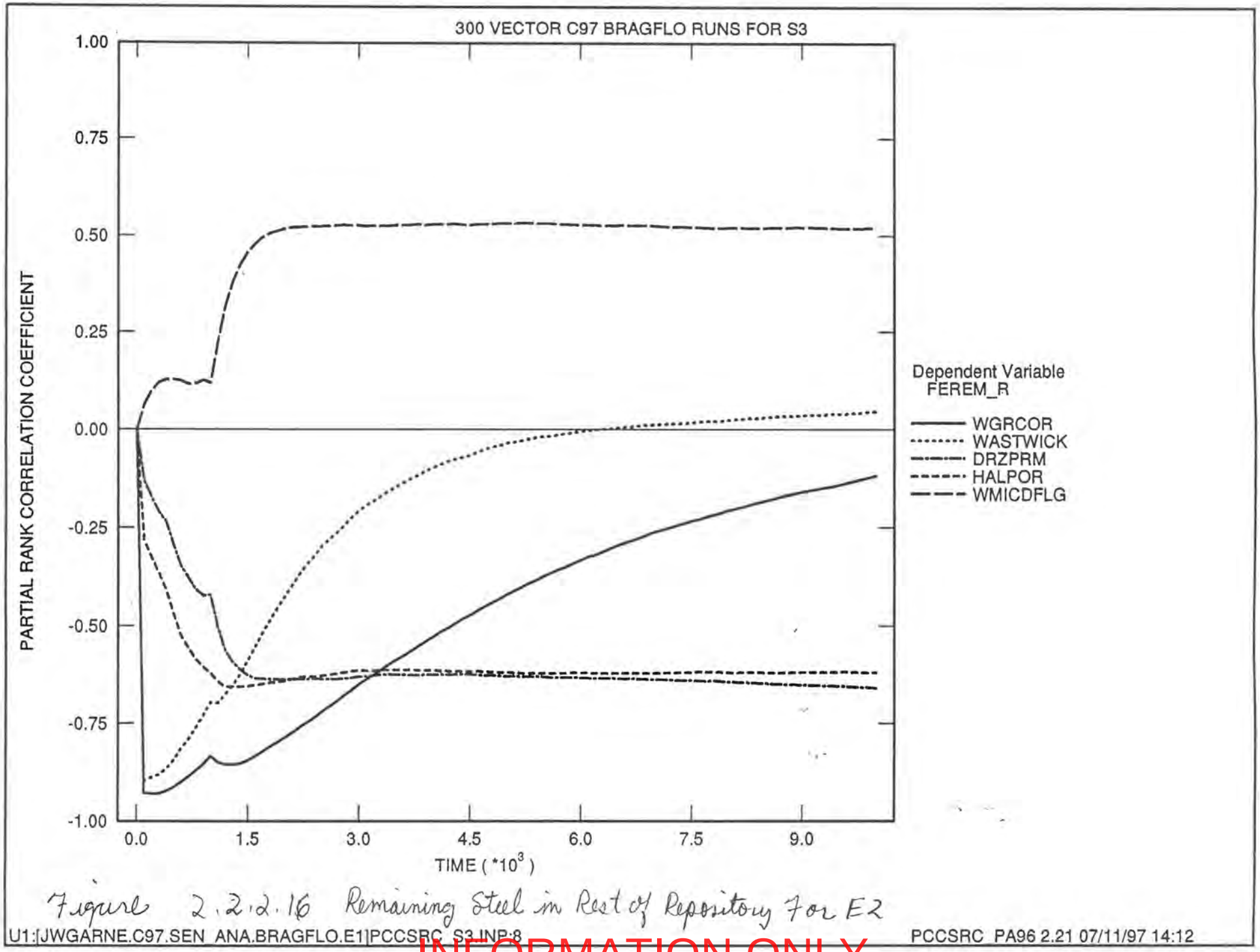

Figure 2.2.2.16 Remaining Steel in Rest of Repository for E2

U1:[JWGARNE.C97.SEN_ANA.BRAGFLO.E1]PCCSRC_S3.INP;8 PCCSRC_PA96 2.21 07/11/97 14:12

SNL WIPP C97: BRAGFLO SIMULATIONS (C97 R1 S5)

Volume-Averaged Pressure in Waste Panel

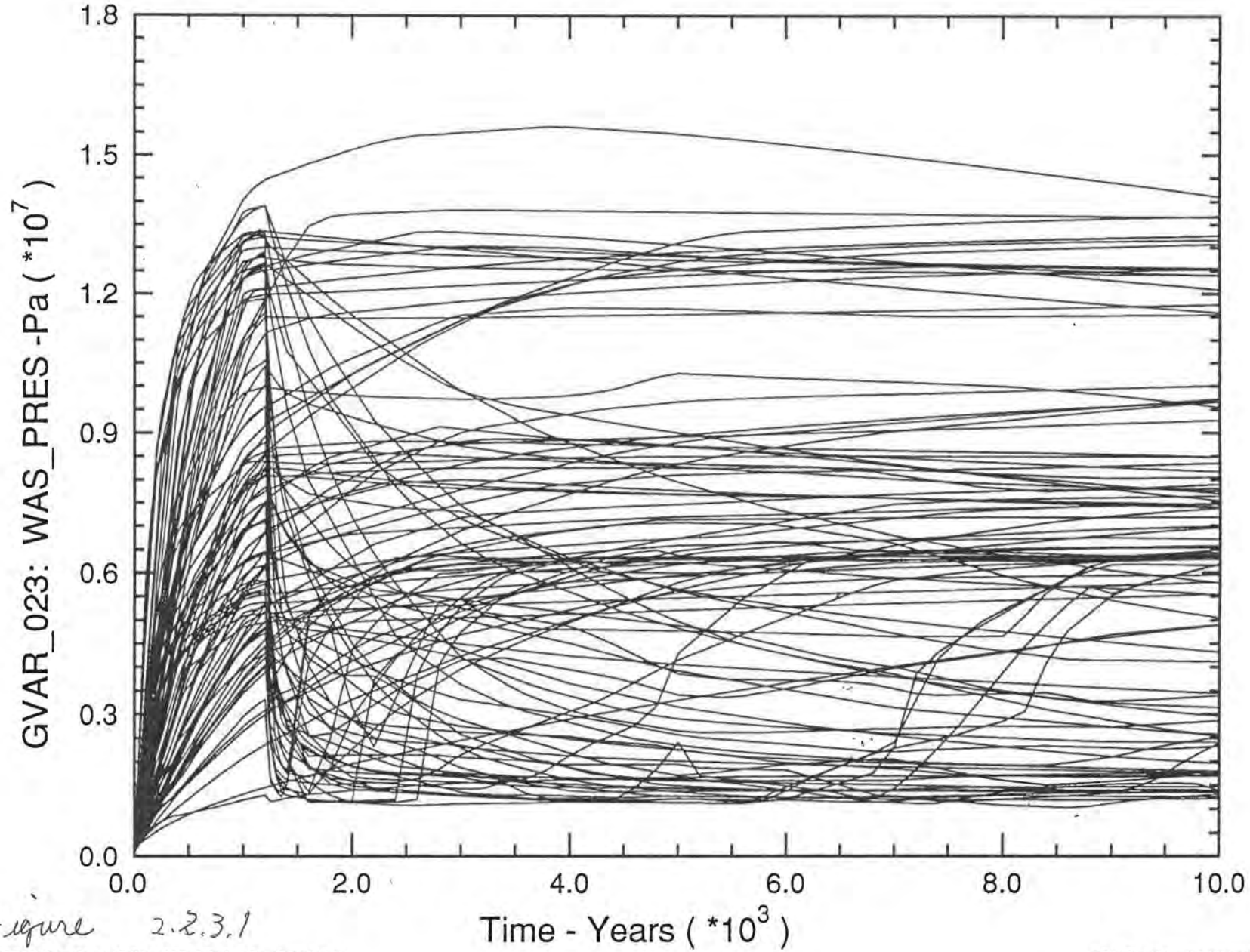

Figure 2.2.3.1

1DRA1:[JEBEAN.C97.SUMMZ.R1S5]SPLAT_R1_S5_H023.INP;1

SPLAT_PA96_2 1.02 05/27/97 09:12:48

SNL WIPP C97: BRAGFLO SIMULATIONS (C97 R1 S3)

Volume-Averaged Pressure in Waste Panel

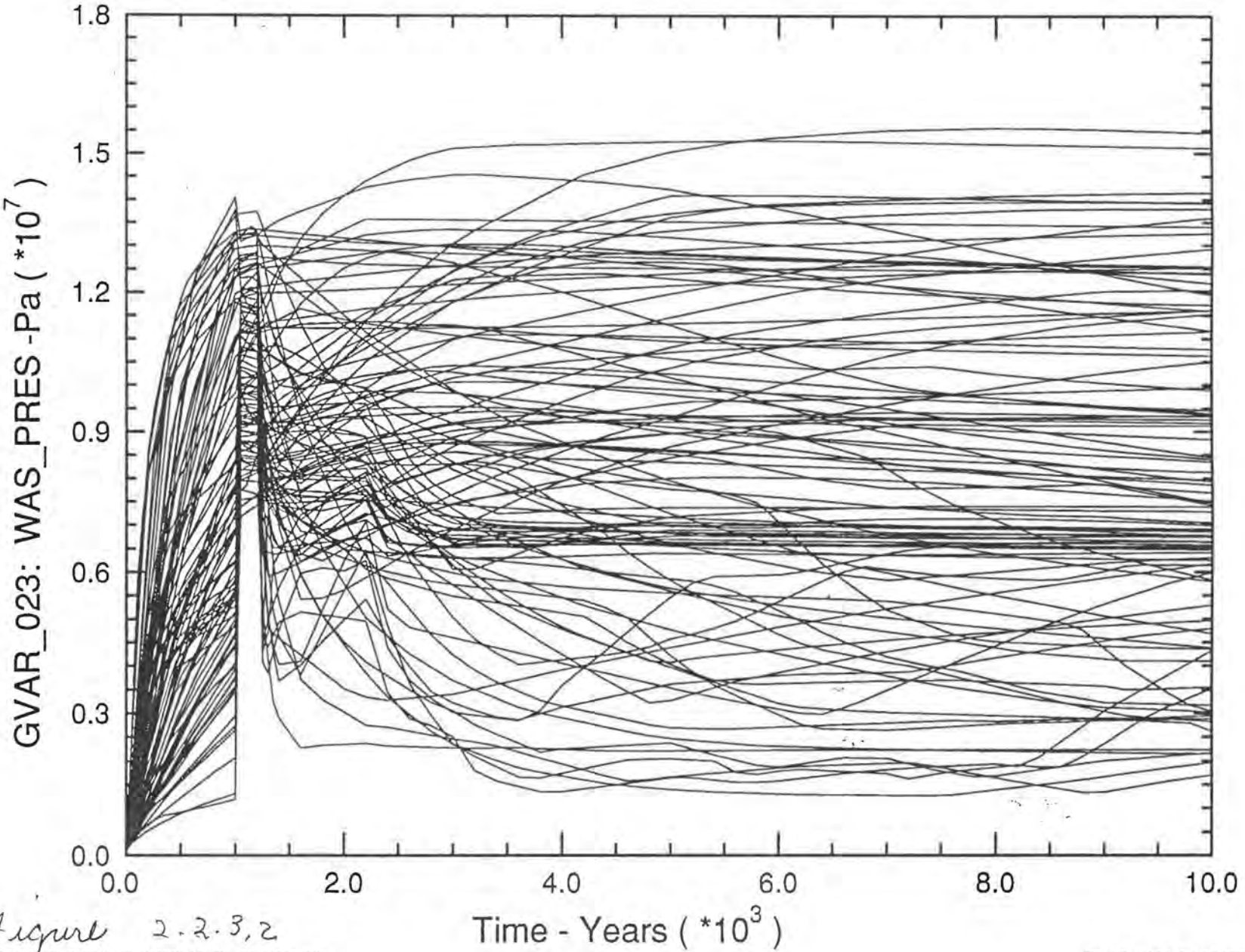

Figure 2.2.3.2

1DRA1:[JEBEAN.C97.SUMMZ.R1S3]SPLAT_R1_S3_H023.INP;1

SPLAT_PA96_2 1.02 05/27/97 08:49:36

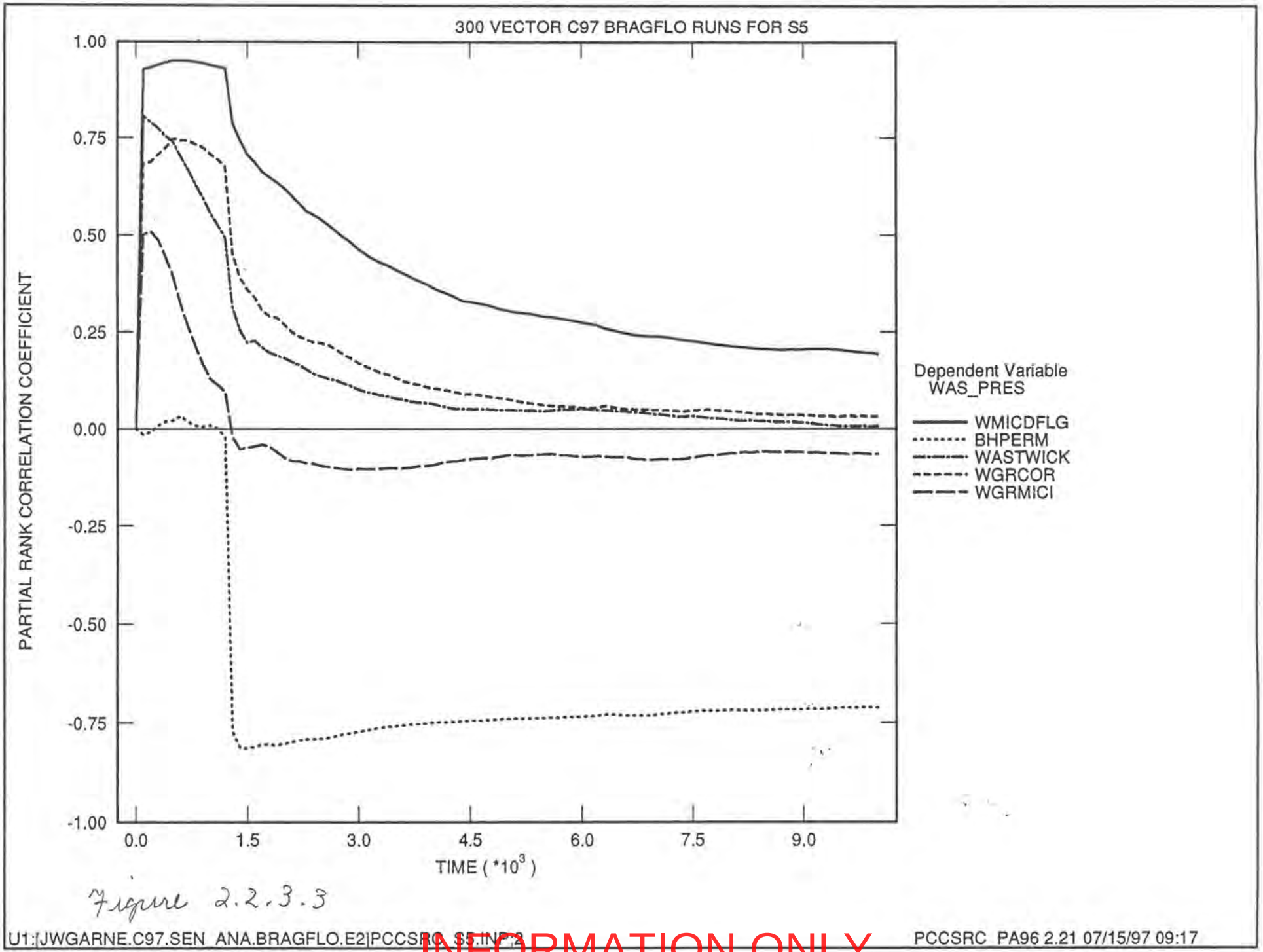

Figure 2.2.3.3

U1:[JWGARNE.C97.SEN_ANA.BRAGFLO.E2]PCCSRC_S5.INP;2 PCCSRC PA96 2.21 07/15/97 09:17

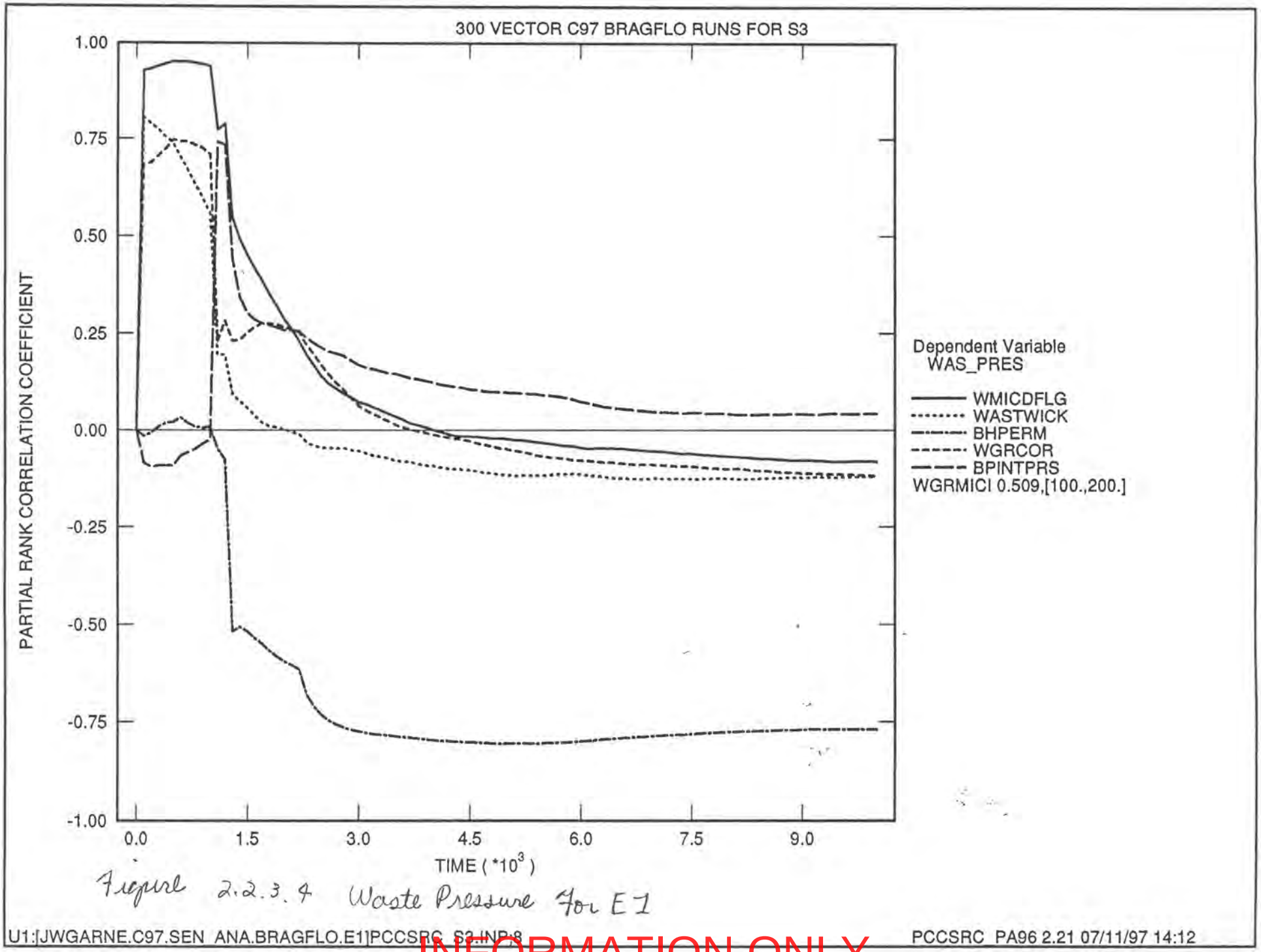

Figure 2.2.3.4 Waste Pressure For E1

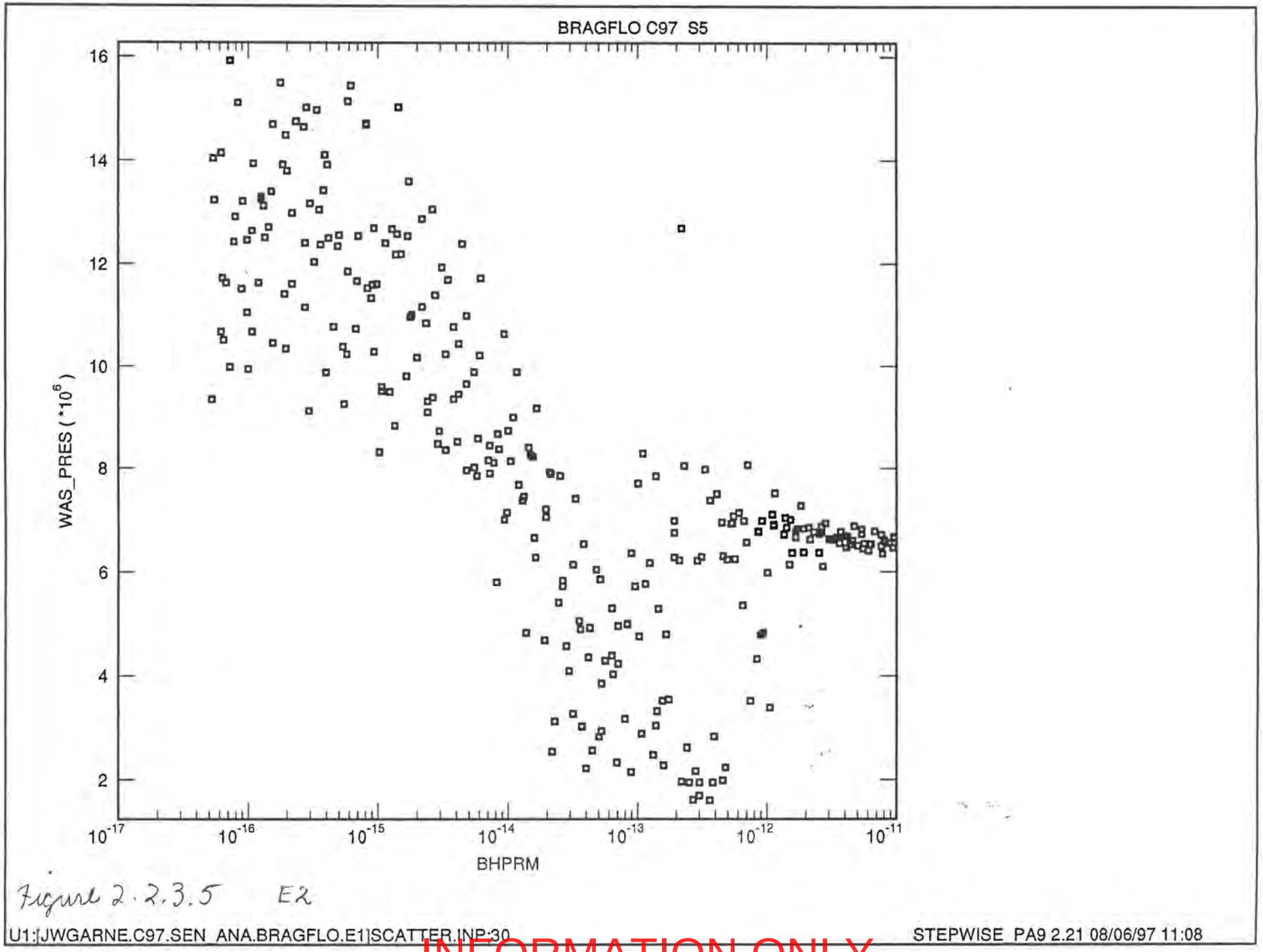

Figure 2.2.3.5 E2

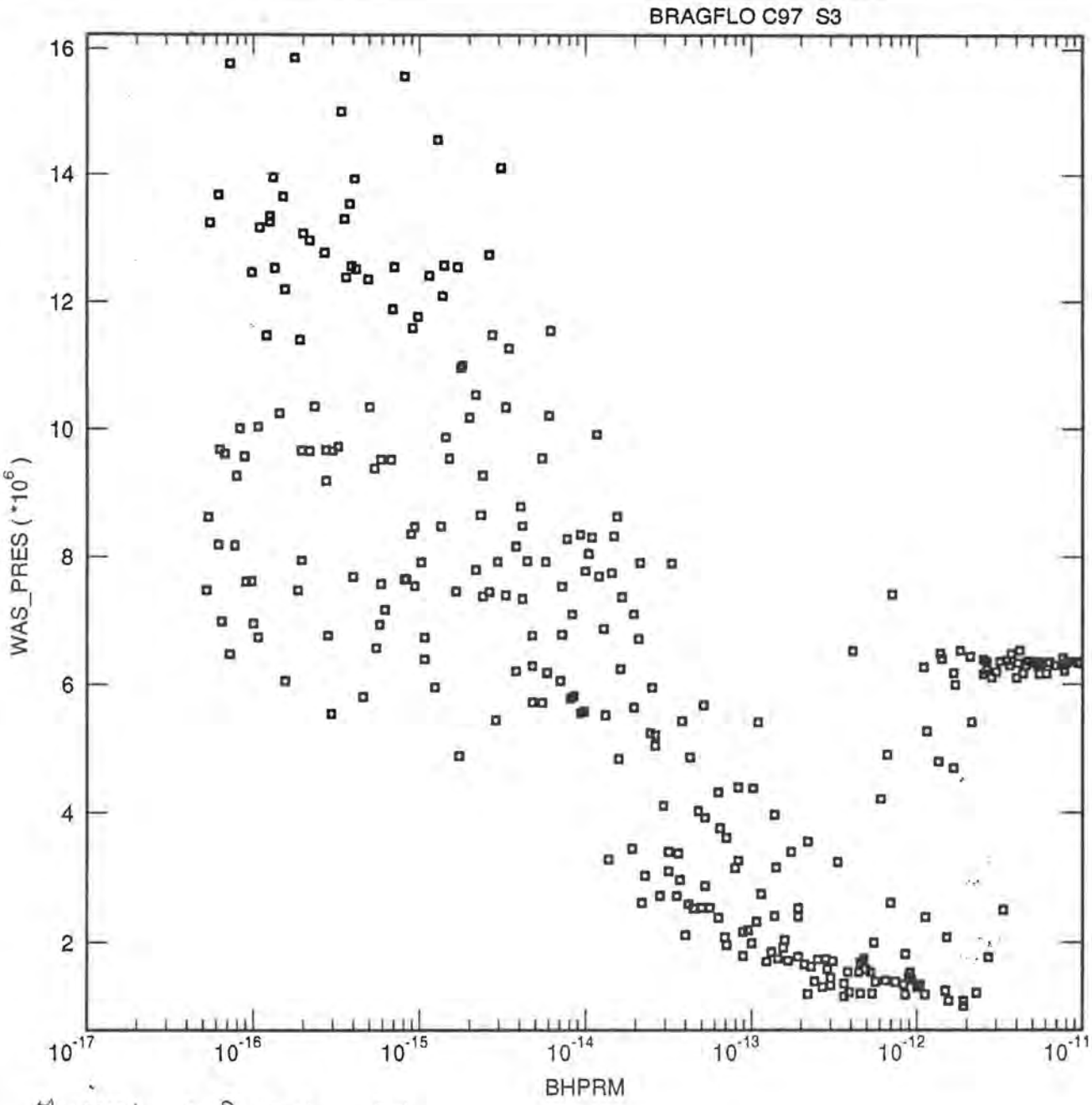

Figure 2.2.3.c E1

U1:[JWGARNE.C97.SEN_ANA.BRAGFLO.E2]SCATTER.INP;4 STEPWISE PA9 2.21 08/06/97 11:04

SNL WIPP C97: BRAGFLO SIMULATIONS (C97 R1 S5)

Volume-Averaged Brine Saturation in Rest of Repository

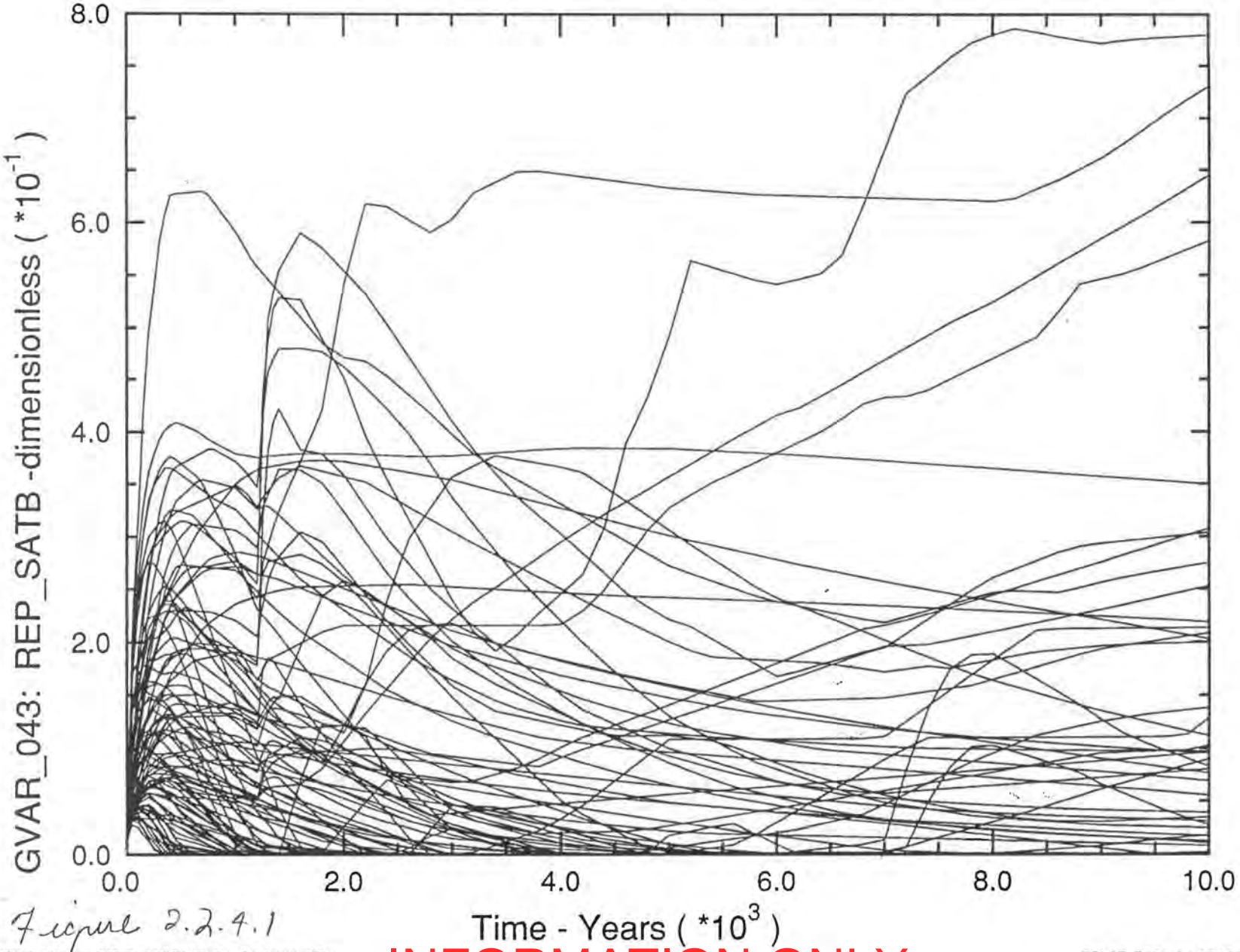

Figure 2.2.4.1

1DRA1:[JEBEAN.C97.SUMMZ.R1S5]SPLAT_R1_S5_H043.INP;1

INFORMATION ONLY

SPLAT_PA96_2 1.02 05/27/97 10:25:44

SNL WIPP C97: BRAGFLO SIMULATIONS (C97 R1 S5)

Volume-Averaged Brine Saturation in Waste Panel

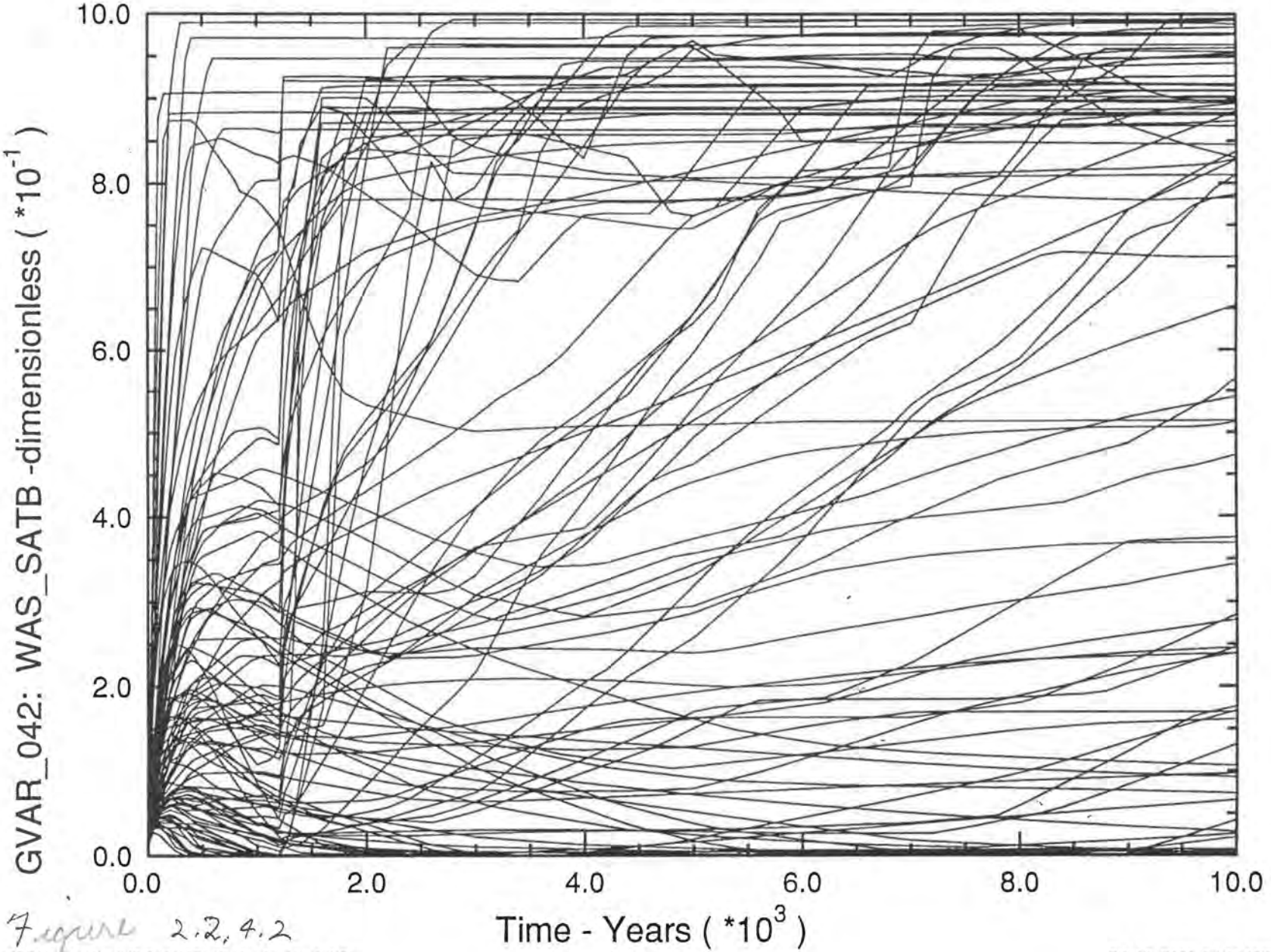

Figure 2.2.4.2

1DRA1:[JEBEAN.C97.SUMMZ.R1S5]SPLAT_R1_S5_H042.INP;1

SPLAT_PA96_2 1.02 05/27/97 10:21:49

SNL WIPP C97: BRAGFLO SIMULATIONS (C97 R1 S3)

Volume-Averaged Brine Saturation in Rest of Repository

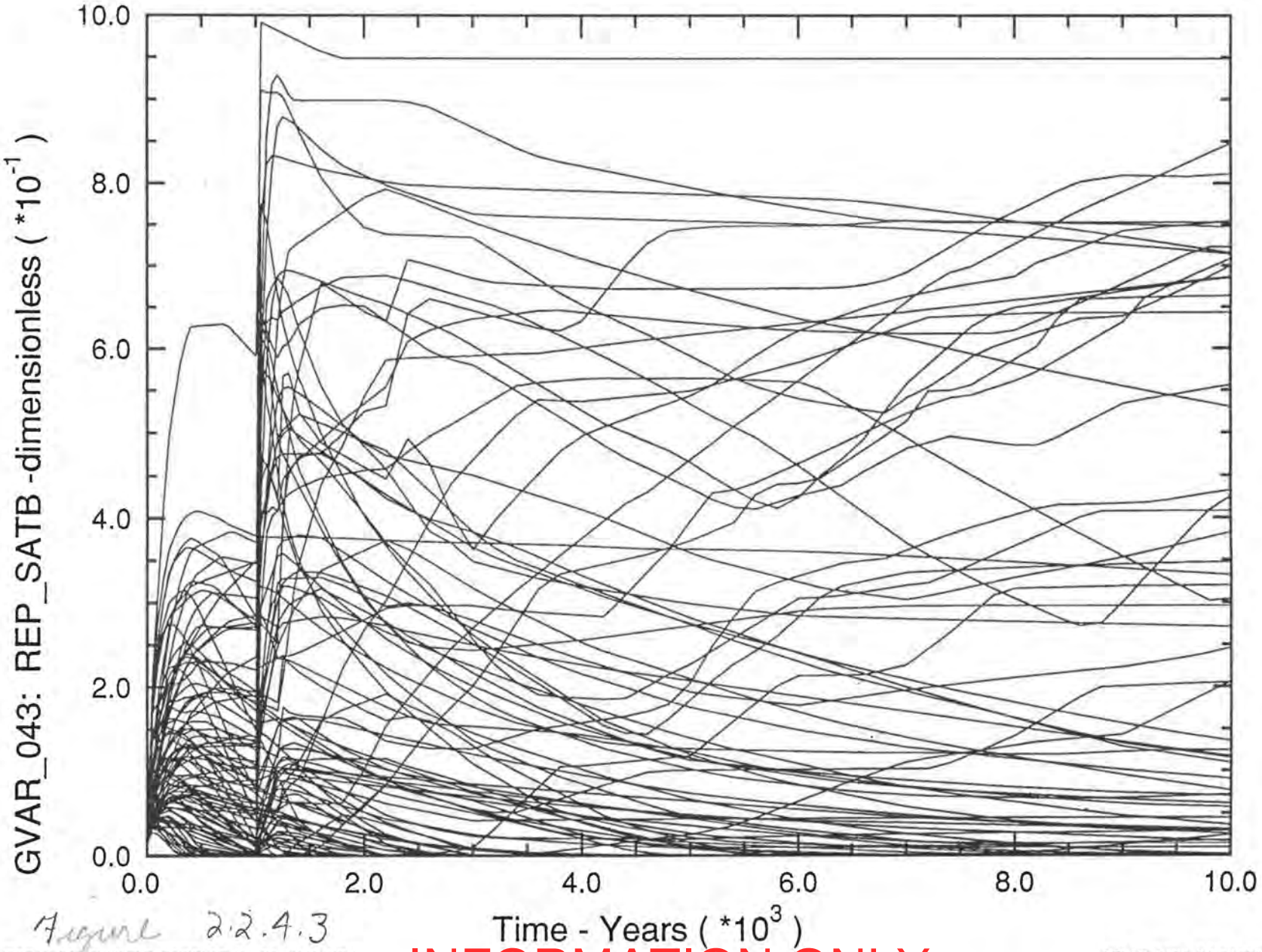

Figure 2.2.4.3

1DRA1:[JEBEAN.C97.SUMMZ.R1S3]SPLAT_R1_S3_H043.INP;1

INFORMATION ONLY

SPLAT_PA96_2 1.02 05/27/97 09:43:02

SNL WIPP C97: BRAGFLO SIMULATIONS (C97 R1 S3)

Volume-Averaged Brine Saturation in Waste Panel

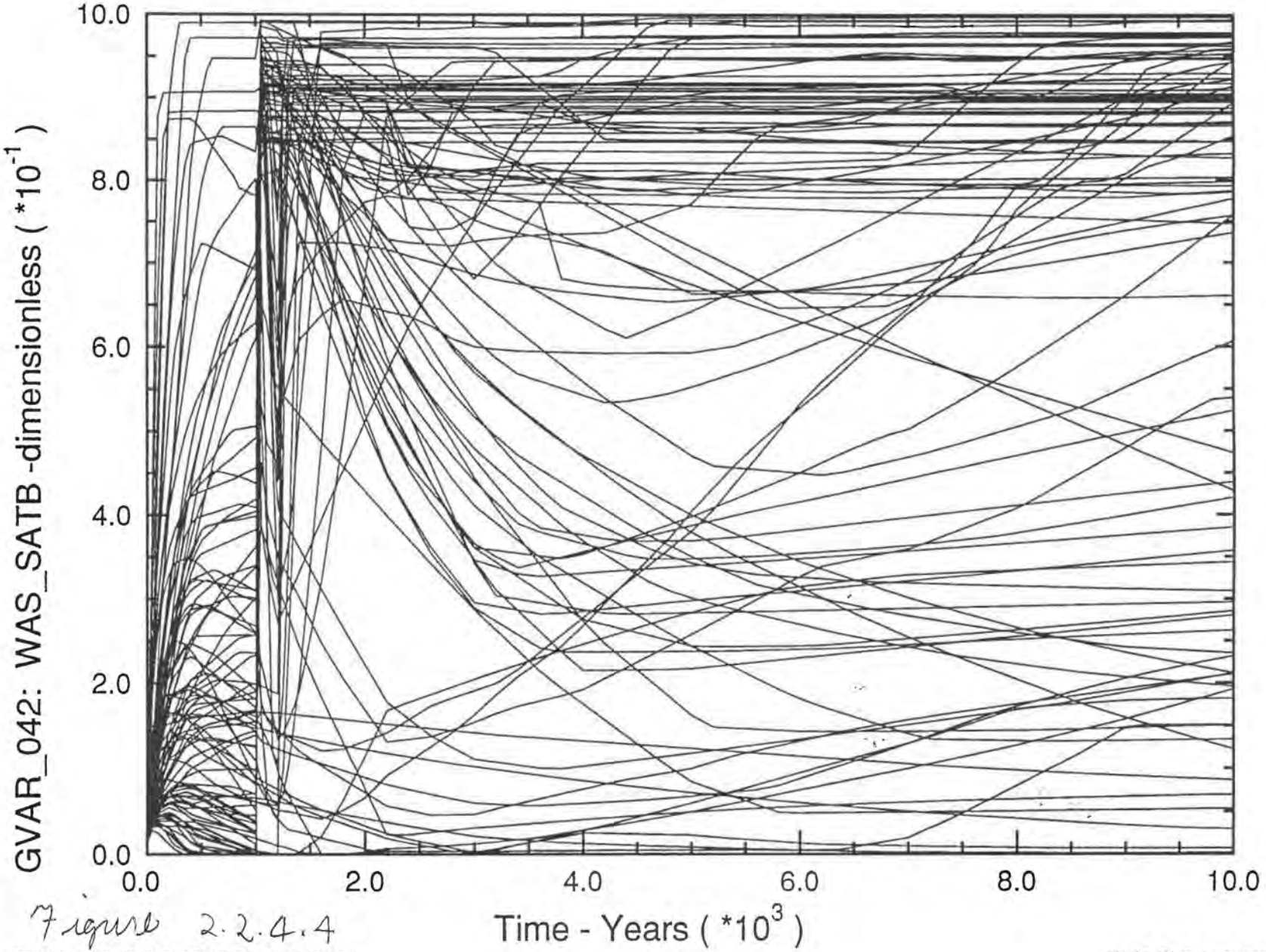

Figure 2.2.4.4

1DRA1:[JEBEAN.C97.SUMMZ.R1S3]SPLAT_R1_S3_H042.INP;1

SPLAT_PA96_2 1.02 05/27/97 09:40:24

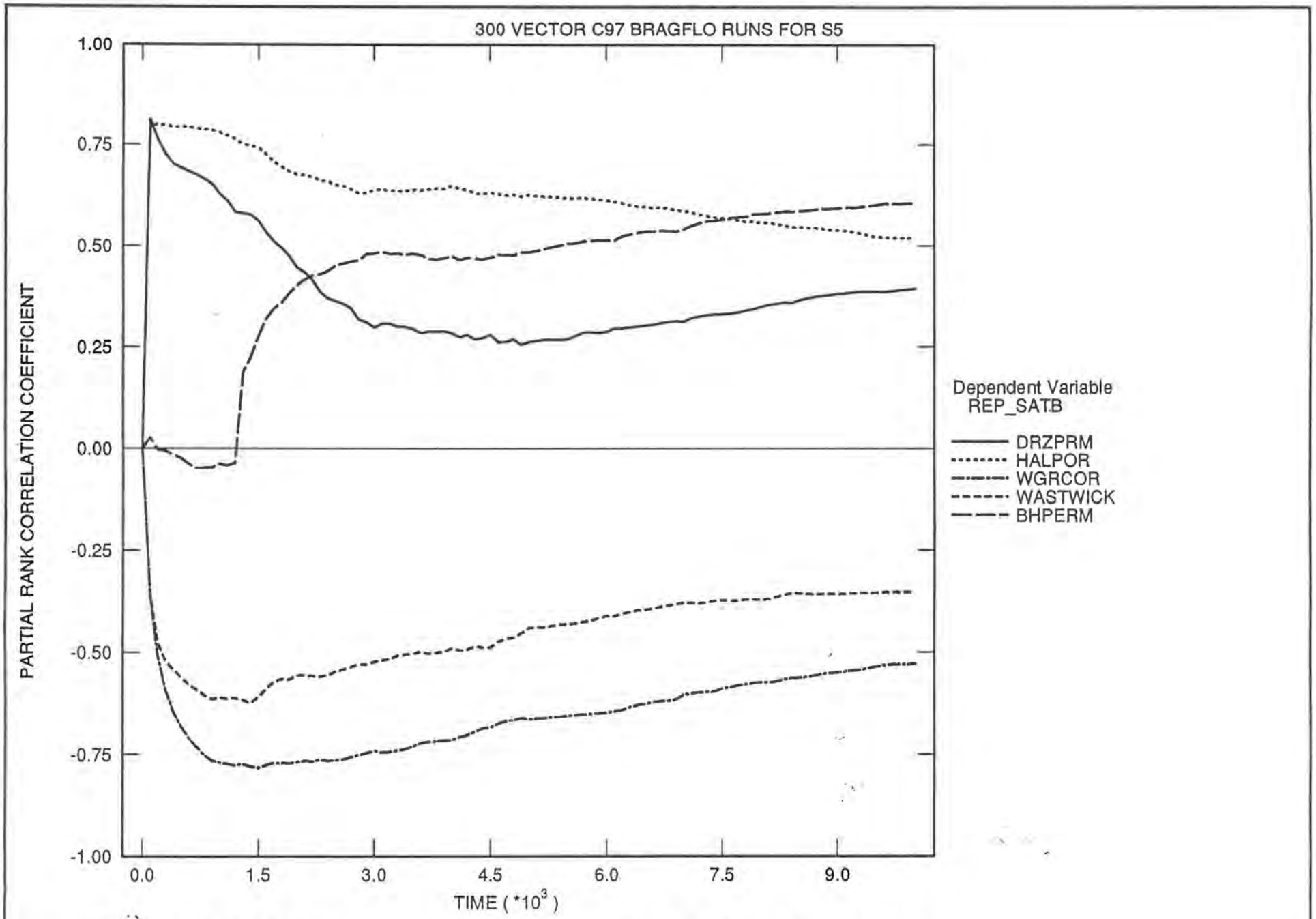

Figure 2.2.4.5 Brine Saturation in Rest. of Repository for E2

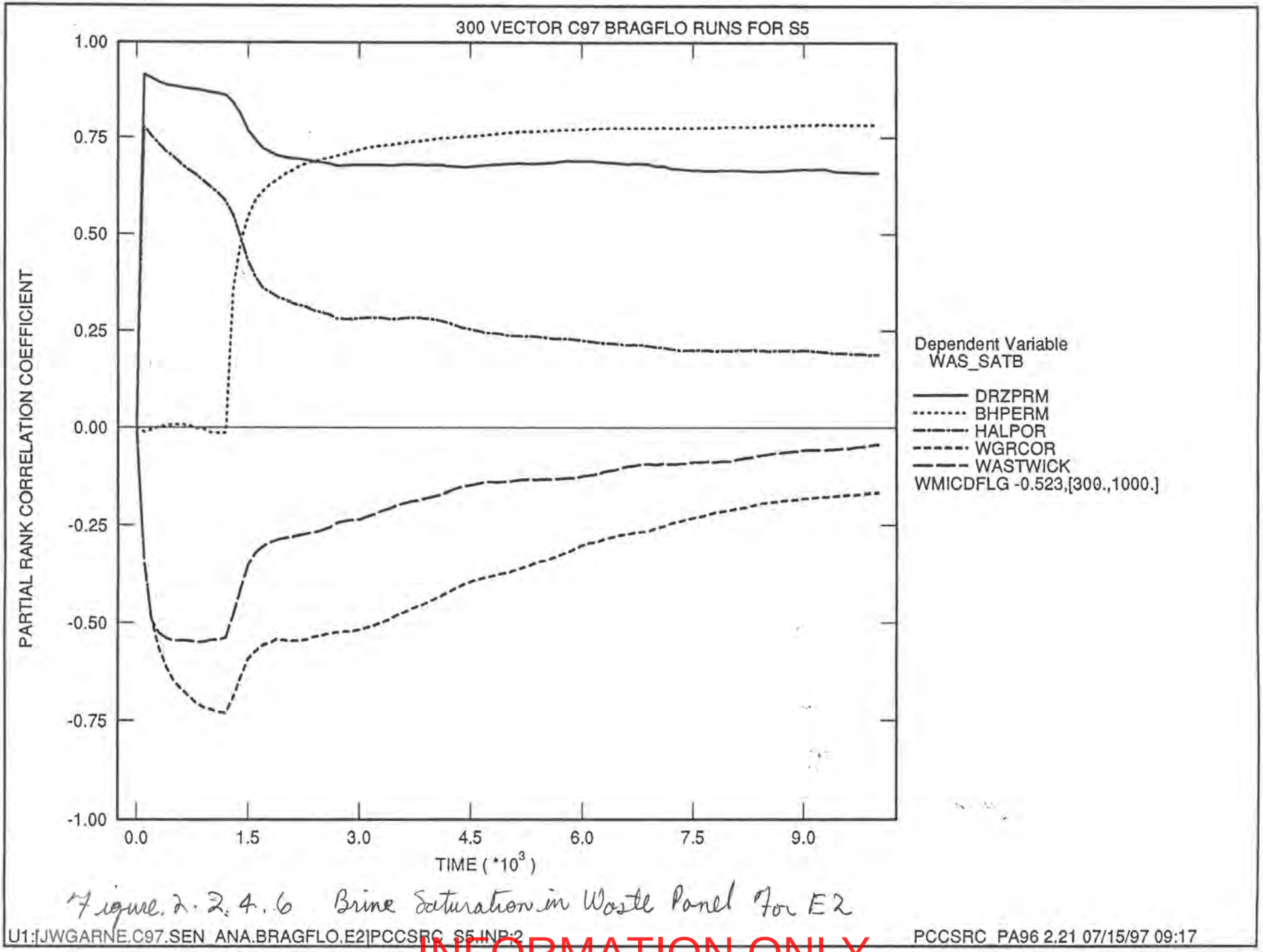

Figure 2.2.4.6 Brine Saturation in Waste Panel for E2

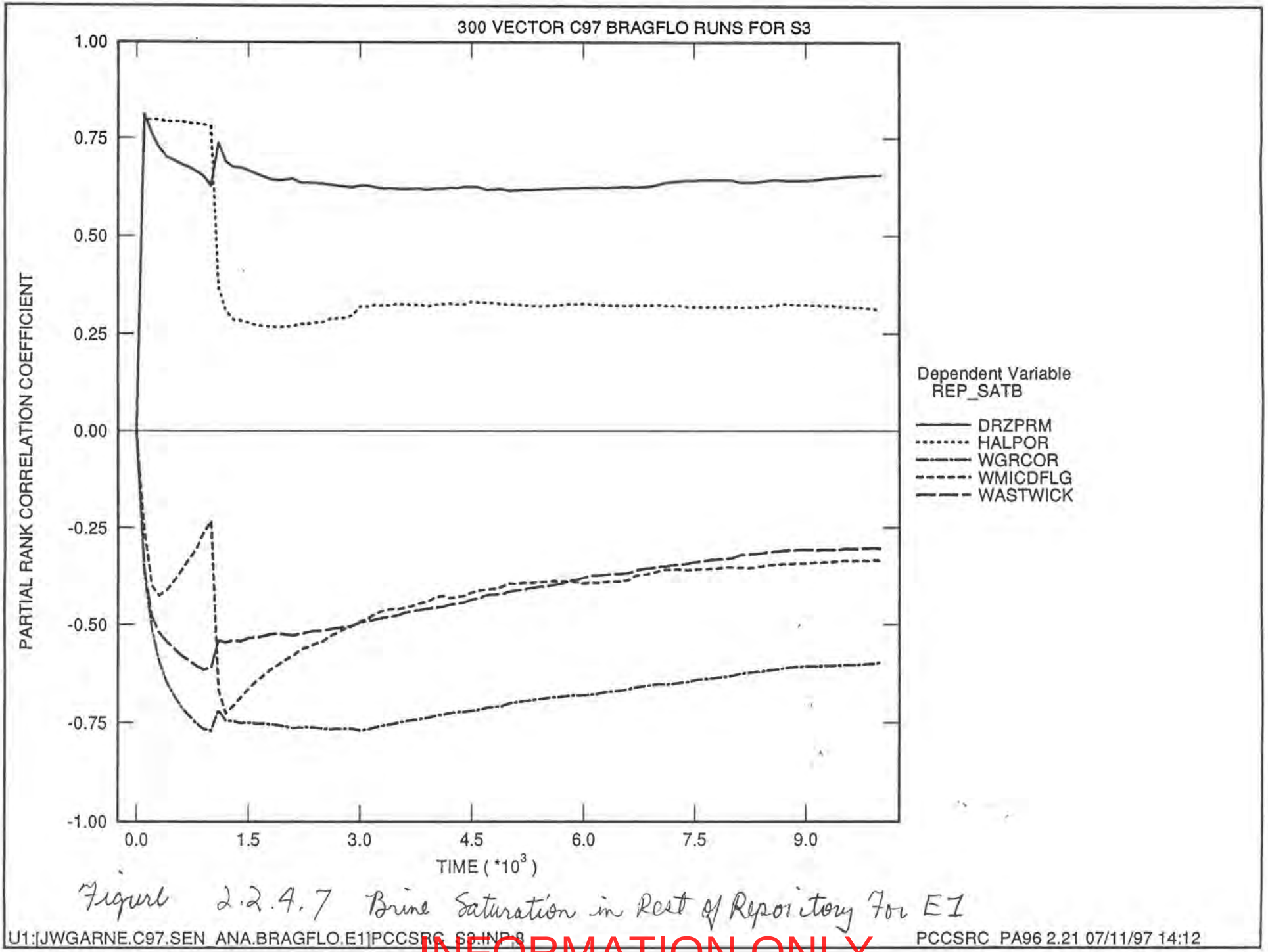

Figure 2.2.4.7 Brine Saturation in Rest of Repository For E1

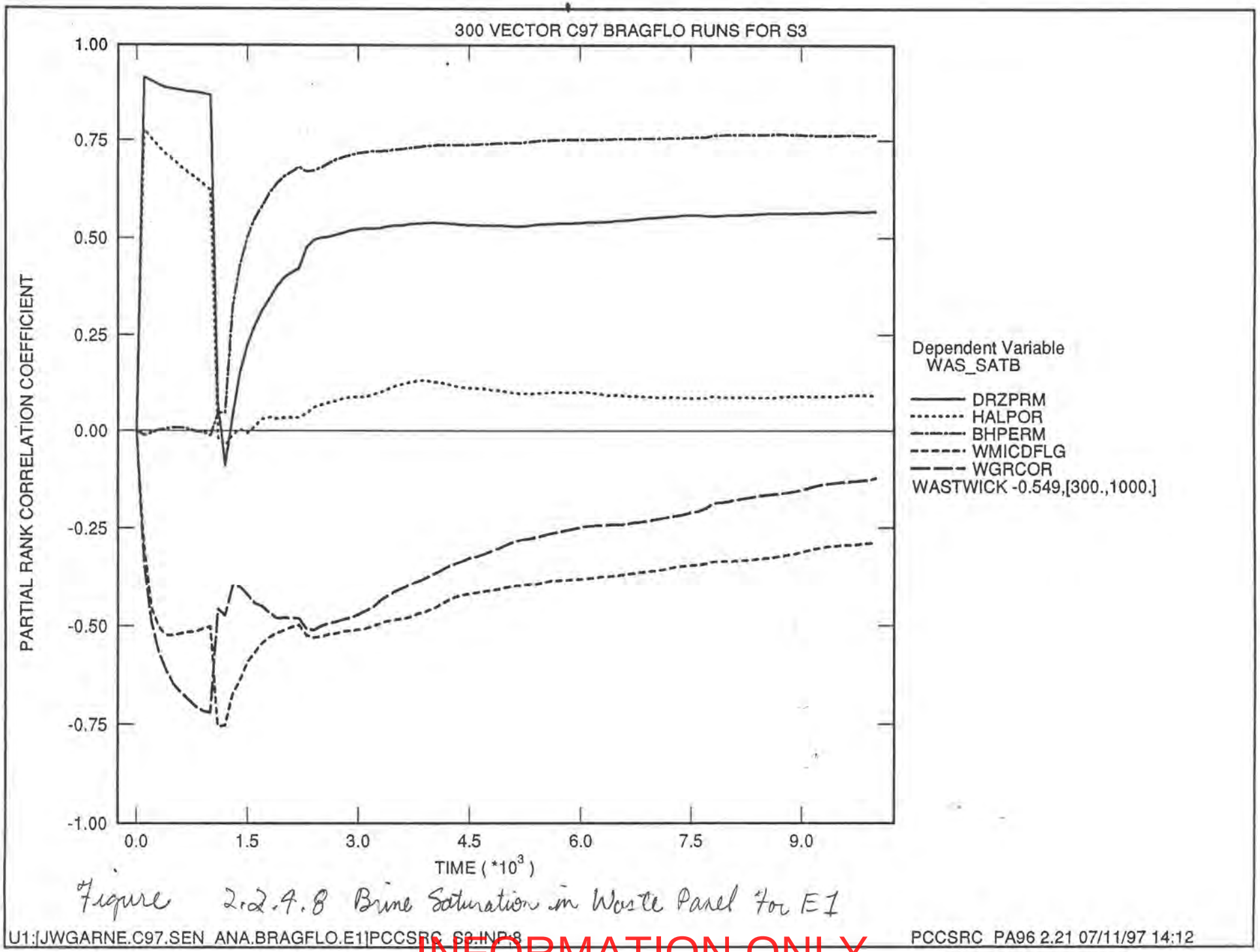

Figure 2.2.4.8 Brine Saturation in Waste Panel for E1

SNL WIPP C97: BRAGFLO SIMULATIONS (C97 R1 S3)

Volume-Averaged Pressure in Brine Pocket

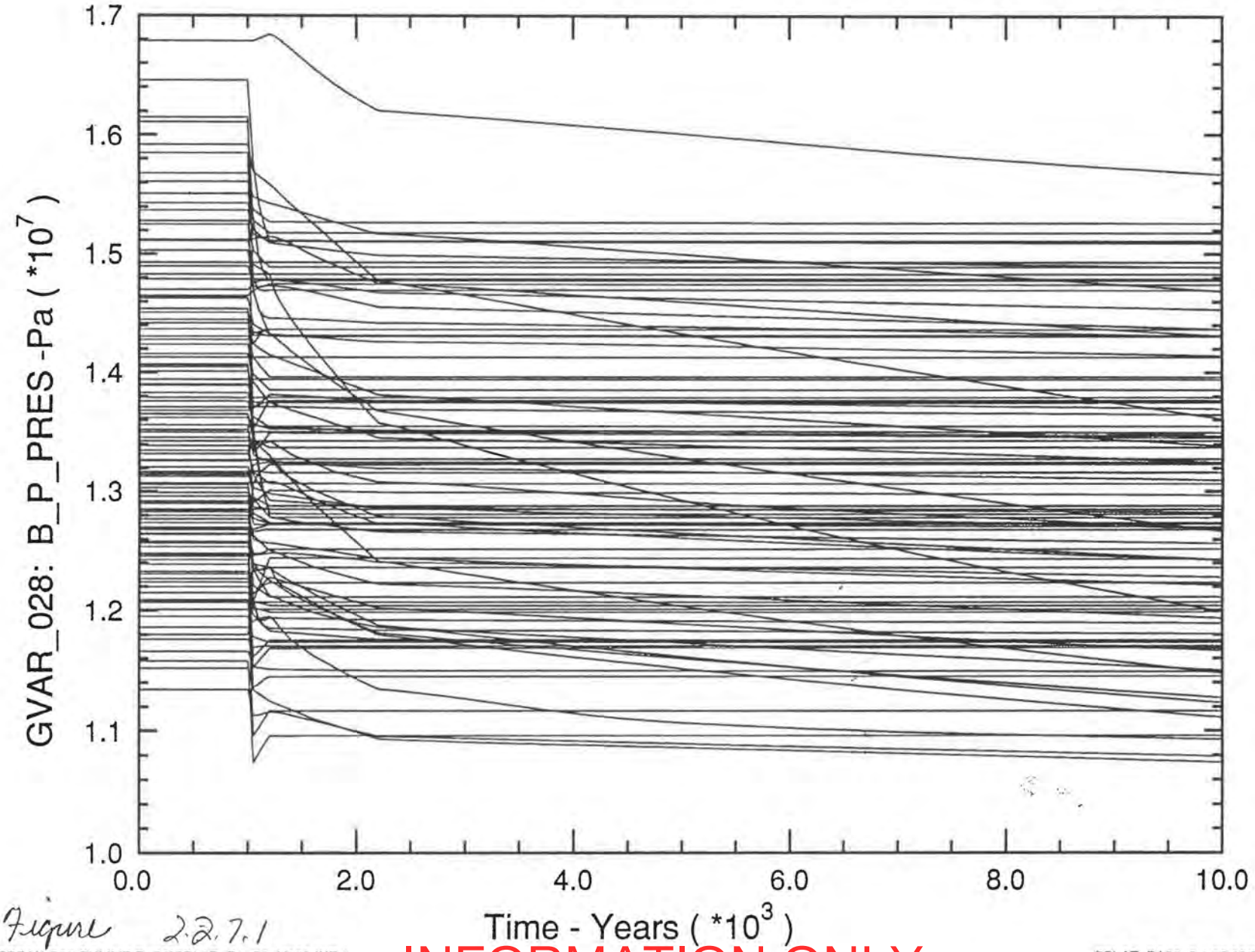

Figure 2.2.7.1

1DRA1:[JEBEAN.C97.SUMMZ.R1S3]SPLAT_R1_S3_H028.INP;1

INFORMATION ONLY

SPLAT_PA96_2 1.02 05/27/97 09:03:07

SNL WIPP C97: BRAGFLO SIMULATIONS (C97 R1 S3)

Brine Volume in Brine Pocket

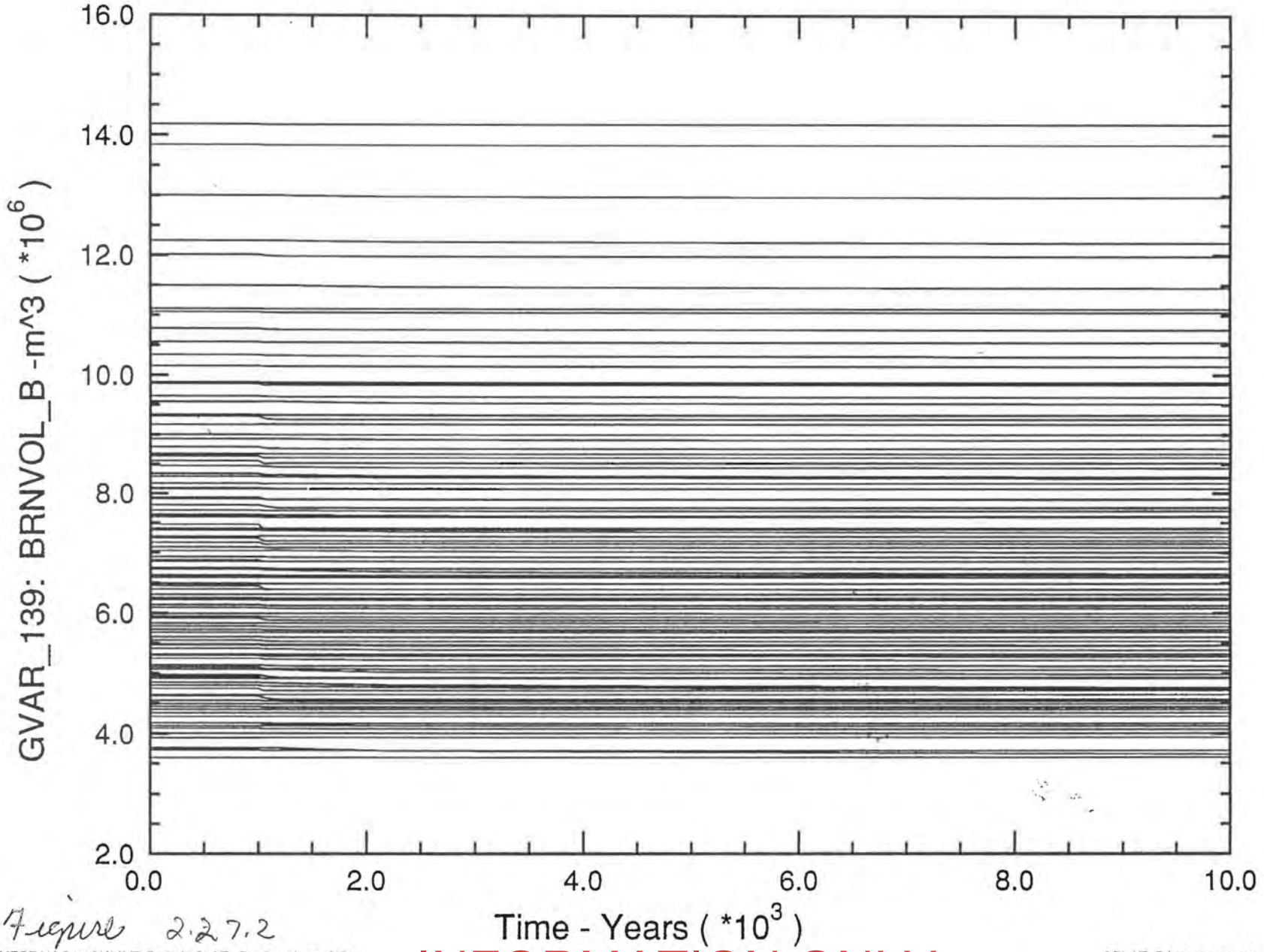

Figure 2.27.2

1DRA1:[JEBEAN.C97.SUMMZ.R1S3]SPLAT_R1_S3_H139.INP;1

SPLAT_PA96_2 1.02 05/27/97 13:59:45

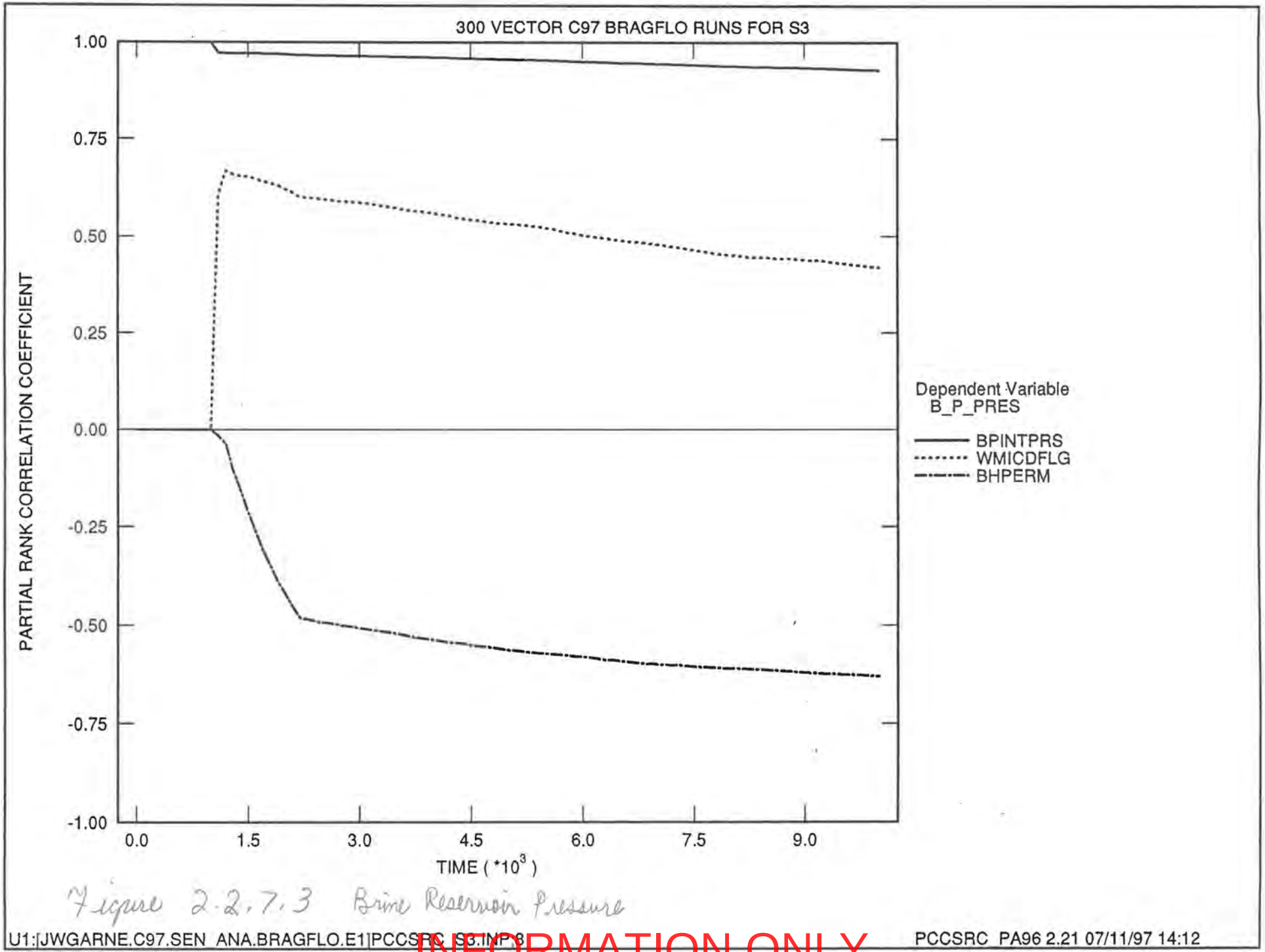

Figure 2.2.7.3 Brine Reservoir Pressure

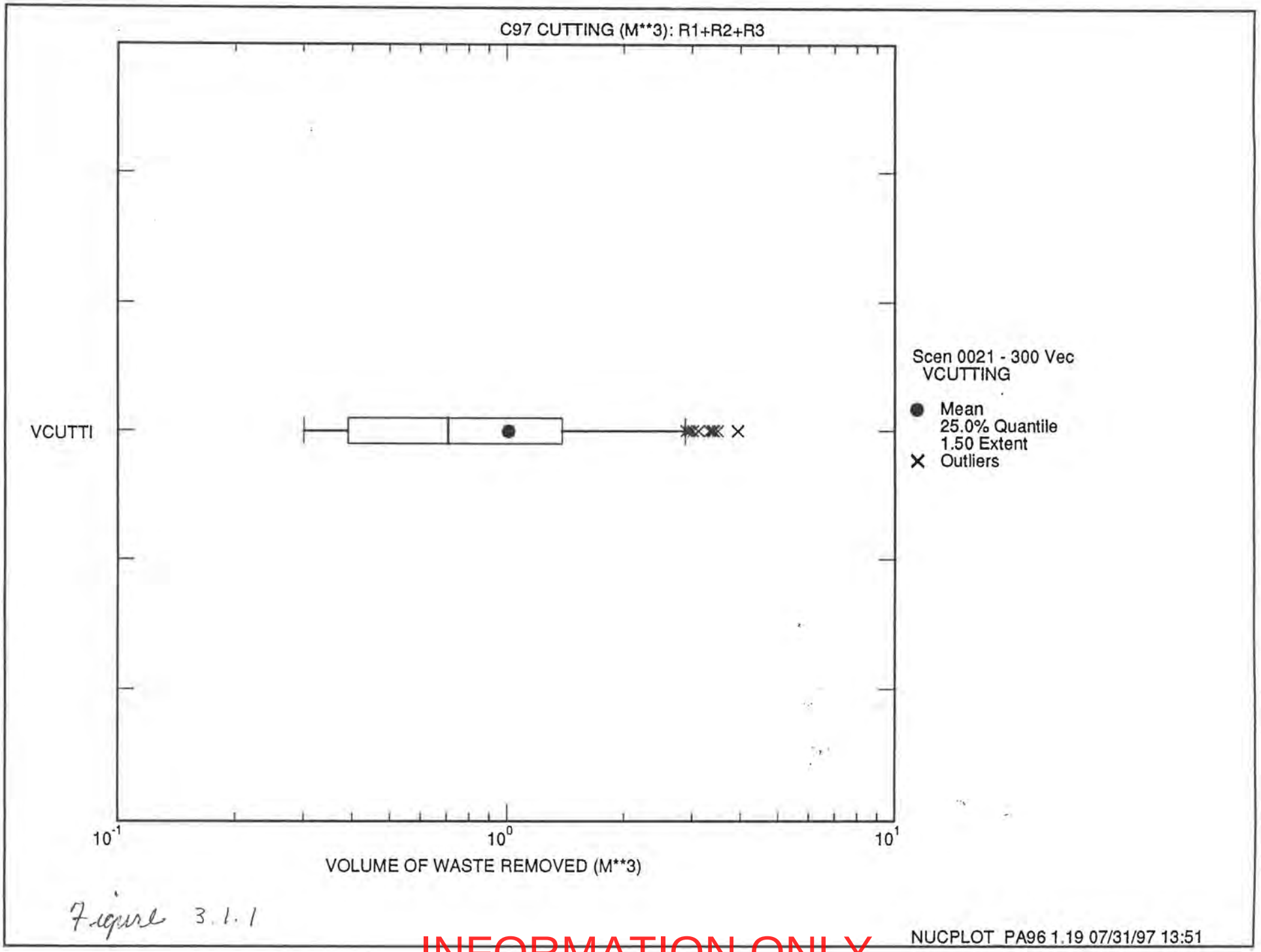

Figure 3.1.1

NUCPLOT PA96 1.19 07/31/97 13:51

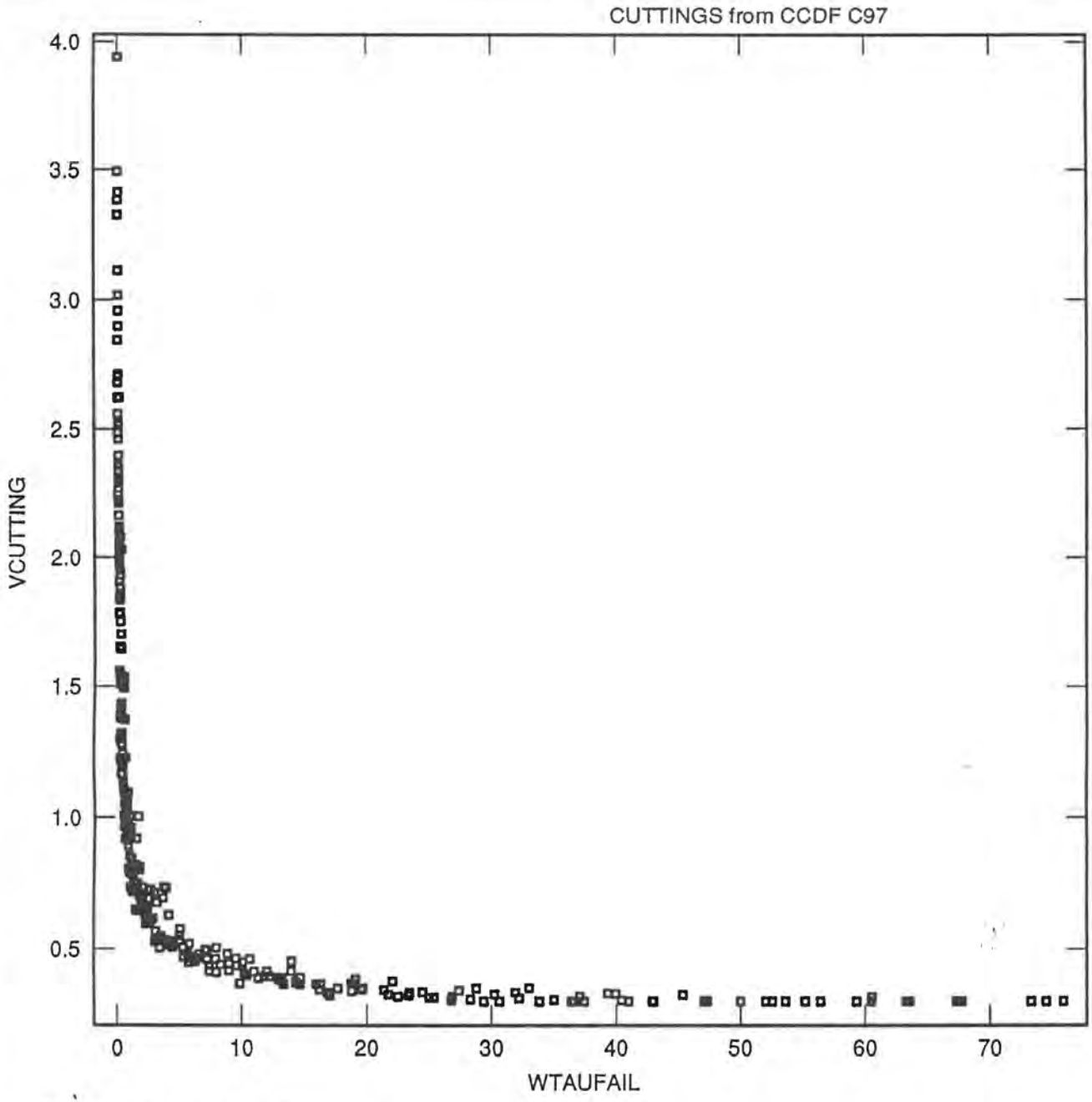

Figure 3.1.2

U1:[JWGARNE.C97.SEN_ANA.CUTTINGS]CUT_SCATNNP:2 STEPWISE PA9 2.21 08/08/97 13:32

SNL WIPP PA: NUTS_ISO SIMULATIONS(C97 R1 S2)

Total Integrated Discharge up Borehole at Culebra

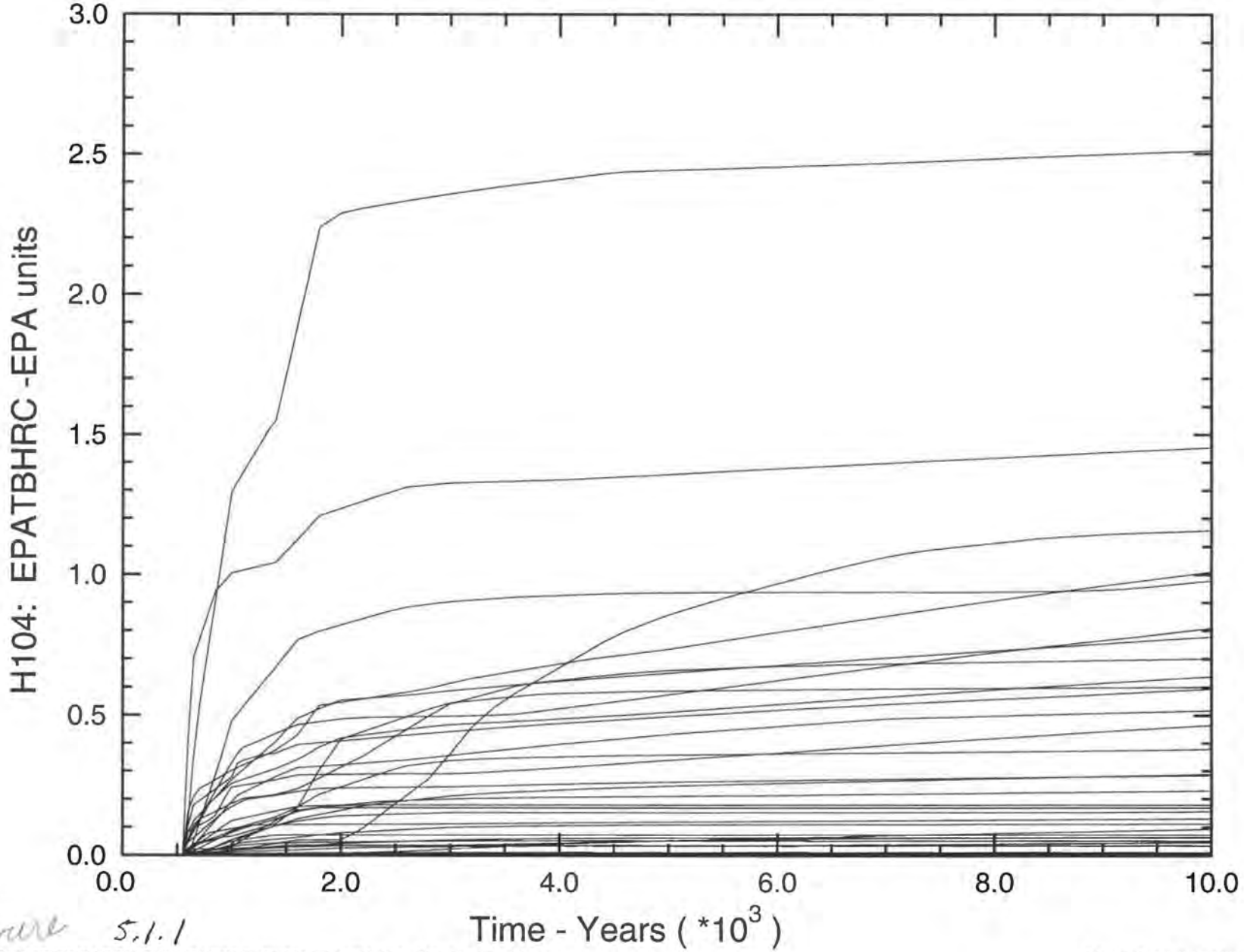

Figure 5.1.1

DISK$TINA_CCA3:[BF.JDMILLE.C97.SUMMZ.NUTS.R1S2]SPLAT_NUTS_ISO_C97_R1S2_H104INP.1

SPLAT_PA96_2 1.02 08/11/97 14:55:00

SNL WIPP PA: NUTS_ISO SIMULATIONS(C97 R1 S3)

Total Integrated Discharge up Borehole at Culebra

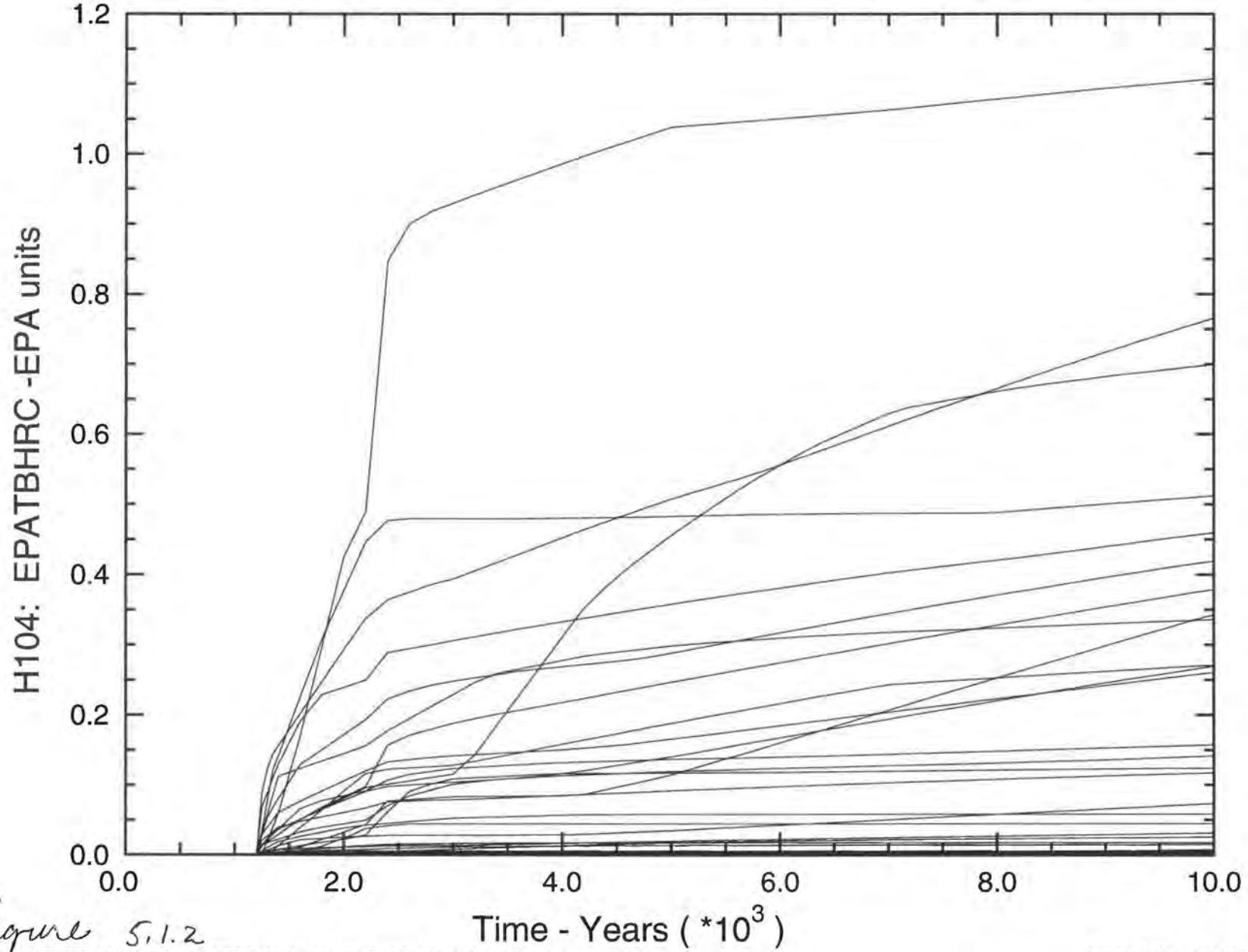

Figure 5.1.2

DISK$TINA_CCA3:[BF.JDMILLE.C97.SUMMZ.NUTS.R1S3]SPLAT_NUTS_ISO_C97_R1S3_H104.INP;1

SPLAT_PA96_2 1.02 08/11/97 14:57:21

SNL WIPP PA: NUTS_ISO SIMULATIONS(C97 R1 S4)

Total Integrated Discharge up Borehole at Culebra

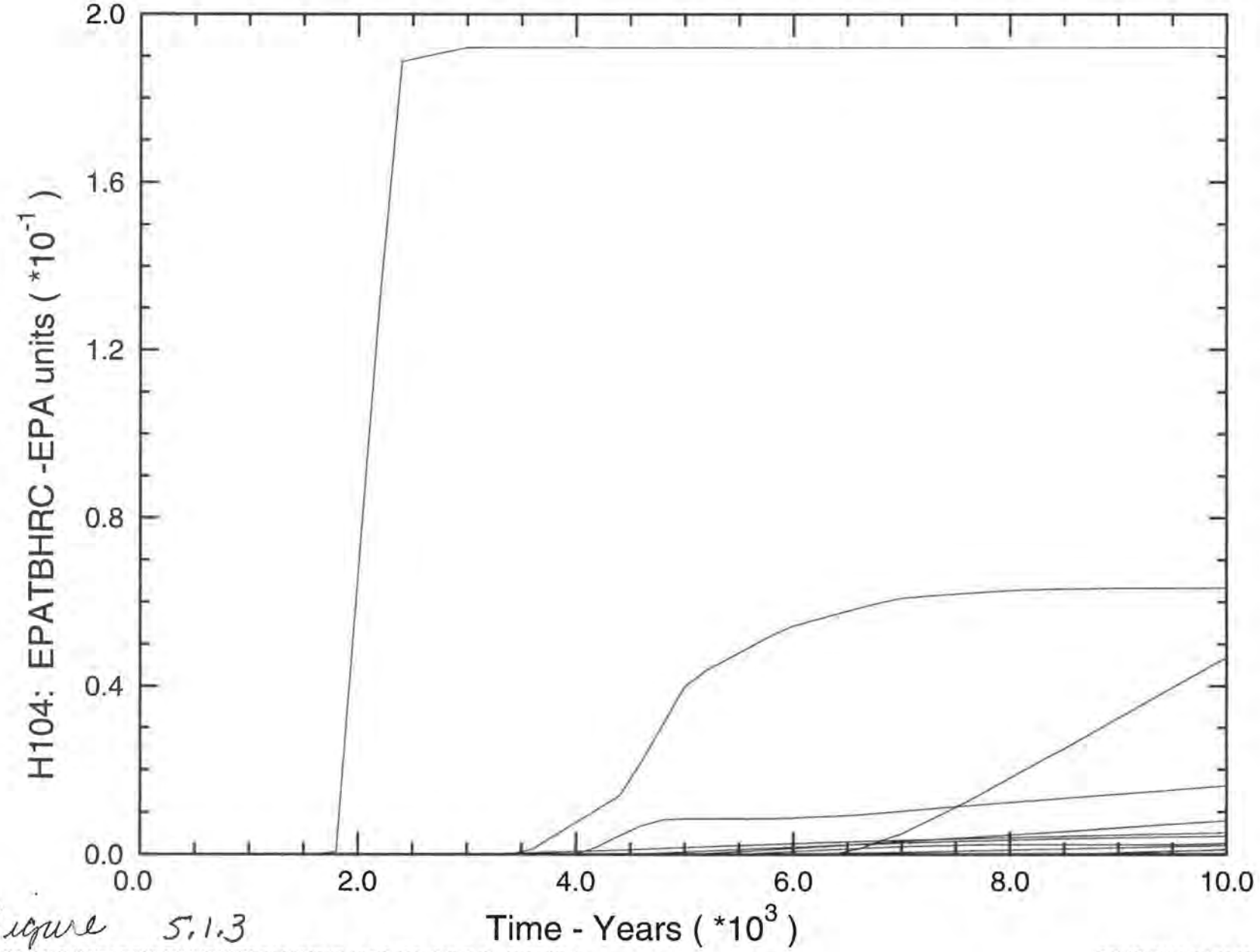

Figure 5.1.3

DISK$TINA_CCA3:[BF.JDMILLE.C97.SUMMZ.NUTS.R1S4]SPLAT_NUTS_ISO_C97_R1S4_H104.INP;1

SPLAT_PA96_2 1.02 08/11/97 14:59:06

SNL WIPP PA: NUTS_ISO SIMULATIONS(C97 R1 S5)

Total Integrated Discharge up Borehole at Culebra

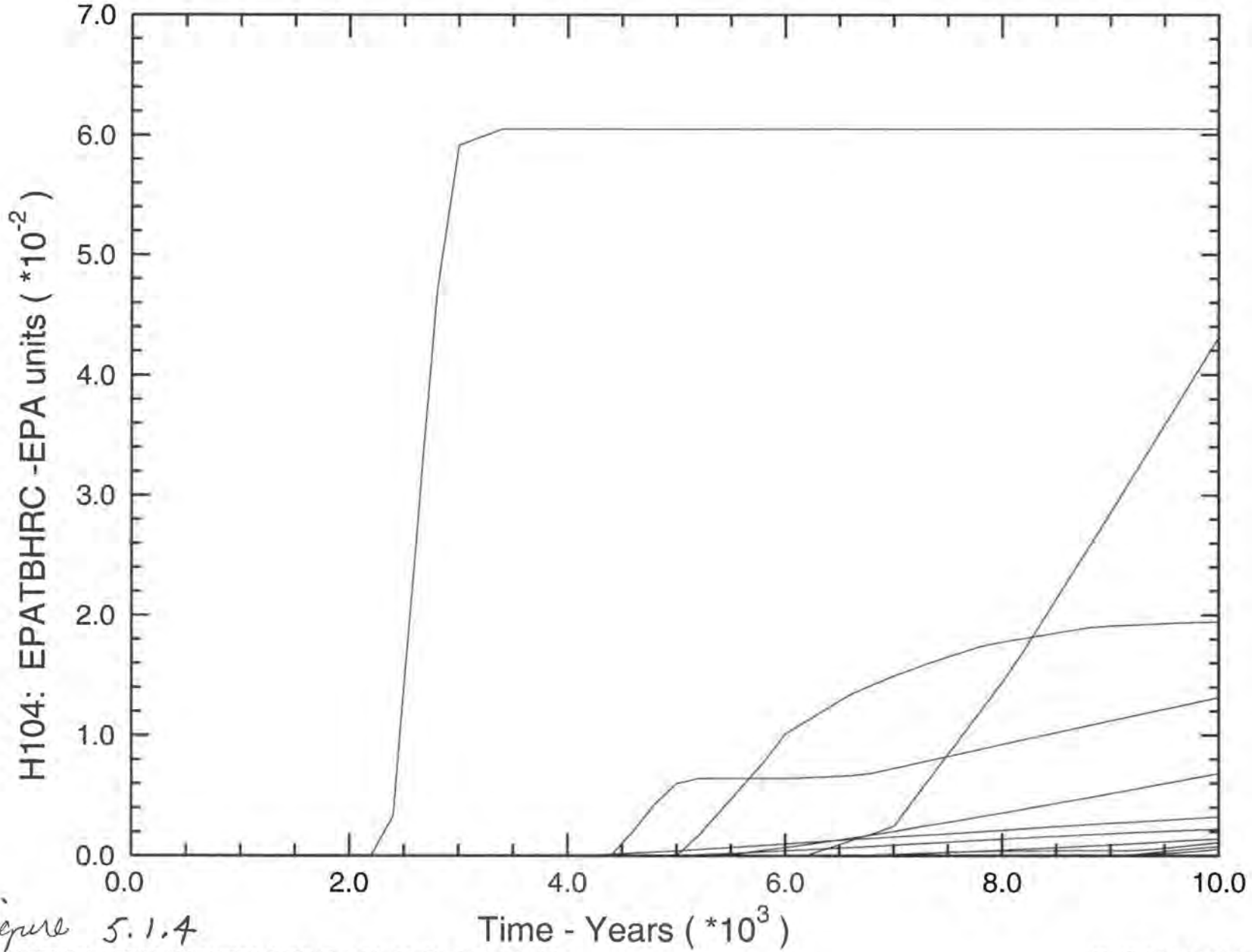

Figure 5.1.4

DISK$TINA_CCA3:[BF.JDMILLE.C97.SUMMZ.NUTS.R1S5]SPLAT_NUTS_ISO_C97_R1S5_H104INP.1

SPLAT_PA96_2 1.02 08/11/97 14:59:39

SNL WIPP PA: PANEL SIMULATIONS (C97 R1 S6 T350)

Total Integrated Discharge up Borehole at Culebra

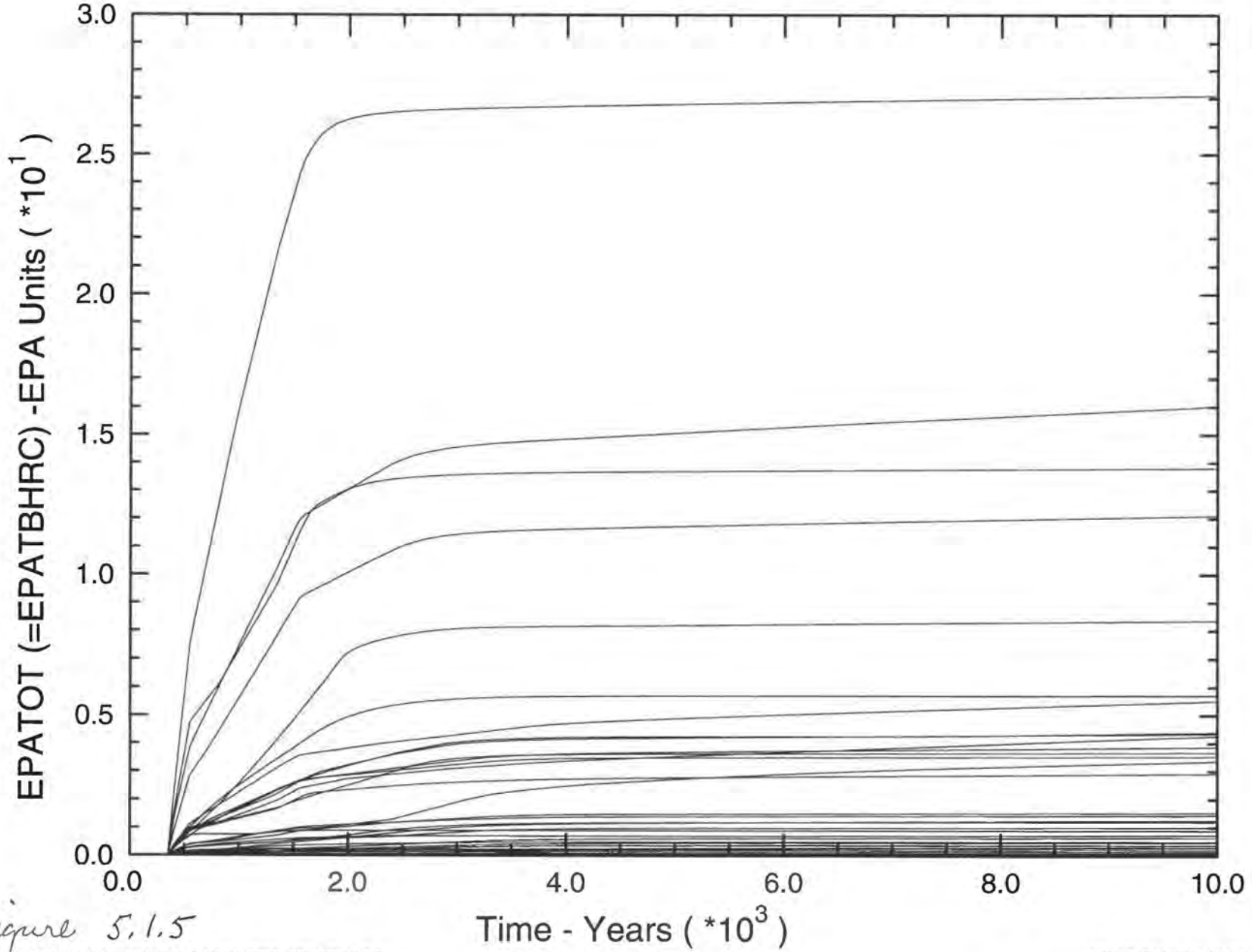

Figure 5.1.5

U1:[JDMILLE.C97.PANEL]ALG_PANEL_C97_R1S6_T350_EPATOT.INP;2

SPLAT_PA96_2 1.02 08/11/97 15:22:45

SNL WIPP PA: PANEL SIMULATIONS (C97 R1 S6 T1000)

Total Integrated Discharge up Borehole at Culebra

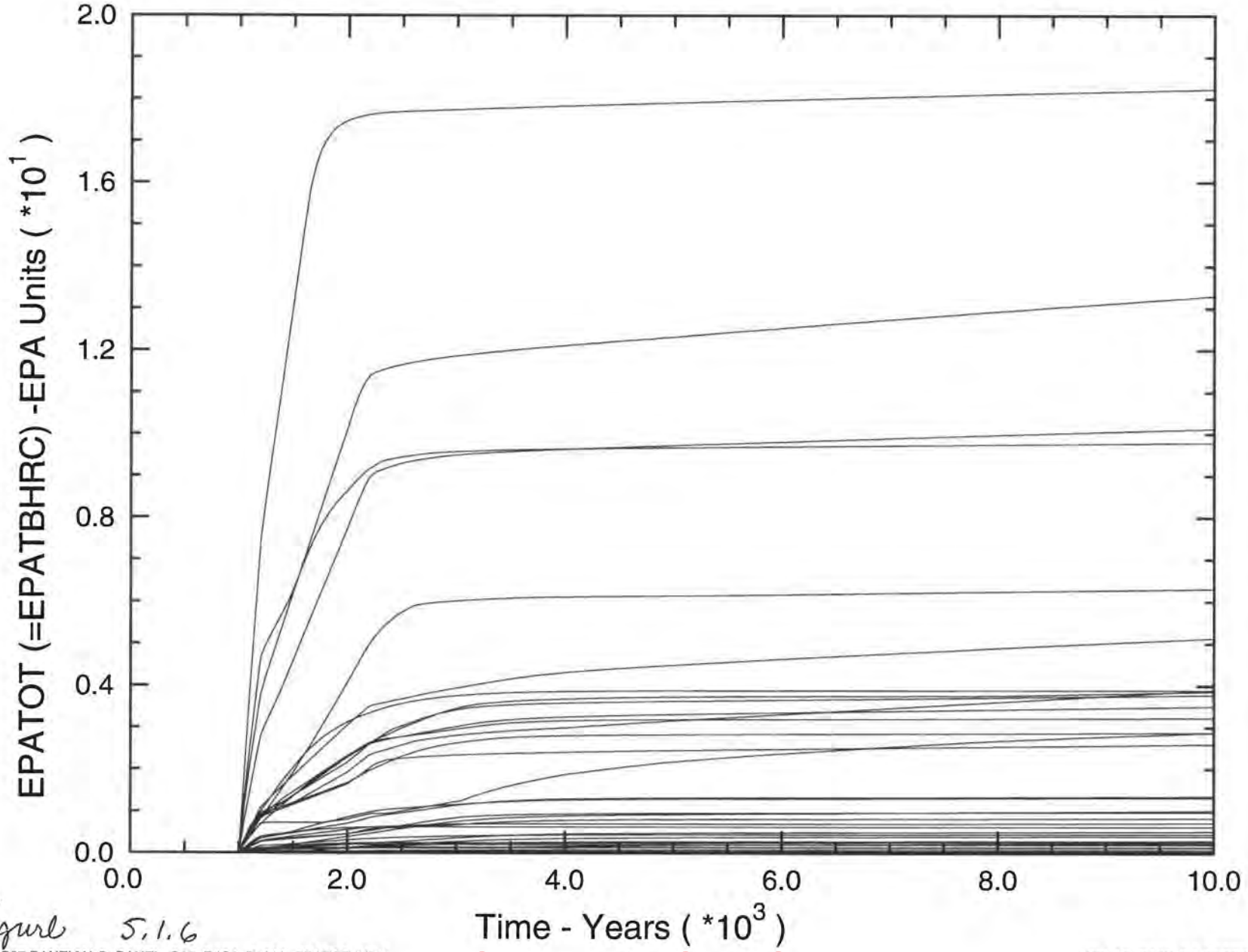

Figure 5.1.6

U1:[JDMILLE.C97.PANEL]ALG_PANEL_C97_R1S6_T1000_EPATOT.INP;2

SPLAT_PA96_2 1.02 08/11/97 15:23:26

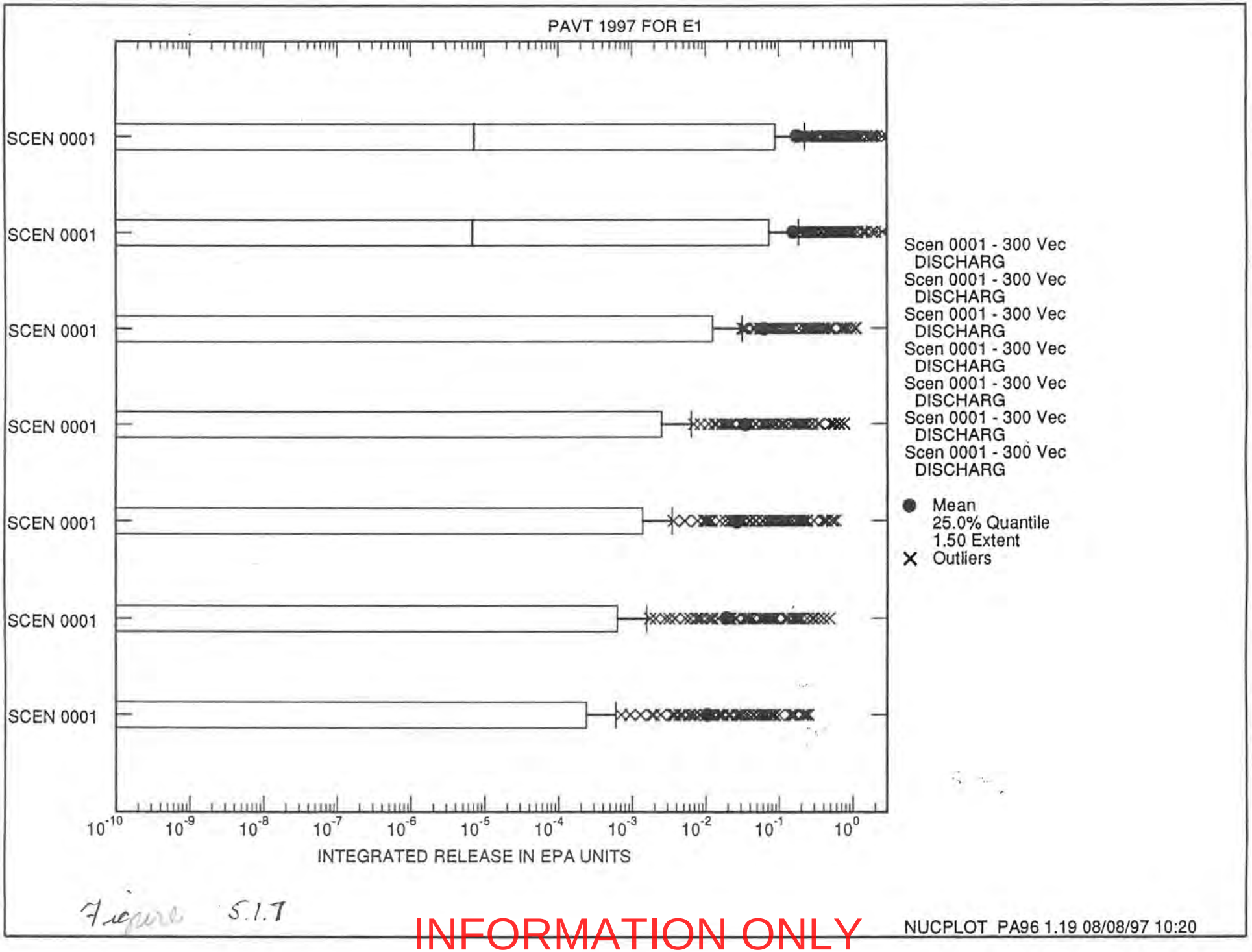

Figure 5.1.7

NUCPLOT PA96 1.19 08/08/97 10:20

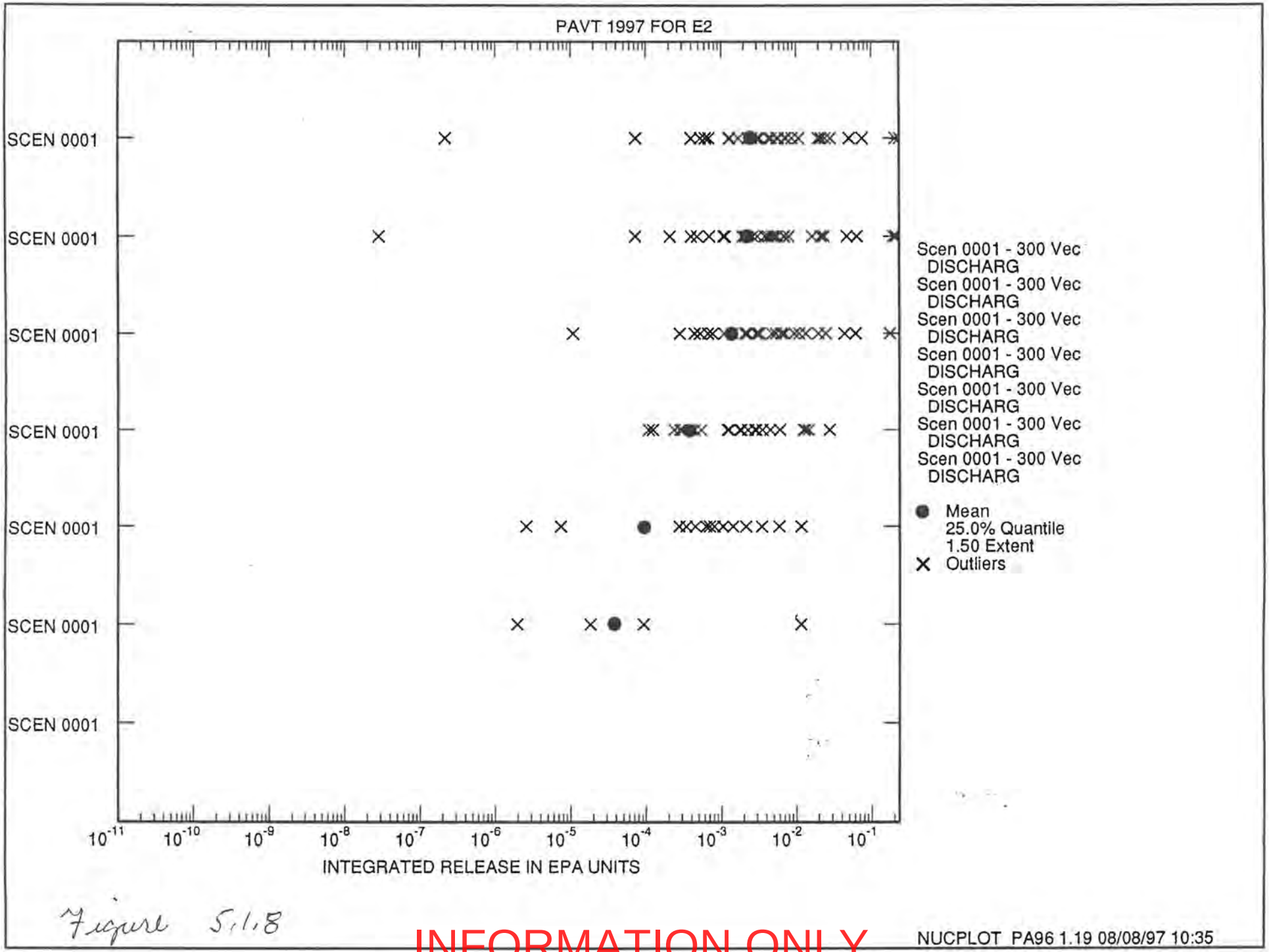

Figure 5.1.8

INFORMATION ONLY

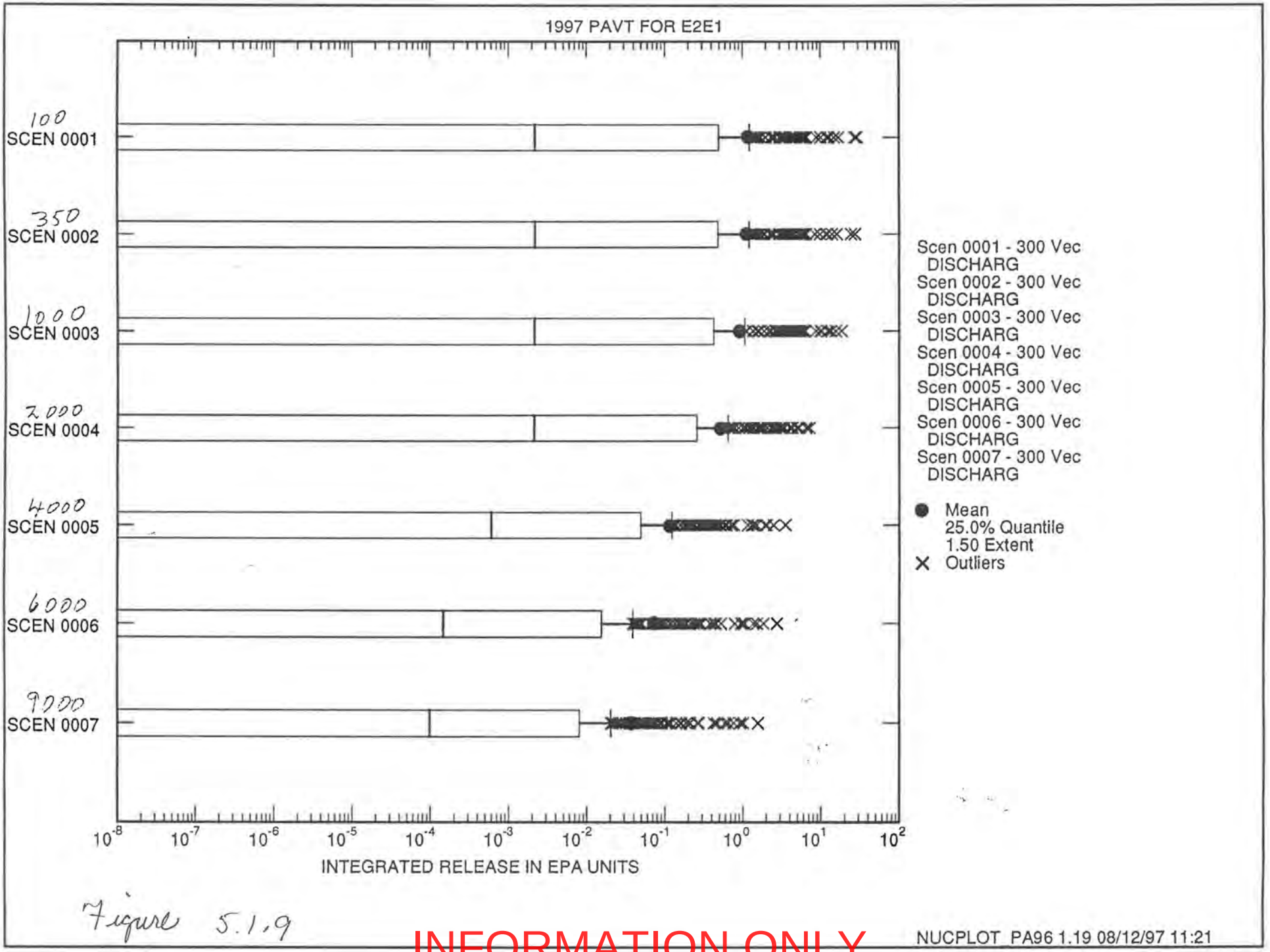

Figure 5.1.9

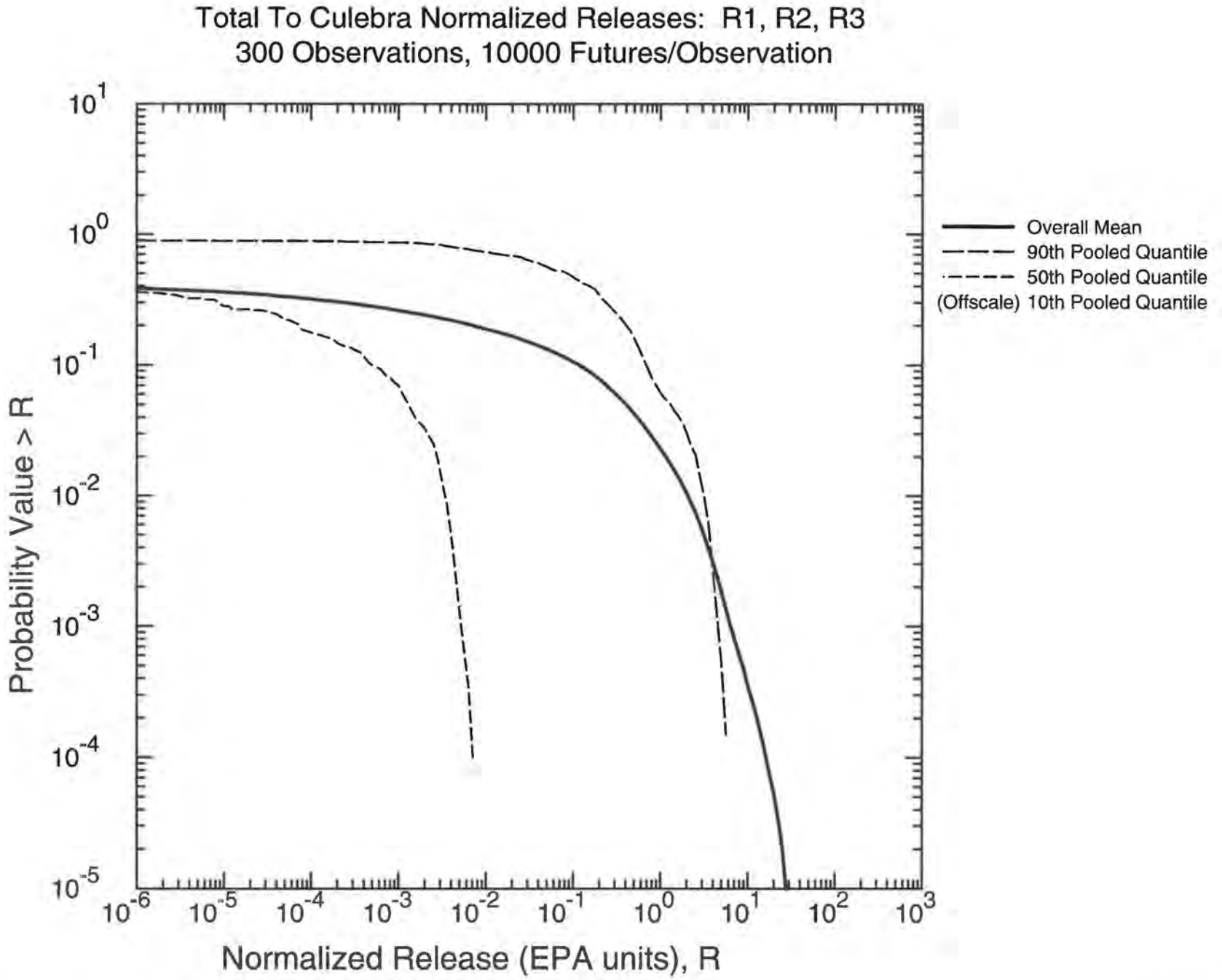

08/13/97 12:13:12

Figure 5.1.1

INFORMATION ONLY

TRI-6342-5556-0

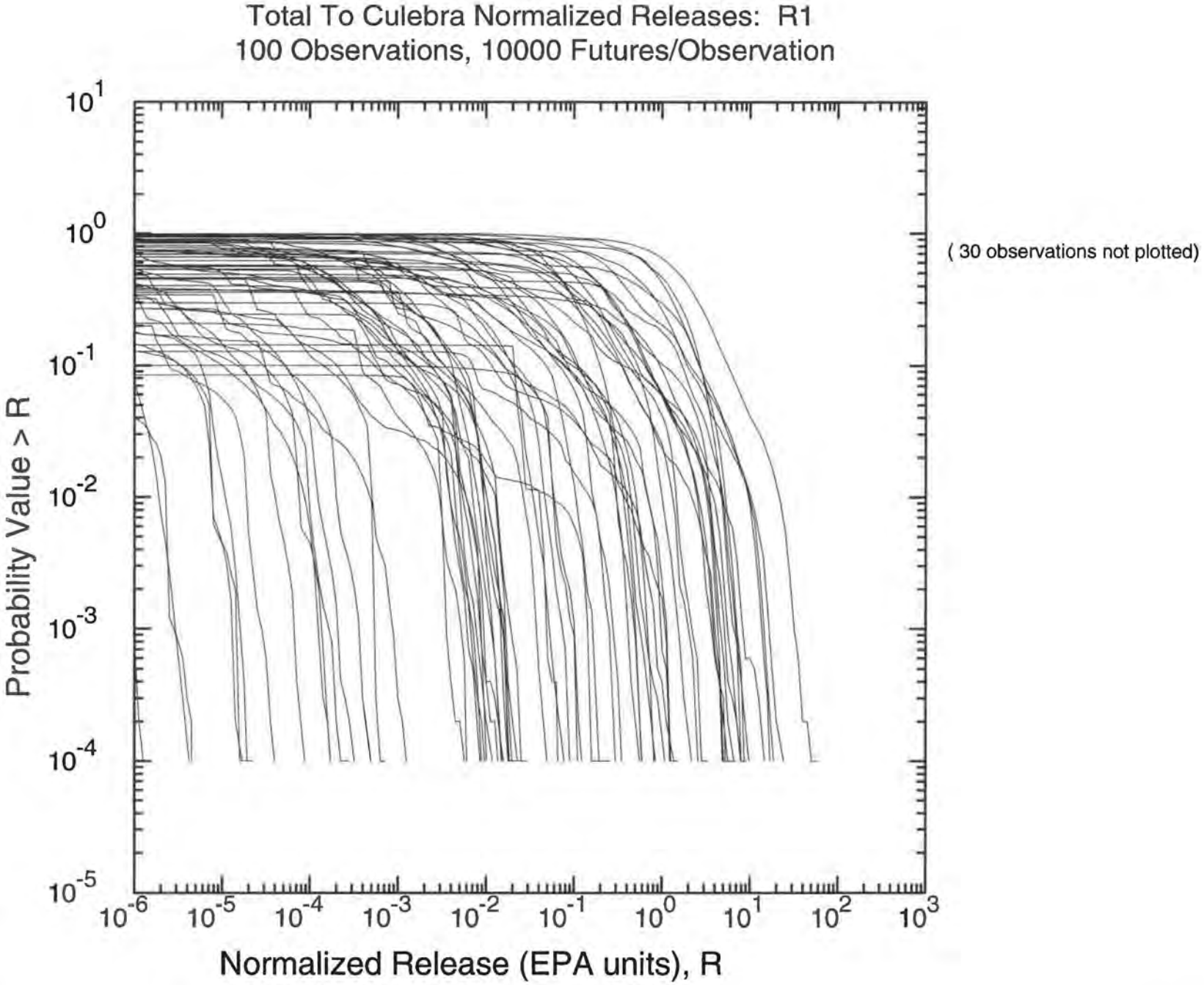

08/13/97 12:13:12

Figure 5.2.1-2

INFORMATION ONLY

TRI-6342-5549-0

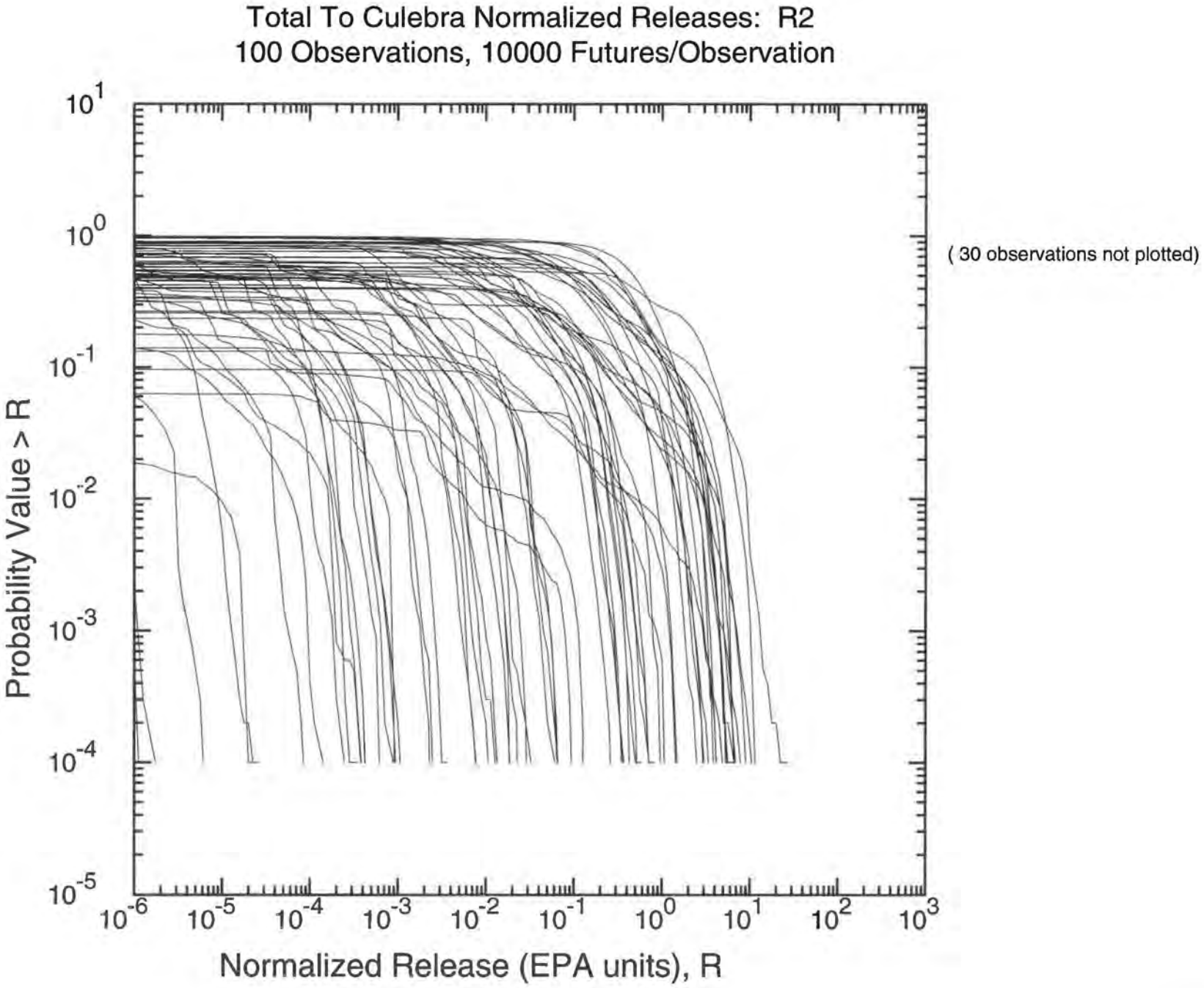

08/13/97 12:13:12

Figure 3.2.3

TRI-6342-5554-0

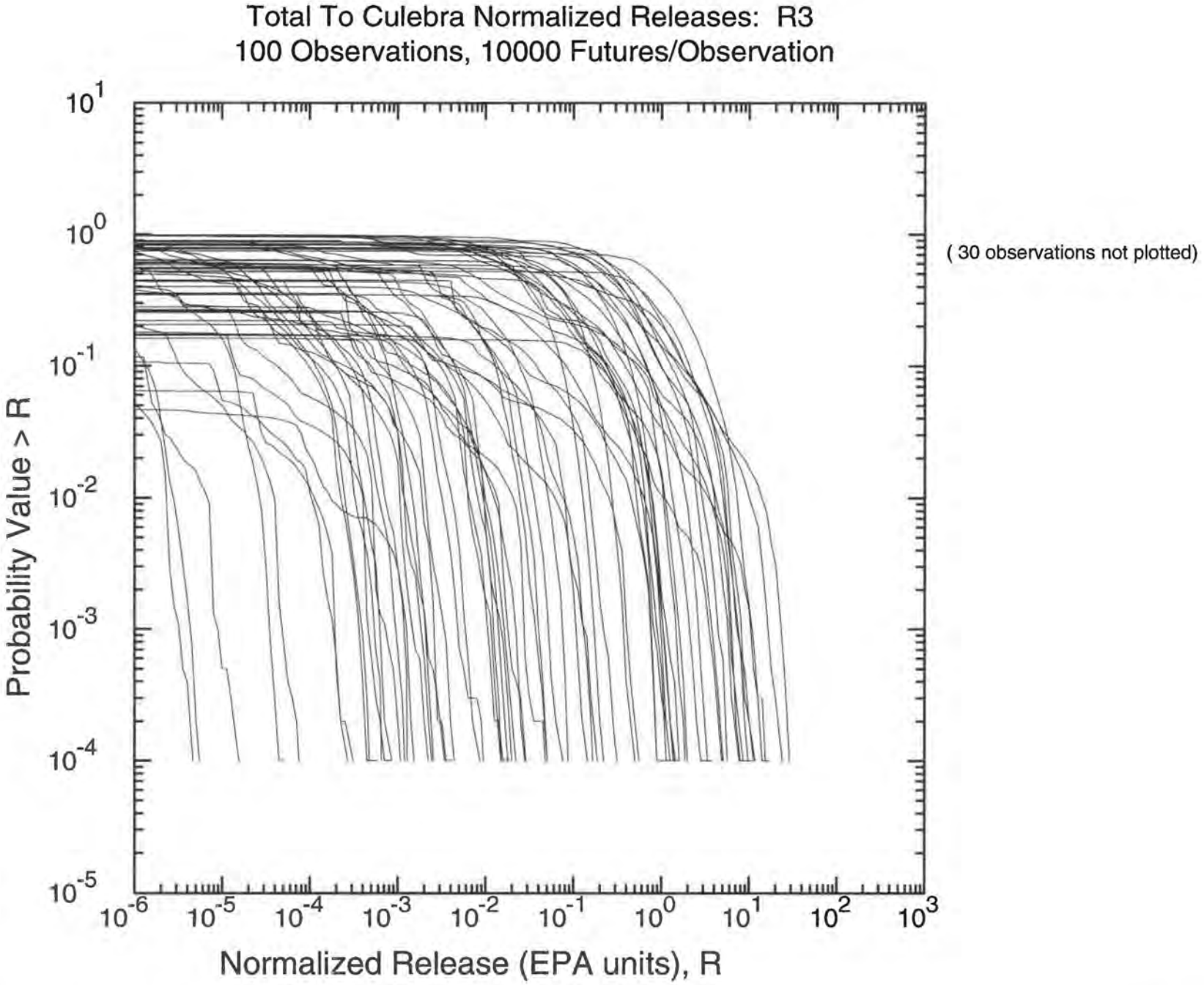

08/13/97 12:13:12

Figure 5.4.4

Total Am241 to Culebra Normalized Releases: R1
100 Observations, 10000 Futures/Observation

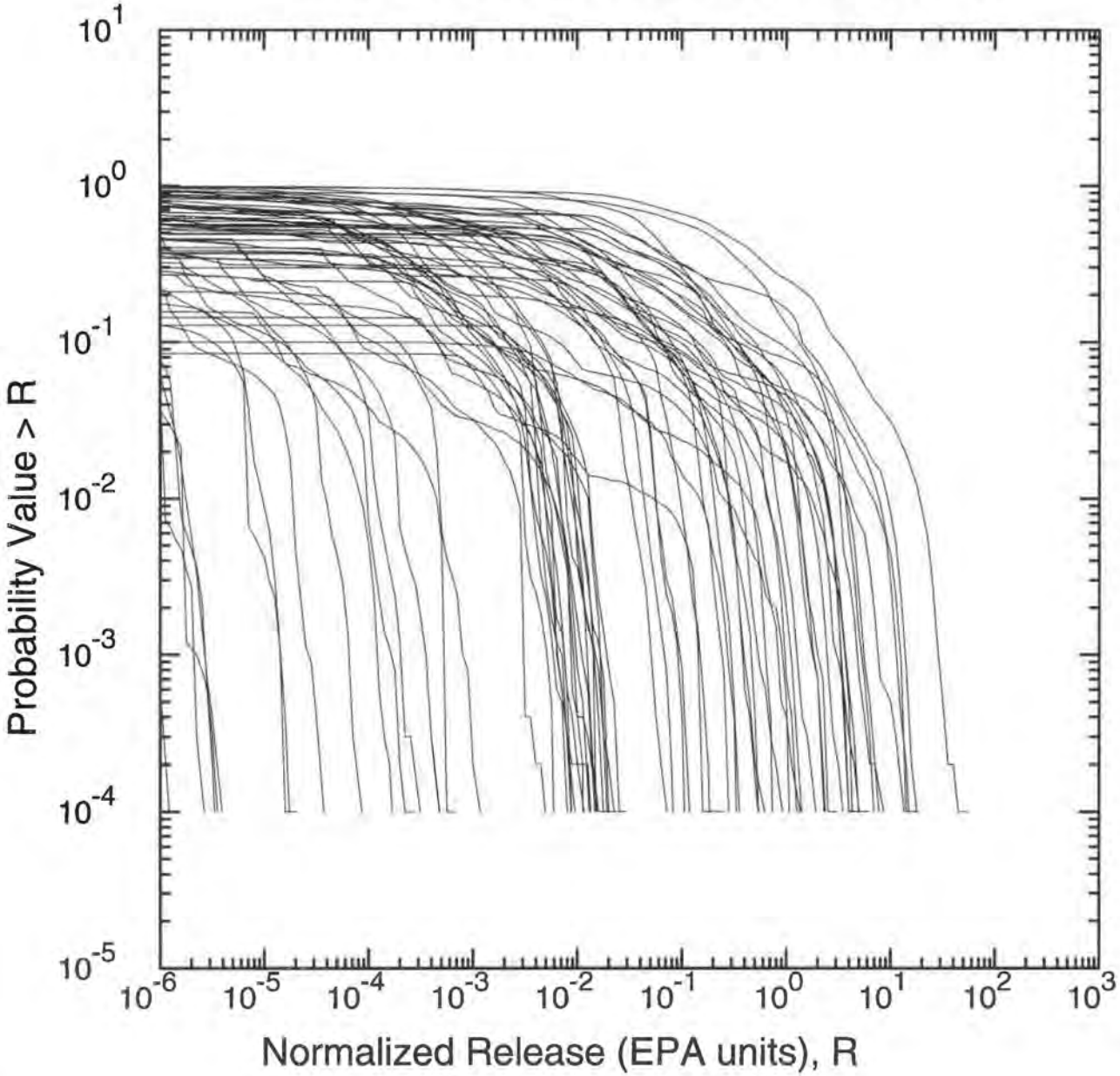

(30 observations not plotted)

08/13/97 12:13:12

Figure 5.2.5-7

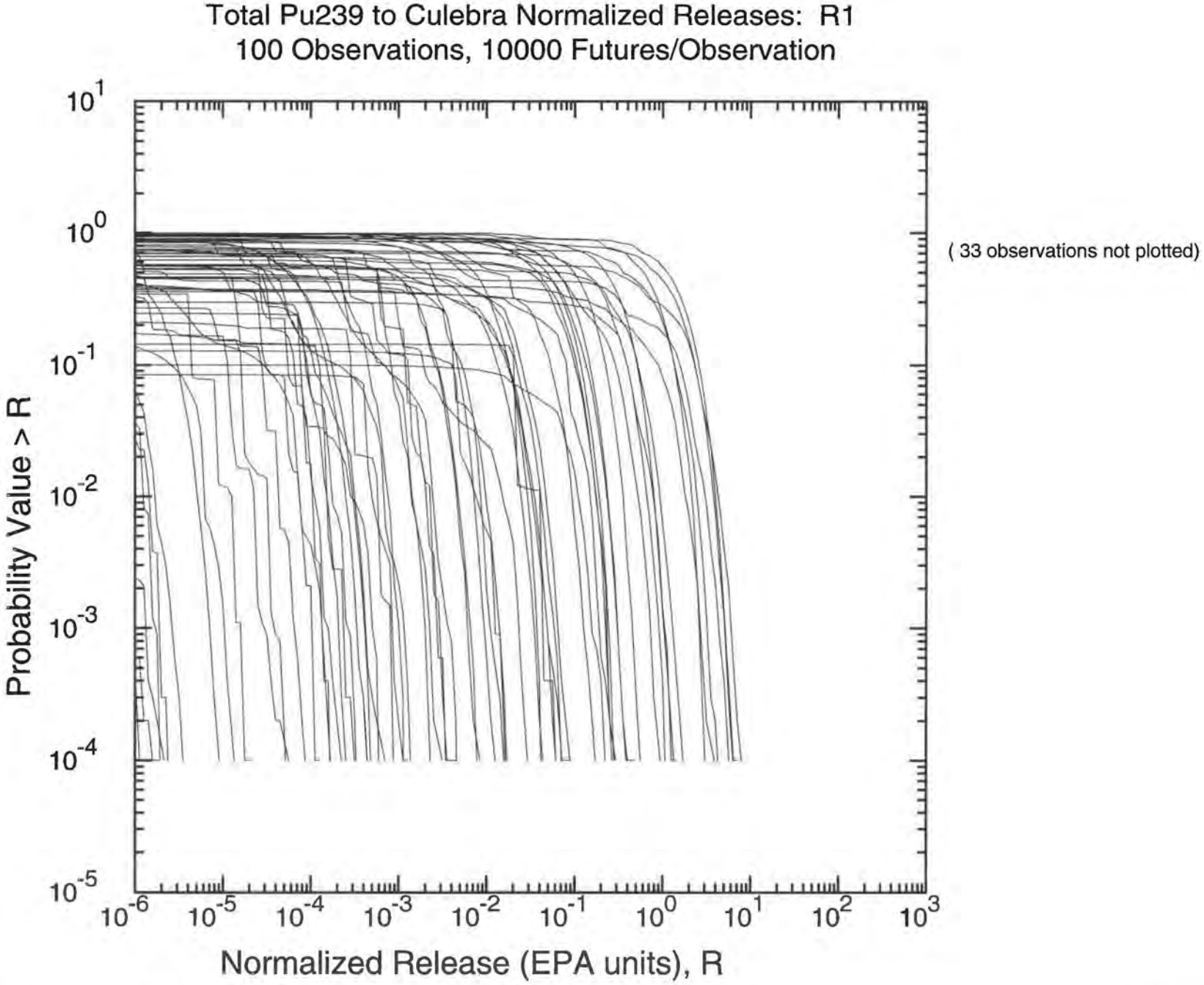

08/13/97 12:13:12

Figure 5.2.7-6

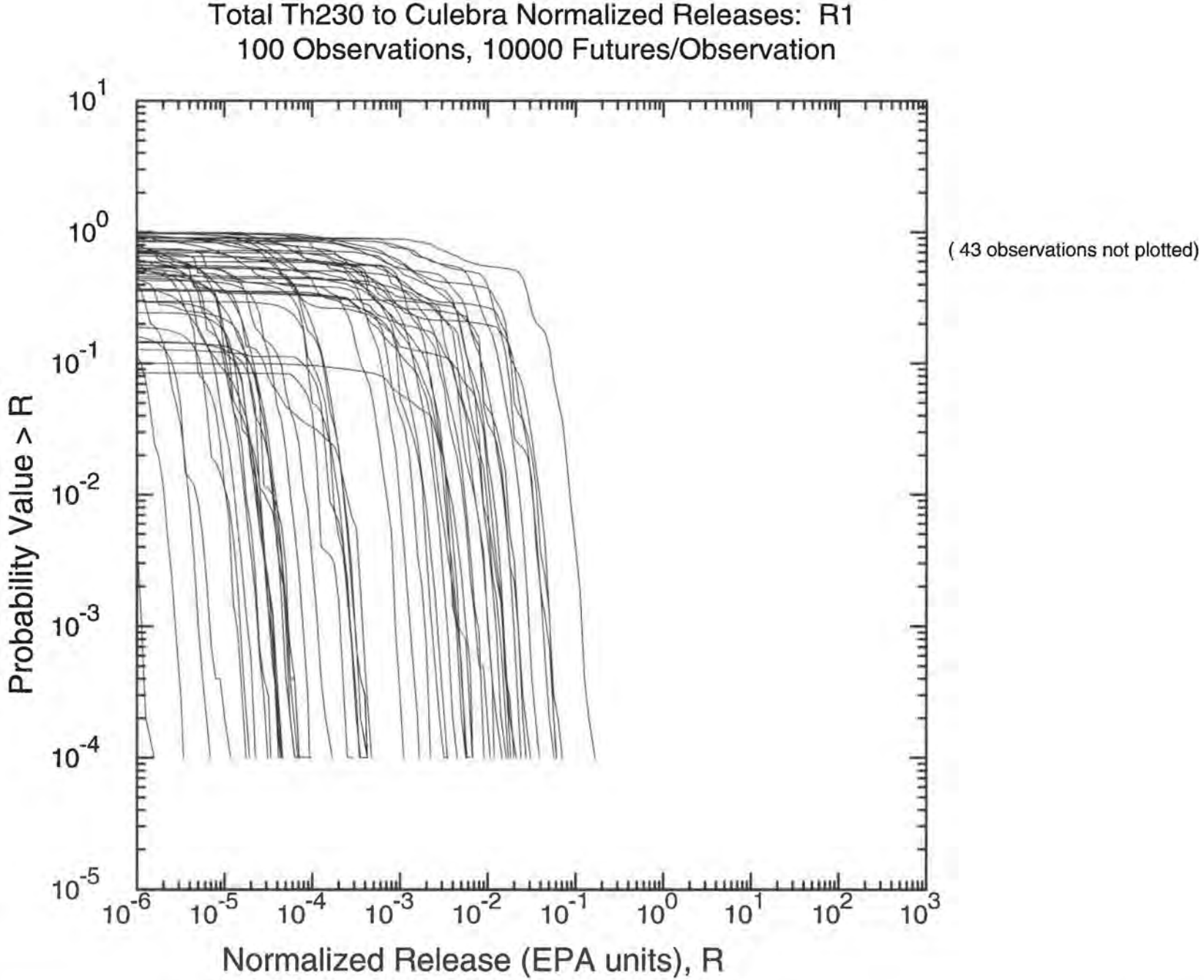

08/13/97 12:13:12

Figure 5.2.7

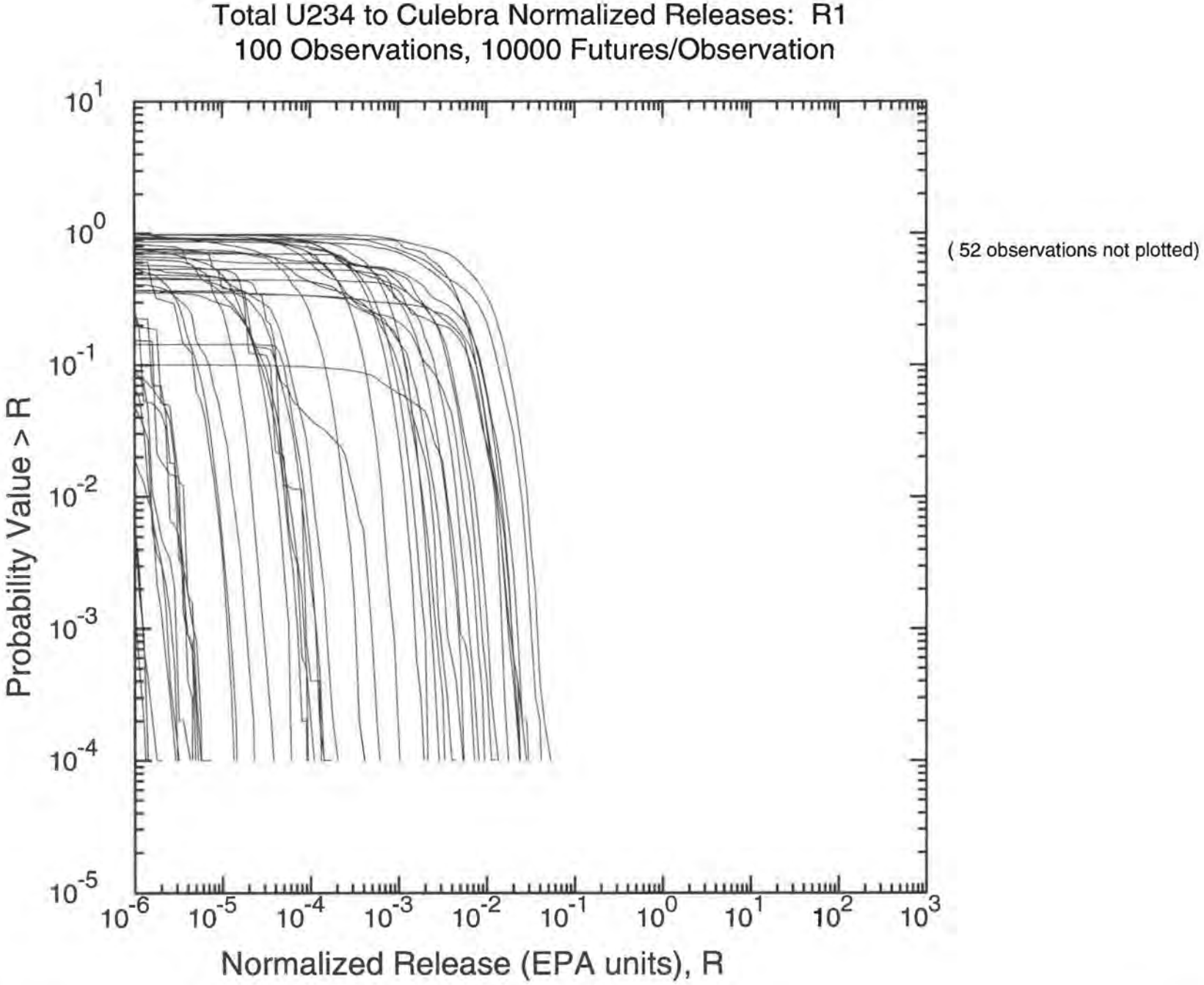

08/13/97 12:13:12

Figure 5.2.8

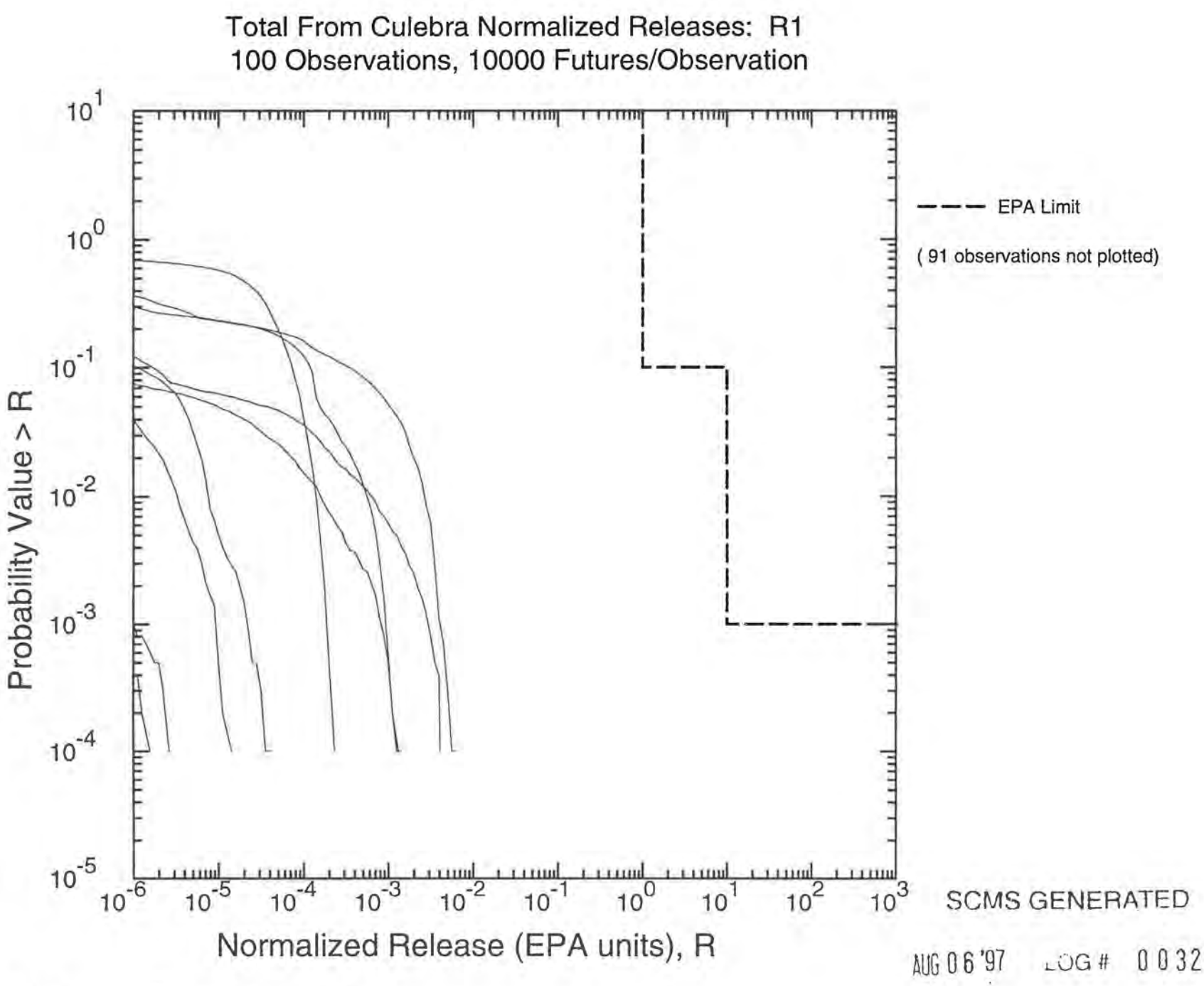
Total From Culebra Normalized Releases: R1
100 Observations, 10000 Futures/Observation
Probability Value > R
Normalized Release (EPA units), R
EPA Limit
(91 observations not plotted)
SCMS GENERATED
AUG 06 '97 LOG # 0032
08/06/97 12:01:17
INFORMATION ONLY

Figure 4.4.1

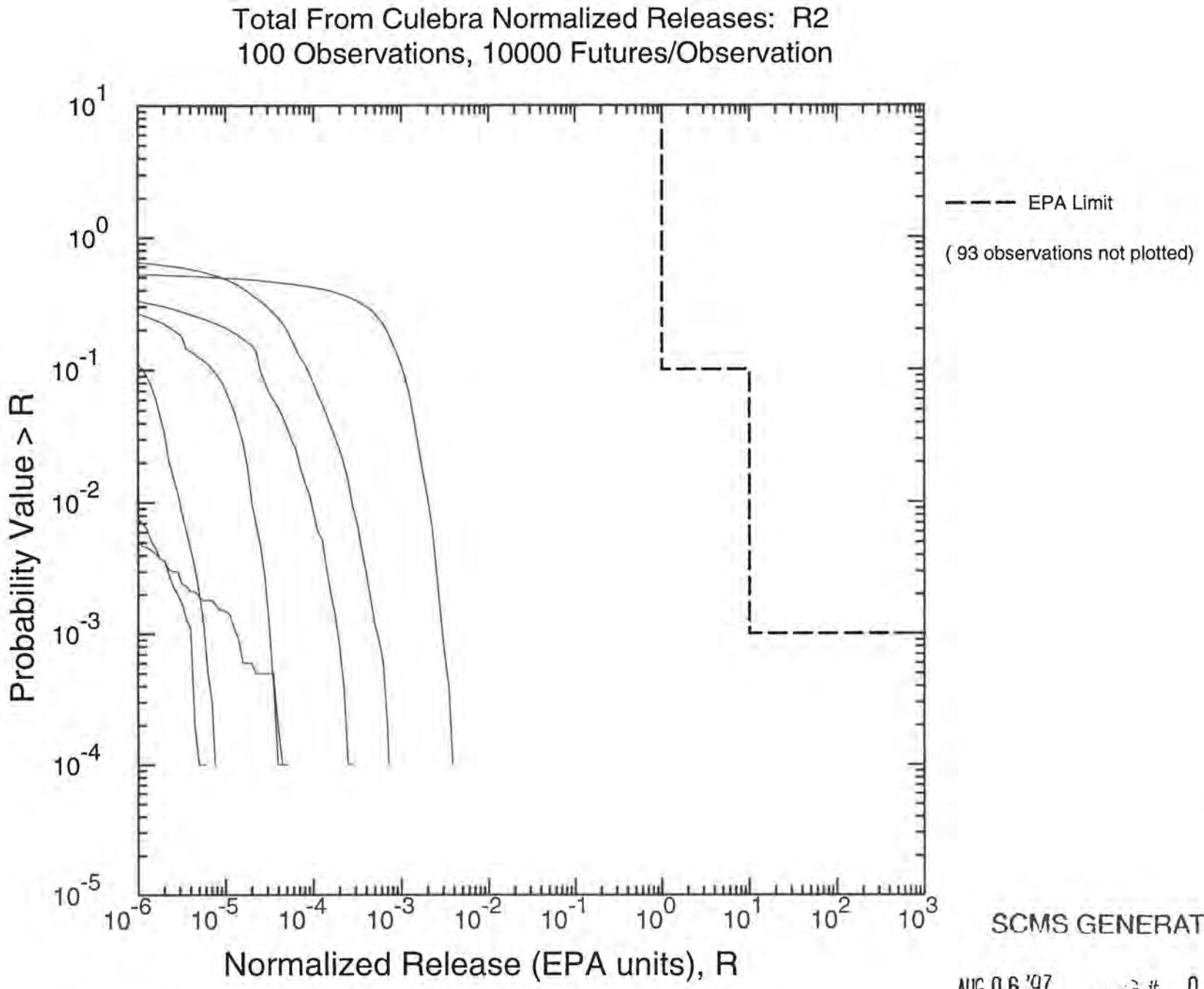

SCMS GENERATED

AUG 06 '97 USG # 0032

08/06/97 12:01:17 Figure 5.4.2

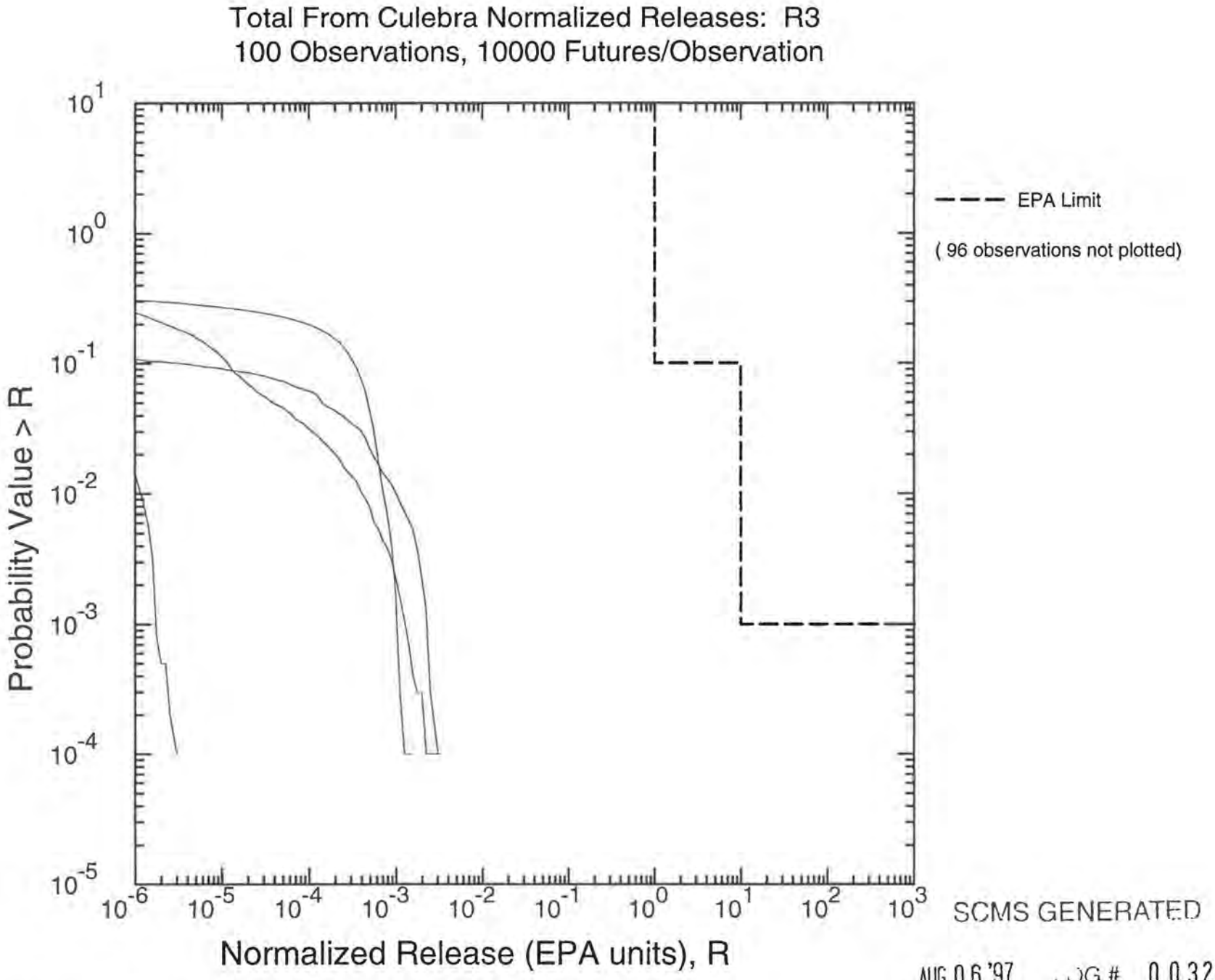

08/06/97 12:01:17

Figure 5.4-3

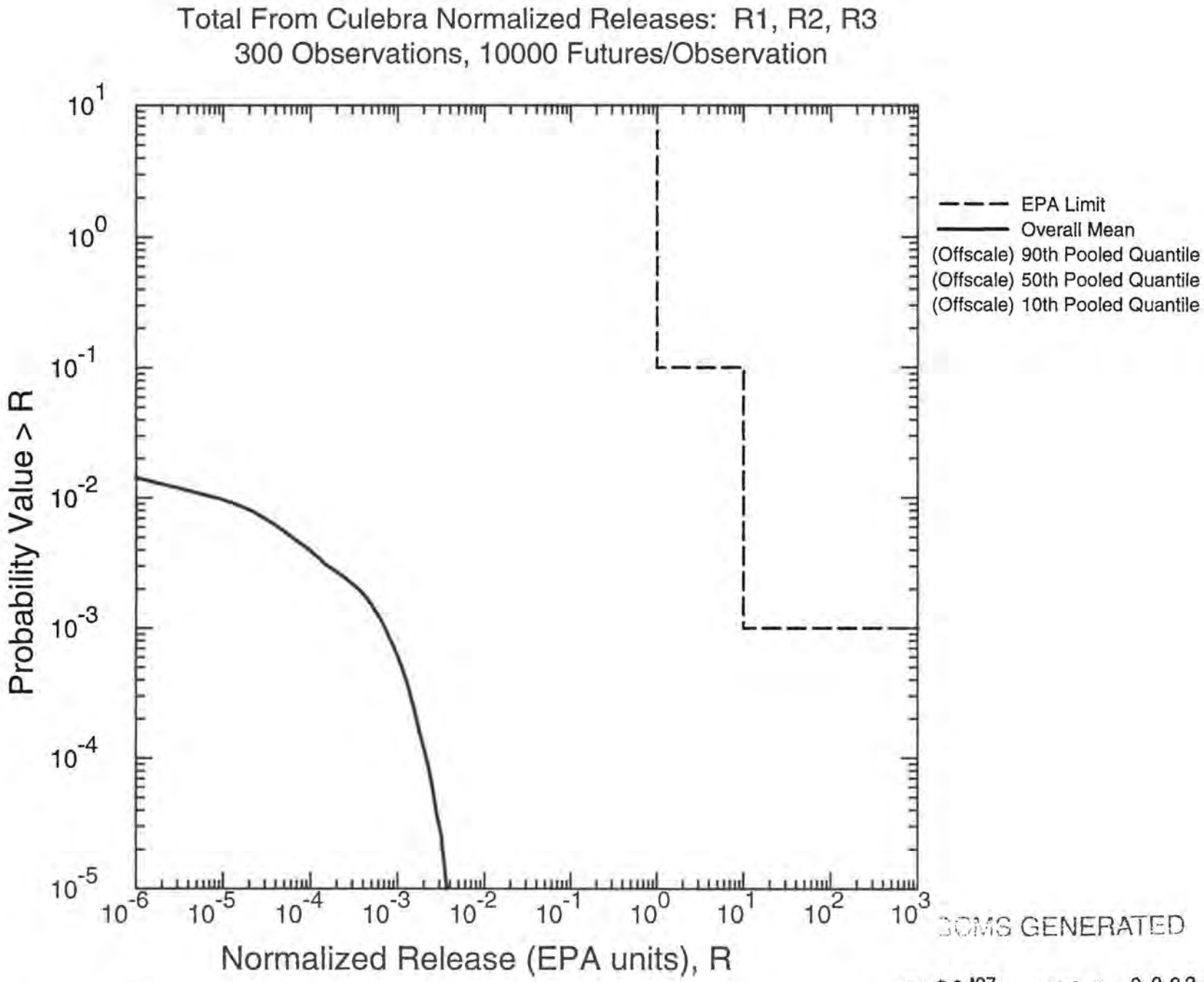

08/06/97 12:01:17 Figure 5.4.4

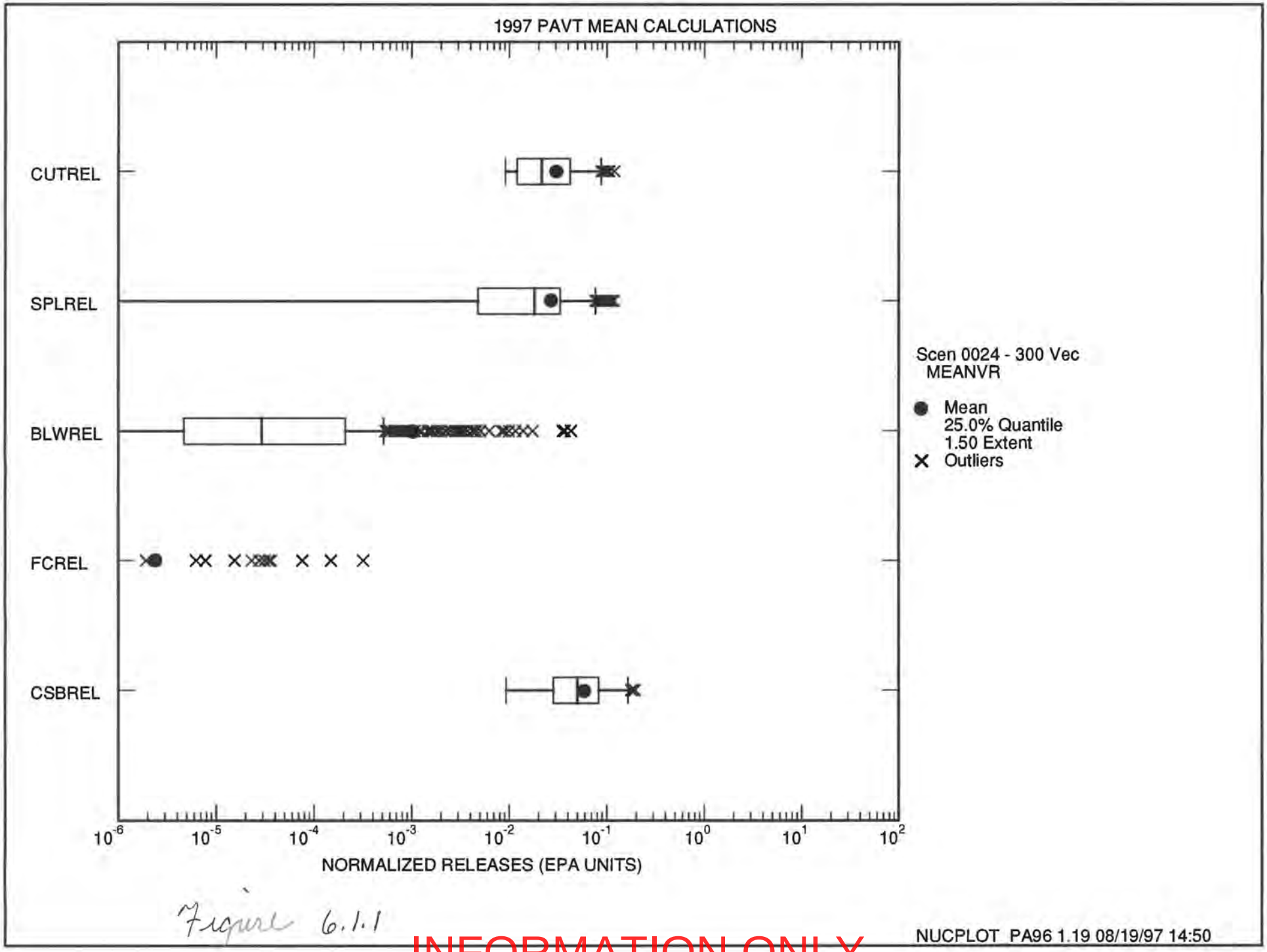

Figure 6.1.1